Applied Mechanics

Dynamics of a Rigid Ship

Jerzy Matusiak

Aalto University
SCIENCE + TECHNOLOGY
LEARNING MATERIAL

Aalto University publication series
SCIENCE + **TECHNOLOGY** 11/2013

Dynamics of a Rigid Ship

Jerzy Matusiak

Aalto University
School of Engineering
Department of Applied Mechanics
Marine Technology

Aalto University publication series
SCIENCE + **TECHNOLOGY** 11/2013

ISBN 978-952-60-5204-5 (printed)
ISBN 978-952-60-5205-2 (pdf)
ISSN-L 1799-4896
ISSN 1799-4896 (printed)
ISSN 1799-490X (pdf)

Unigrafia Oy
Helsinki 2013

Finland

441 697
Printed matter

Preface

This textbook is a result of the work started in 1996 when I joined a very interesting, newly formed Specialist Committee working on Ship Stability within the International Towing Tank Conference (ITTC). Thanks to this group of international enthusiastic scholars in the field, it became clear for me that both the research and the rules' development in the field of ship stability will proceed in the direction of including ship dynamics into account. Moreover, this development will require sophisticated mathematical models of ship dynamics based on the first principles and taking realistically into account the environmental, often very hostile, conditions. These models should be verified and thoroughly validated.

I am very grateful to Professor Eero-Matti Salonen for his valuable comments and corrections he has made to the original manuscript. I want to thank my colleagues Messrs Teemu Manderbacka and Otto Puolakka, the assistants in the course on ship dynamics, for their valuable remarks concerning the lecture notes that were the bases of this report.

I also want to thank Dr. Timo Kukkanen for reviewing the manuscript.

Contents

List of symbols

A	amplitude, area
A_p	propeller plane area
a	added mass coefficient, coefficient
b	added damping coefficient
C_B	volumetric block coefficient
C_D	drag coefficient
C_L	lift coefficient
C_T	total resistance coefficient
C_B	thrust loading coefficient
D	propeller diameter, drag
E	energy
$\boldsymbol{F}$	force vector
f	function
g	constant of gravitational acceleration
G	centre of gravity
$\mathbf{G}$	moment of external forces

h	angular momentum
h	water depth
H	transfer function
H_S	significant wave height
$\boldsymbol{I}$	matrix comprising components of mass moment of inertia of the body
I,J,K	unit vectors of the Earth-fixed co-ordinate system
i, j,k	unit vectors of the body-fixed co-ordinate system
k	wave number, retardation function
K	coefficient
J	advance number
K,M,N	components of the moment of external forces
L	ship length, lift
M	Bending moment
m	ship mass, spectral moment
n	propeller revolutions per second
$\boldsymbol{n}$	vector normal to the body surface and pointing outwards of the fluid domain
p,q,r	angular velocities in the body-fixed co-ordinate system
p	pressure

P	power
q	load distribution
Q	shear force
r	radius
$\boldsymbol{R}$	position vector
R	resistance
S	wetted surface, spectral density
t	time, thrust deduction factor
T	draft, thrust, period
$\mathbf{T}$	transformation matrix
$\mathbf{U}$	ship velocity vector
u,v,w	translational velocities in the body-fixed co-ordinate system, flow velocity components in x-, y- and z-directions
V	ship speed
$\boldsymbol{v}$	flow velocity vector
w	wake factor
x, y, z	co-ordinates of the body-fixed co-ordinate system
X,Y,Z	co-ordinates of the inertial co-ordinate system

	components of the hydrodynamic forces acting on ship hull in the body fixed co-ordinate system
Z	number of propellers
α	angle of attack
∇	volumetric displacement
β	drift angle
γ	flow angle, Euler angle
δ	rudder angle
ε	air-flow angle, phase
θ	pitch
λ	characteristic value, wave length
μ	ship course in respect to waves, heading angle
ρ	water density
ρ_a	air density
ϕ	roll, velocity potential
ψ	yaw
ω	angular velocity
$\mathbf{\Omega}$	angular velocity vector
ξ	critical damping ratio

ξ_j	motion component in the j-th degree of freedom
ζ	wave elevation

1. Introduction

The term ship dynamics means all operational conditions of a vessel where inertia forces of a ship motion play a role. All situations that differ from the ideal still water condition with a ship at constant heading and constant forward speed fall into the category of ship dynamics. Traditionally ship dynamics is dealt with using different simplified mathematical sub-models termed sea-keeping, manoeuvring, structural vibration and dynamic stability. The term *directional stability and control* is sometimes used meaning a subclass of the manoeuvring. These sub-models are characterized by different assumptions. Usually these assumptions concern the linearity of the responses with respect to the excitation. Thanks to these assumptions it is possible, using relatively simple algorithms, to predict certain limited classes of a ship's behaviour. The shortcoming of these sub-models is that they are not capable to cope with a wide range of vessel's behaviour pertinent to ship safety.

A linear model of ship dynamics in waves called sea-keeping is well established. In most cases, this model gives a sufficiently accurate prediction of loads and ship motions. Perhaps the biggest benefit of using a linear model is that prediction of exceeding a certain level of load or response can be easily derived. Analysis is conveniently conducted in the frequency domain. The most serious shortcoming of the linearity assumption is that it precludes prediction of certain classes of ship responses. The linear models cannot predict the loss of ship stability in waves, parametric resonance of roll, and asymmetry of sagging and hogging. Ship steering and manoeuvring motion are disregarded.

Simulation of ship manoeuvring is usually conducted for the still water condition. Time-domain simulation of ship motion is restricted to in-plane

motion comprising of surge, yaw and sway motion components only. This means that heeling motion, which is a crucial motion component when ship safety is concerned, is disregarded. If waves are encountered, their effect is taken into account as a steady state one.

The main reason for making simplifications in the ship dynamics models was the poor performance of computers at the time the methods were being developed (1960's). On the other hand, a lot of theoretical development done at this time resulted in the analytical models that are still valid and very much applicable.

This course on ship dynamics attempts to present a unified theory covering nonlinear seakeeping and manoeuvring. This model is nearly free of the linearity assumptions and makes it possible to evaluate a ship's responses in the time domain. The model can be used as a basis for an advanced ship-handling simulator. The forthcoming updated rules concerning stability of an intact vessel will allow for a direct simulation of ship behaviour in waves as a direct stability assessment. It is believed that the theory presented in the course covers the requirements of the method to be used in this task.

The lecture notes for this course can also be used as the theoretical manual of the *LaiDyn* software. This computer program has a modular structure. The separate modules represent the forces developed by rudders and propellers, hydrodynamic reaction due to hull motion, wave and wind forces. Mathematical models of these forces are based on basic ship hydrodynamics; they are presented in detail in the lecture notes. The above-mentioned reaction forces are used as the excitation to the general model of a rigid body motion in the six-degrees-of-freedom. This general model, known from the classical mechanics, is recalled at the beginning of the course. Next a simplified model of ship dynamics, restricted to the in-plane motion, is presented. This model is known as manoeuvring. This is a simplification used amongst the others in the ship-handling simulators used for training deck officers and pilots. The sub-models representing the action of propellers and rudders are introduced in the context of manoeuvring. Numerical implementation of the manoeuvring simulation and the exemplary results are also given.

In Chapter 6, a mathematical model of sea surface waves is presented. This is done both for regular and irregular waves. Nonlinearities associated with wave motion are discussed.

In Chapter 7, hydrodynamic reaction forces acting on a ship in waves are discussed. This is done using a classical potential flow model and making an allowance for the most important nonlinearities to be taken into account in the simulation.

Chapter 8 presents a simple, one-degree-of-freedom model of a rigid body motion in waves. This chapter can be understood as an introduction to sea-keeping theory.

The model in Chapter 8 is expanded to the linear model of ship motions in the six-degrees-of-freedom (classical sea-keeping theory) in the beginning of Chapter 9.

This is followed in Chapter 10 by a presentation of the nonlinear time-domain model utilized in *LaiDyn*. This can be thought of as a summary of what was presented earlier as the separate sub-models and a numerical implementation of the integration routine.

Chapter 11 presents several applications of the *LaiDyn* method. A broad range of ship dynamic problems is discussed and illustrated by example simulations and model test results.

Internal loads acting on a rigid ship operating in waves are discussed in Chapter 12. This discussion is mainly based on research conducted by Timo Kukkanen (2012).

2. Basic assumptions

A ship is regarded as a rigid intact body. Hull rigidity means that ship deformations are not taken into account. This assumption is reasonable, as the deformations of a ship or a boat are a few centimetres at most, while motions and wave amplitudes are measured in metres. Thus the argument is that hull deformations do not affect global motions. For the sake of simplicity, damage to the hull and flooding are not taken into account either. Other assumptions are presented in the subsequent sections.

3. Co-ordinate systems and kinematics used for describing ship motion

Three co-ordinate systems are used for describing ship motion. These are presented in Figure 1.

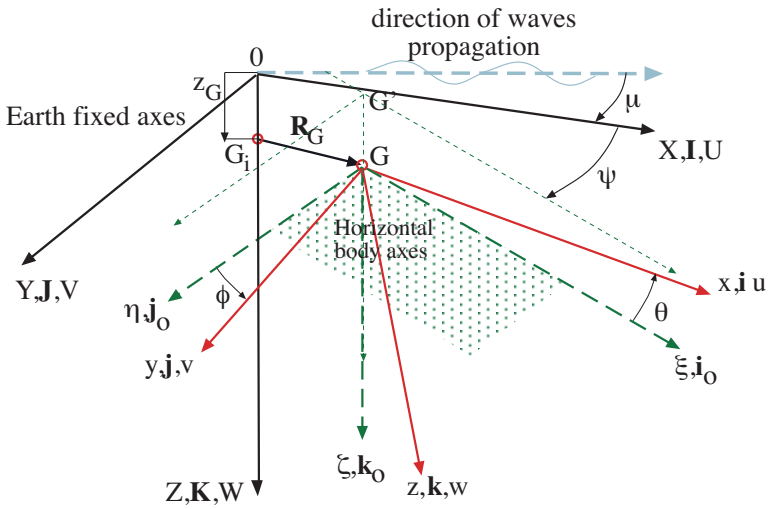

Fig. 3.1 Co-ordinate systems used in ship dynamics.

An inertial Cartesian co-ordinate system fixed to Earth is denoted by *XYZ*. This co-ordinate system is used when giving the navigational position of a vessel. The *X-Y* plane coincides with the still water level. The origin *0* of this co-ordinate system is located at the vertical passing through the initial location G_i of the ship's centre of gravity. *X*-axis is usually selected so that it points to the initial direction of ship's bow. The basis vectors of this co-ordinate system are **I**, **J** and **K**. Direction of surface waves propagation makes angle μ with axis *X*. G denotes the ship's centre of gravity. It is the

origin of the moving Cartesian co-ordinate system *xyz* fixed with the ship with the *x*-axis pointing towards the bow. This system is called the body-fixed co-ordinate system. The basis vectors of this body-fixed co-ordinate system are **i**, **j** and **k**. The so-called horizontal body axes co-ordinate system (Hamamoto & Kim, 1993) denoted as $\xi\eta\zeta$ also moves also with the ship so that the plane ξ–η is parallel to the still water plane *X*-*Y*. The axes *X* and ξ make an angle ψ, which is the deviation from the initial course. The main role of this auxiliary co-ordinate system is to enable a definition of the angular orientation of the vessel. We also use this co-ordinate system to define linear motion components. Namely, the motion along the ξ-axis is called *surge*. The motion components along the η- and ζ-axes are called *sway* and *heave* respectively.

When describing ship motion we are interested in its position in the inertial co-ordinate system *XYZ*. The position of a rigid body is uniquely defined by the position of a certain selected point (e.g. the origin) of the body and by the angular orientation. Thus the position of a rigid body moving in three dimensional space is uniquely defined by six quantities. These are called as the generalized co-ordinates and denoted by $\mathrm{X} = \{X_\mathrm{G}, Y_\mathrm{G}, Z_\mathrm{G}, \phi, \theta, \psi\}^\mathrm{T}$.

It is convenient, as above, although not necessary, to select the body's centre of gravity as the origin. Thus the vector $\boldsymbol{R}_\mathrm{G}=X_\mathrm{G}\mathbf{I}+Y_\mathrm{G}\mathbf{J}+Z_\mathrm{G}\mathbf{K}$ gives the translational position of the body. The components (X_G, Y_G and Z_G) of this vector are three of the generalized co-ordinates. The time differentiation of the position vector yields the velocity of the origin of ship as

$$\mathbf{U} = \dot{\mathbf{R}}_G = \dot{X}_G\mathbf{I} + \dot{Y}_G\mathbf{J} + \dot{Z}_G\mathbf{K} = u\mathbf{i} + v\mathbf{j} + w\mathbf{k} \quad (3.1)$$

Here $\dot{X}_G, \dot{Y}_G, \dot{Z}_G$ and *u, v, w* are the velocity components of the velocity **U** of the ship's centre of gravity with respect to the inertial system expressed in the inertial and in the body-fixed system, respectively. In the marine field the angular position of a vessel is given by the so-called modified Euler angles (ψ, θ and ϕ in Fig. 3.1). The angular position means angular orientation of the body with respect to the inertial co-ordinate system *XYZ*.

Euler angles are the remaining three generalized co-ordinates describing the position of a rigid body. The angular position also rules the relation between the velocity components of Equation 3.1 expressed in two different frames.

In order to obtain this relation, let us rotate the inertial co-ordinate system to the orientation of the body-fixed system in the three subsequent stages as shown in Fig. 3.2.

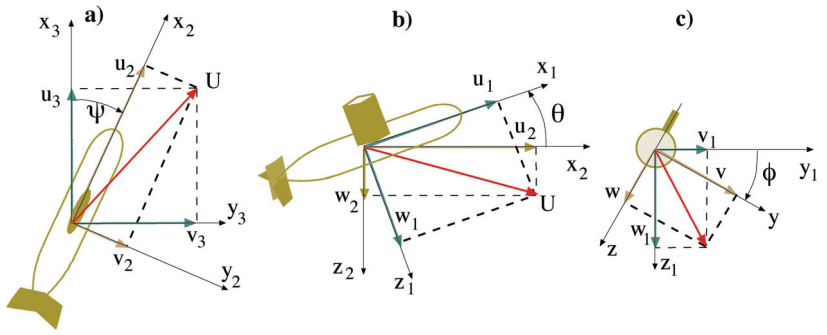

Fig. 3.2 Definition of the Euler angles as a sequence of three rotations. Figures (a), (b) and (c) are represented so that the rotation axes z, y and x are perpendicular to the plane of the paper.

We start with the co-ordinate system $x_3y_3z_3$ having the origin in the body's centre of gravity and the angular orientation the same as that of the inertial co-ordinate system XYZ. We rotate this system (see Fig. 3.2a) through the angle ψ about the axis z_3. As a result we get the co-ordinate system $x_2y_2z_2$. This angle is called the *yaw*.

The relation of the velocity components between these two co-ordinate systems can be expressed as follows (Fossen, 1994; Clayton&Bishop, 1982; Salonen, 1999).

$$\begin{Bmatrix} u_3 \\ v_3 \\ w_3 \end{Bmatrix} = \begin{bmatrix} \cos\psi & -\sin\psi & 0 \\ \sin\psi & \cos\psi & 0 \\ 0 & 0 & 1 \end{bmatrix} \begin{Bmatrix} u_2 \\ v_2 \\ w_2 \end{Bmatrix} \tag{3.2}$$

The subsequent rotations (*pitch* and *roll*) about the *y*- and *x*-axis respectively (see figures 3b and 3c) yield the transformations

$$\begin{Bmatrix} u_2 \\ v_2 \\ w_2 \end{Bmatrix} = \begin{bmatrix} \cos\theta & 0 & \sin\theta \\ 0 & 1 & 0 \\ -\sin\theta & 0 & \cos\theta \end{bmatrix} \begin{Bmatrix} u_1 \\ v_1 \\ w_1 \end{Bmatrix}$$
$$\begin{Bmatrix} u_1 \\ v_1 \\ w_1 \end{Bmatrix} = \begin{bmatrix} 1 & 0 & 0 \\ 0 & \cos\phi & -\sin\phi \\ 0 & \sin\phi & \cos\phi \end{bmatrix} \begin{Bmatrix} u \\ v \\ w \end{Bmatrix} \tag{3.3}$$

Combining (3.2) and (3.3) and noting that the velocity components in the $x_3y_3z_3$ co-ordinate system are the same as those of the *XYZ* inertial system, the one gets

$$\begin{Bmatrix} \dot{X}_G \\ \dot{Y}_G \\ \dot{Z}_G \end{Bmatrix} = \begin{bmatrix} \cos\psi\cos\theta & \cos\psi\sin\theta\sin\phi - \sin\psi\cos\phi & \cos\psi\sin\theta\cos\phi + \sin\psi\sin\phi \\ \sin\psi\cos\theta & \sin\psi\sin\theta\sin\phi + \cos\psi\cos\phi & \sin\psi\sin\theta\cos\phi - \cos\psi\sin\phi \\ -\sin\theta & +\cos\theta\sin\phi & \cos\theta\cos\phi \end{bmatrix} \begin{Bmatrix} u \\ v \\ w \end{Bmatrix} = \mathbf{T}_1(\gamma) \begin{Bmatrix} u \\ v \\ w \end{Bmatrix}. \tag{3.4}$$

with $\mathbf{T}_1$ being the transformation matrix from the body co-ordinate system to the inertial co-ordinate system. Transformation matrix is dependent upon the Euler angles (γ depicts the Euler angles).

Angular velocity $\boldsymbol{\Omega}$ of the ship in the body fixed co-ordinate system is

$$\boldsymbol{\Omega} = p\mathbf{i} + q\mathbf{j} + r\mathbf{k}, \tag{3.5}$$

where p, q and r are the respective x-, y- and z-directional components of the angular velocity. The dependence of the derivatives of the Euler angles and angular velocity components of (3.5) is as follows (Fossen, 1994; Clayton&Bishop, 1982)

$$\begin{Bmatrix} \dot{\phi} \\ \dot{\theta} \\ \dot{\psi} \end{Bmatrix} = \begin{bmatrix} 1 & \sin\phi\tan\theta & \cos\phi\tan\theta \\ 0 & \cos\phi & -\sin\phi \\ 0 & \sin\phi/\cos\theta & \cos\phi/\cos\theta \end{bmatrix} \begin{Bmatrix} p \\ q \\ r \end{Bmatrix} = \mathbf{T}_2(\gamma) \begin{Bmatrix} p \\ q \\ r \end{Bmatrix} \tag{3.6}$$

with $\mathbf{T}_2$ being the transformation matrix of the angular velocities in the body-fixed co-ordinate system to the angular velocities expressed using the Euler angles. This matrix is also dependent upon the Euler angles.

A shorter notation for a relation between the velocities expressed in two frames can be used:

$$\dot{\mathbf{X}} = \begin{bmatrix} \mathbf{T}_1(\gamma) & \mathbf{0}_{3\times3} \\ \mathbf{0}_{3\times3} & \mathbf{T}_2(\gamma) \end{bmatrix} \dot{\mathbf{x}} \tag{3.7}$$

where vector

$$\dot{\mathbf{X}} = \begin{Bmatrix} \mathbf{U} \\ \dot{\gamma} \end{Bmatrix} = \left\{ \dot{X}_G, \dot{Y}_G, \dot{Z}_G, \dot{\phi}, \dot{\theta}, \dot{\psi} \right\}^T \tag{3.8}$$

comprises both the velocity components in the Earth-fixed co-ordinate system and the time derivatives of the Euler angles. The matrices $\mathbf{0}_{3x3}$ are of a size three times three and they comprise zeros. Vector

$$\dot{\mathbf{x}} = \begin{Bmatrix} \mathbf{U} \\ \Omega \end{Bmatrix} = \left\{ u, v, w, p, q, r \right\}^T \tag{3.9}$$

comprises both the linear and the angular velocities in the moving body-fixed co-ordinate system.

4. General form of equations of motion

The general equations of motion of a rigid body can be described by two vector equations.

4.1 Equations of translational motion

The translational motion describing the motion of ship origin G stems from Newton's second law and is of the form

$$\mathbf{F} = \mathrm{m}\frac{\mathrm{d}\mathbf{U}}{\mathrm{d}t}, \tag{4.1}$$

where $\mathbf{F}$ is the vector of the external forces, m is the mass of a rigid body and $\mathbf{U}$ is the velocity of the centre of gravity of the body with respect to the inertial co-ordinate system. It is not easy to express external forces acting on a ship in the inertial *XYZ* co-ordinate system. It is easier and more logical to have them expressed in the co-ordinate system moving with the ship, that is, in the body-fixed system. Equation (4.1) expressed in the body-fixed co-ordinate system *xyz* is (Salonen, 1999)

$$\mathbf{F} = \frac{\delta}{\delta t}\left(\mathrm{m}\mathbf{U}\right) + \boldsymbol{\Omega} \times \mathrm{m}\mathbf{U}, \tag{4.2}$$

where $\delta/\delta t$ denotes the time derivative in the moving co-ordinate system. It is feasible to separate the gravity mg$\mathbf{K}$ and other forces *X*,*Y* and *Z* from the total force vector $\mathbf{F}$. Thus

$$\mathbf{F} = X\mathbf{i} + Y\mathbf{j} + Z\mathbf{k} + \mathrm{mg}\mathbf{K}. \tag{4.3}$$

Note that the reaction forces *X,Y* and *Z* are given in the body-fixed co-ordinate system *xyz*. With a separation of external forces presented above the vector equation (4.2) can be expressed in the component form as follows (Clayton&Bishop, 1982)

$$\begin{aligned} \mathrm{m}\left(\dot{u} + qw - rv\right) &= X - \mathrm{m}g\sin\theta \\ \mathrm{m}\left(\dot{v} + ru - pw\right) &= Y + \mathrm{m}g\cos\theta\sin\phi \\ \mathrm{m}\left(\dot{w} + pv - qu\right) &= Z + \mathrm{m}g\cos\theta\cos\phi. \end{aligned} \tag{4.4}$$

It is interesting to note that the angular motion of a ship causes nonlinear cross-coupling velocity terms to appear in the equations of a translational motion.

Sometimes it is more convenient to have the origin of the body-fixed co-ordinate system located somewhere else than at the centre of gravity. In ship dynamics this point may be located for instance at the intersection of three planes: the main frame, the centreplane and the waterplane. If we denote by $\mathbf{r}_G = x_G\mathbf{i} + y_G\mathbf{j} + z_G\mathbf{k}$ the position of the ship's centre of gravity in the new body fixed coordinate system, then the component equations of (4.2) appear as (Triantafyllou& Hover, 2003):

$$\begin{aligned} &\mathrm{m}\left[\dot{u} + qw - rv + \dot{q}z_G - \dot{r}y_G + \left(qy_G + rz_G\right)p - \left(q^2 + r^2\right)x_G\right] \\ &= X - \mathrm{m}g\sin\theta \\ &\mathrm{m}\left[\dot{v} + ru - pw + \dot{r}x_G - \dot{p}z_G + \left(rz_G + pz_G\right)q - \left(r^2 + p^2\right)y_G\right] \\ &= Y + \mathrm{m}g\cos\theta\sin\phi \\ &\mathrm{m}\left[\dot{w} + pv - qu + \dot{p}y_G - \dot{q}x_G + \left(px_G + qy_G\right)r - \left(p^2 + q^2\right)z_G\right] \\ &= Z + \mathrm{m}g\cos\theta\cos\phi. \end{aligned} \tag{4.4a}$$

Here, *u, v* and *w* are now the velocity components of the new origin.

4.2 Equations of angular motion

The angular motion is governed by the vector equation

$$\boldsymbol{G} = \frac{\mathrm{d}\boldsymbol{h}}{\mathrm{d}t} = \frac{\delta\boldsymbol{h}}{\delta t} + \boldsymbol{\Omega}\times\boldsymbol{h} \tag{4.5}$$

where $\boldsymbol{G} = K\mathbf{i} + M\mathbf{j} + N\mathbf{k}$ is the moment of external forces about the centre of gravity and $\mathbf{h}$ is the angular momentum given in the form

$$\mathbf{h} = \ddot{\mathbf{I}} \cdot \boldsymbol{\Omega} = \begin{bmatrix} I_x & -I_{xy} & -I_{xz} \\ -I_{yx} & I_y & -I_{yz} \\ -I_{zx} & -I_{zy} & I_z \end{bmatrix} \begin{Bmatrix} p \\ q \\ r \end{Bmatrix} \tag{4.6}$$

Matrix $\ddot{\mathbf{I}}$ comprises the elements of the mass moment of inertia of the body. If we assume that the considered body consists of N masses m_i, the definitions of the elements of matrix $\ddot{\mathbf{I}}$ are:

Diagonal terms	Cross-inertia terms
$I_x = \sum_{i=1}^{N} m_i \left(y_i^2 + z_i^2 \right)$	$I_{xy} = I_{yx} = \sum_{i=1}^{N} m_i x_i y_i$
$I_y = \sum_{i=1}^{N} m_i \left(x_i^2 + z_i^2 \right)$	$I_{xz} = I_{zx} = \sum_{i=1}^{N} m_i x_i z_i$
$I_z = \sum_{i=1}^{N} m_i \left(x_i^2 + y_i^2 \right)$	$I_{yz} = I_{zy} = \sum_{i=1}^{N} m_i y_i z_i .$

(4.7)

Equation (4.5) in the component form is (Clayton&Bishop, 1982)

$$\begin{aligned} &I_x \dot{p} - I_{xy} \dot{q} - I_{xz} \dot{r} + \left(I_z r - I_{zx} p - I_{zy} q \right) q - \left(I_y q - I_{yz} r - I_{yx} p \right) r = K \\ &I_y \dot{q} - I_{yx} \dot{p} - I_{yz} \dot{r} + \left(I_x p - I_{xy} q - I_{xz} r \right) r - \left(I_z r - I_{zx} p - I_{zy} q \right) p = M \\ &I_z \dot{r} - I_{zx} \dot{p} - I_{zy} \dot{q} + \left(I_y q - I_{yz} r - I_{yx} p \right) p - \left(I_x p - I_{xy} q - I_{xz} r \right) q = N. \end{aligned} \tag{4.8}$$

For the origin located off the ship's centre of gravity but with axes of a new co-ordinate system parallel to the original one, equations of the angular motion get somewhat more complicated form (Fossen, 1994):

$$
\begin{aligned}
&I_x\dot{p} - I_{xy}\dot{q} - I_{xz}\dot{r} + \left(I_z r - I_{zx}p - I_{zy}q\right)q - \left(I_y q - I_{yz}r - I_{yx}p\right)r \\
&+ m\left[y_G\left(\dot{w} - uq + vp\right) - z_G\left(\dot{v} - wp + ur\right)\right] = K \\
&I_y\dot{q} - I_{yx}\dot{p} - I_{yz}\dot{r} + \left(I_x p - I_{xy}q - I_{xz}r\right)r - \left(I_z r - I_{zx}p - I_{zy}q\right)p \\
&+ m\left[z_G\left(\dot{u} - vr + wq\right) - x_G\left(\dot{w} - uq + vp\right)\right] = M \\
&I_z\dot{r} - I_{zx}\dot{p} - I_{zy}\dot{q} + \left(I_y q - I_{yz}r - I_{yx}p\right)p - \left(I_x p - I_{xy}q - I_{xz}r\right)q \\
&+ m\left[x_G\left(\dot{v} - wp + ur\right) - y_G\left(\dot{u} - vr + wq\right)\right] = N.
\end{aligned}
\tag{4.9}
$$

Moreover, the elements of the mass moment of inertia of the body used in 4.9 are changed according to Steiner's rule as follows

$$
\begin{aligned}
I_x &= \left(I_x\right)_G + \mathrm{m}\left(y_G^2 + z_G^2\right) \\
I_y &= \left(I_y\right)_G + \mathrm{m}\left(x_G^2 + z_G^2\right) \\
I_z &= \left(I_z\right)_G + \mathrm{m}\left(x_G^2 + y_G^2\right) \\
I_{xy} &= \left(I_{xy}\right)_G + \mathrm{m}x_G y_G \\
I_{yz} &= \left(I_{yz}\right)_G + \mathrm{m}y_G z_G \\
I_{zx} &= \left(I_{zx}\right)_G + \mathrm{m}z_G x_G,
\end{aligned}
\tag{4.10}
$$

with the moment of inertia terms on RHS being defined by Equation 4.7 in the co-ordinate system having the origin in the Centre of Gravity *G*.

Equations (4.8) or (4.9) yield the angular motion of the body in terms of angular velocity components *p*, *q* and *r* expressed in the moving co-ordinate system *xyz*. These equations and expressions (4.4) are the final equations governing total rigid body motion in six degrees of freedom. In order to solve them we need to specify the external (fluid) forces *X,Y,Z* and moments *K,M,N* acting on a body. Moreover we use equations (3.4) and (3.6) to express body velocities in the inertial co-ordinate system. Numerical integration of these equations yields the instantaneous position and orientation of a ship in the inertial co-ordinate system *XYZ*.

The main problem of ship dynamics is not really in the equations of motion as such. The main issue is to construct the appropriate mathematical models describing the external (fluid) forces **F** and moments **G** caused by waves, by

the ship-to-water interaction or caused by other factors. Thus the problem is in hydrodynamics.

5. In-plane motion of a ship – manoeuvring

In plane motion approximation is commonly used when considering surface vessel's manoeuvring. Normally, only a still water condition (that is, no surface waves) is considered. The motion is restricted to three degrees of freedom, namely: surge (translation along the *x*-axis), sway (translation along the *y*-axis) and yaw (rotation around the *z*-axis). Heel is usually disregarded, although it may be important during manoeuvring. Moreover, the starboard-port symmetry of a ship is used. As a result, equations of motion reduce to the following set of three equations:

$$\begin{aligned} \mathrm{m}(\dot{u} - rv) &= X \\ \mathrm{m}(\dot{v} + ru) &= Y \\ I_z\dot{r} &= N. \end{aligned} \tag{5.1}$$

If the origin of the body-fixed co-ordination system is not located at the centre of gravity the equations of motion are of the somewhat more complex form (Triantafyllou&Hover, 2003)

$$\begin{aligned} \mathrm{m}\left(\dot{u} - rv - x_G r^2\right) &= X \\ \mathrm{m}\left(\dot{v} + ru + x_G\dot{r}\right) &= Y \\ I_z\dot{r} + \mathrm{m}x_G\left(\dot{v} + ur\right) &= N, \end{aligned} \tag{5.1a}$$

where x_G is the x co-ordinate value of the centre of gravity. Note that in the manoeuvring model, the origin of the body-fixed co-ordinate system is usually located at the mid-section of a ship. So the selected origin is denoted by the subscript 0. The moment of inertia I_z in Equation 5.1a is also defined

in the same co-ordinate system. If the moment of inertia related to the Centre-of-Gravity *G* is used, then the equations of motion are of the form

$$\begin{aligned} &\mathrm{m}\left(\dot{u} - rv - x_G r^2\right) = X \\ &\mathrm{m}\left(\dot{v} + ru + x_G \dot{r}\right) = Y \\ &\left(I_z + \mathrm{m}x_G^2\right)\dot{r} + \mathrm{m}x_G\left(\dot{v} + ur\right) = N. \end{aligned} \tag{5.1b}$$

5.1 Slow motion approximation for the hydrodynamic forces

The hydrodynamic forces *X, Y* and moment *N* consist mainly of the forces acting on the hull and of the forces generated by the control surfaces (rudders, propellers, etc.) of a vessel. In principle there are three basic models used in describing hull forces. In the manoeuvring theory, it is customary to use the so-called *slow motion derivatives* model for hull forces. This approach does not attempt to model the physics of the complicated flow over the manoeuvring hull. It is simply assumed that the forces are dependent upon the motion variables (*u*, *v* and *r*), their time derivatives, hull geometry and the rudder angle δ. The Taylor series expansion of forces is used. In detail, the following expression, illustrated with the aid of a two-variable function *f=f(x,y)*, is used:

$$\begin{aligned} f(h,k) &= f(0,0) + \frac{\partial f(0,0)}{\partial x}h + \frac{\partial f(0,0)}{\partial y}k \\ &+ \frac{1}{2}\left(\frac{\partial^2 f(0,0)}{\partial x^2}h^2 + 2\frac{\partial^2 f(0,0)}{\partial x \partial y}hk + \frac{\partial^2 f(0,0)}{\partial y^2}k^2\right) + \frac{1}{6}(.....) + R_3 \end{aligned} \tag{5.5}$$

5.2 Linear model of a ship's in-plane motion

The *x*-directional vessel velocity is decomposed into the initial constant *U* and the perturbed part *u* as follows:

$$\mathrm{u} := \mathrm{U} + \mathrm{u}, \text{ where } |\mathrm{u}| << \mathrm{U}. \tag{5.6}$$

Moreover, sway velocity is assumed to be much smaller than the forward ship speed that is $|v| << U$. Thus in the following *u* means the deviation from

the initial velocity U. The linear model of ship manoeuvring is obtained by dropping the nonlinear terms in the equations of motion (5.1a), as follows:

$$\begin{aligned} m\dot{u} &= X_{lin} \\ m\left(\dot{v} + Ur + x_G\dot{r}\right) &= Y_{lin} \\ I_z\dot{r} + mx_G\left(\dot{v} + Ur\right) &= N_{lin}, \end{aligned} \tag{5.7}$$

In general, the linear approximations of X, Y and N are:

$$\begin{aligned} X_{lin} &= X_{\dot{u}}\dot{u} + X_u u + X_{\dot{v}}\dot{v} + X_v v + X_{\dot{r}}\dot{r} + X_r r + X_\delta\delta \\ Y_{lin} &= Y_{\dot{u}}\dot{u} + Y_u u + Y_{\dot{v}}\dot{v} + Y_v v + Y_{\dot{r}}\dot{r} + Y_r r + Y_\delta\delta \\ N_{lin} &= N_{\dot{u}}\dot{u} + N_u u + N_{\dot{v}}\dot{v} + N_v v + N_{\dot{r}}\dot{r} + N_r r + N_\delta\delta. \end{aligned} \tag{5.8}$$

In (5.8), the so-called *hydrodynamic derivatives* are used, as in the following example

$$X_{\dot{u}} \equiv \frac{\partial X}{\partial \dot{u}}, Y_u \equiv \frac{\partial Y}{\partial u}, Y_{\dot{u}} \equiv \frac{\partial Y}{\partial \dot{u}}, etc$$

and δ is the rudder angle.

As a result the following set of three linear equations of motions is obtained:

$$\begin{aligned} \left(X_{\dot{u}} - m\right)\dot{u} + X_u u + X_{\dot{v}}\dot{v} + X_v v + X_{\dot{r}} + X_r r + X_\delta\delta &= 0 \\ Y_{\dot{u}}\dot{u} + Y_u u + \left(Y_{\dot{v}} - m\right)\dot{v} + Y_v v + \left(Y_{\dot{r}} - mx_G\right)\dot{r} + \left(Y_r - mU\right)r + Y_\delta\delta &= 0 \\ N_{\dot{u}}\dot{u} + N_u u + \left(N_{\dot{v}} - mx_G\right)\dot{v} + N_v v + \left(N_{\dot{r}} - I_z\right)\dot{r} + \left(N_r - mx_G U\right)r + N_\delta\delta &= 0. \end{aligned} \tag{5.9}$$

The terms

$$-X_{\dot{u}}, -Y_{\dot{v}} \text{ and } -N_{\dot{r}} \tag{5.10}$$

are known as *added masses*. The name stems from the fact that accelerating the body entrained by the fluid requires a larger force than the corresponding force needed to achieve the same acceleration in the vacuum or in a gas. Thus the effect of the fluid entraining the accelerated body is the same as that of the mass of a body. This means that in a sense the surrounding fluid increases the mass of a body by an amount called *added*

mass. Added masses and moments of inertia of the typical ship shapes have positive values of the same order of magnitude as the corresponding ship's quantities. More on this subject is dealt with in Section 6.3.

The terms

$$X_{\dot{v}}, X_v, X_{\dot{r}} \text{ and } X_r$$

depict the influence of sway and yaw motion on the *x*-directional force acting on a hull. This influence is usually disregarded. Also the effect of rudder deflection on the ship resistance is in most cases not taken into account, i.e. X_δ=0. The effect of surge motion on sway force Y and yaw moment N are usually disregarded as well, that is:

$$Y_{\dot{u}} = Y_u = N_{\dot{u}} = N_u = 0.$$

Next, let us examine the nature of the remaining terms:

$$X_u, Y_r, Y_v, N_v, N_r, Y_\delta \text{ and } N_\delta . \qquad (5.11)$$

The first of these, X_u multiplied by the velocity change u, gives the change in the force component X. Ship resistance, which is a negative force component X, increases with ship speed. Thus X_u has to be negative. The physical meanings of the other terms are explained with the aid of Figure 5.1.

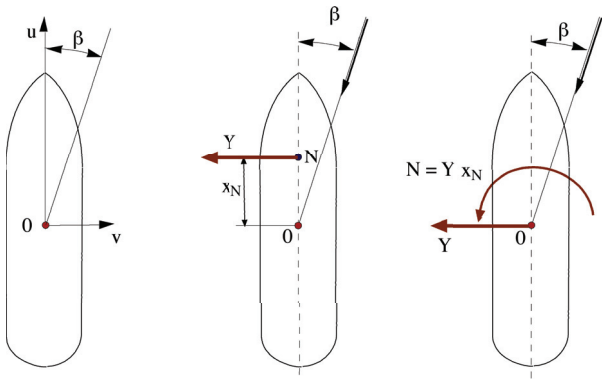

Fig. 5.1 Forces acting on a ship in an oblique flow.

Apart from the bow-wards oriented velocity u, if a ship also has y-directional velocity v, the inflow to the hull resembles the flow over a low aspect ratio airfoil set at angle of attack β. Angle β is actually a drift angle of the ship. As a result of an oblique flow, a negative side force Y develops. This force acts normally at some point N located between the stem (extreme bow) and mid-ship. Moving this force to the origin 0 results in a yawing moment, $N = Y x_N$. It is clear from Figure 5.1 that for the positive v-motion of a ship, both the side force Y and the yaw moment N are negative. Thus both terms Y_v and N_v have to be negative, too. For a positive pure yaw motion the opposing yaw moment also has to be negative. Thus the term N_r has to be negative, too. It is not possible to give a general conclusion about the sign of Y_r in this situation.

5.3 Straight line stability

Next we consider a ship represented by a linear manoeuvring model (5.9) and with the rudder fixed to the neutral positional; that is, the following equations have to be considered

$$\begin{aligned} \left(Y_{\dot v} - \mathrm{m}\right)\dot v + Y_v v + \left(Y_{\dot r} - mx_G\right)\dot r + \left(Y_r - mU\right)r &= 0 \\ \left(N_{\dot v} - \mathrm{m}x_G\right)\dot v + N_v v + \left(N_{\dot r} - I_z\right)\dot r + \left(N_r - mx_G U\right)r &= 0. \end{aligned} \tag{5.12}$$

The surge equation was dropped because in the linear form it does not affect other equations. As a result two linear homogeneous differential equations (5.12) of the first order were obtained. These can be presented in matrix form as follows:

$$\begin{bmatrix} Y_{\dot v} - \mathrm{m} & Y_{\dot r} - mx_G \\ N_{\dot v} - \mathrm{m}x_G & N_{\dot r} - I_z \end{bmatrix} \begin{Bmatrix} \dot v \\ \dot r \end{Bmatrix} = \begin{bmatrix} -Y_v & mU - Y_r \\ -N_v & mx_G U - N_r \end{bmatrix} \begin{Bmatrix} v \\ r \end{Bmatrix} \tag{5.13}$$

or in a phase plane (v, r) as

$$\begin{aligned} \dot v &= a_{11} v + a_{12} r \\ \dot r &= a_{21} v + a_{22} r, \end{aligned} \tag{5.14}$$

where the a_{ij} coefficients are:

$$
\begin{aligned}
a_{11} &= \frac{\left(I_z - N_{\dot r}\right)Y_v + \left(Y_{\dot r} - mx_G\right)N_v}{\left(m - Y_{\dot v}\right)\left(I_z - N_{\dot r}\right) - \left(mx_G - Y_{\dot r}\right)\left(mx_G - N_{\dot v}\right)} \\
a_{12} &= \frac{-\left(I_z - N_{\dot r}\right)\left(mU - Y_r\right) - \left(Y_{\dot r} - mx_G\right)\left(mx_G U - N_r\right)}{\left(m - Y_{\dot v}\right)\left(I_z - N_{\dot r}\right) - \left(mx_G - Y_{\dot r}\right)\left(mx_G - N_{\dot v}\right)} \\
a_{21} &= \frac{\left(N_{\dot v} - \mathrm{m}x_G\right)Y_v + \left(m - Y_{\dot v}\right)N_v}{\left(m - Y_{\dot v}\right)\left(I_z - N_{\dot r}\right) - \left(mx_G - Y_{\dot r}\right)\left(mx_G - N_{\dot v}\right)} \\
a_{22} &= \frac{-\left(N_{\dot v} - \mathrm{m}x_G\right)\left(mU - Y_r\right) - \left(m - Y_{\dot v}\right)\left(mx_G U - N_r\right)}{\left(m - Y_{\dot v}\right)\left(I_z - N_{\dot r}\right) - \left(mx_G - Y_{\dot r}\right)\left(mx_G - N_{\dot v}\right)}.
\end{aligned}
\tag{5.15}
$$

Differentiating the first of the equations (5.14) yields:

$$
\ddot v = a_{11}\dot v + a_{12}\dot r\,. \tag{5.16}
$$

Moreover, the first of the equations (5.14) can be written as

$$
a_{12} r = \dot v - a_{11} v\,. \tag{5.14c}
$$

Substituting into the equation (5.16) the second of the equations (5.14) and equation (5.14c) as follows

$$
\begin{aligned}
\ddot v &= a_{11}\dot v + a_{12}\dot r = a_{11}\dot v + a_{12}\left[a_{21} v + a_{22}\frac{1}{a_{12}}\left(\dot v - a_{11} v\right)\right] \\
&= a_{11}\dot v + a_{12}a_{21} v + a_{22}\dot v - a_{22}a_{11} v
\end{aligned}
\tag{5.17}
$$

yields a homogeneous linear ordinary differential equation

$$
\ddot v - \left(a_{11} + a_{22}\right)\dot v + \left(a_{11}a_{22} - a_{12}a_{21}\right)v = 0 \tag{5.17a}
$$

having solutions of the form $e^{\lambda t}$ or $te^{\lambda t}$, where t is time and λ is a characteristic value. As a result, the sway equation can be presented as the characteristic equation

$$
\lambda^2 - \left(a_{11} + a_{22}\right)\lambda + a_{11}a_{22} - a_{12}a_{21} = 0 \tag{5.18}
$$

The solution of the sway equation (5.17a) is stable if the real valued roots λ_1 and λ_2 of the characteristic equation (5.18) are negative. If roots λ are complex values then their real part has to be negative in order to insure the straight line stability. This requires that the following holds (Kreyszig, 1993)

$$\begin{aligned} -a_{11} - a_{22} &> 0 \\ a_{11}a_{22} - a_{12}a_{21} &> 0. \end{aligned} \tag{5.19}$$

The first condition of the straight line stability is obtained using the first of the conditions (5.19), the definitions (5.15) of the constants a_{11} and a_{22} and assuming that the mass centre is close to the geometrical centre, i.e. $x_G \approx 0$. Moreover, the coupling terms

$$Y_{\dot{r}}, Y_r, N_{\dot{v}} \text{ and } N_v$$

are small when compared to the other terms. As the terms $Y_{\dot{v}} \approx -m, N_{\dot{r}} \approx -I_z$, the common denominator of equations (5.15) is positive and thus can be disregarded. The terms depicting drag (Y_v and N_r) are both large negative values. As a result the following terms:

$$\begin{aligned} a_{11} &= \frac{Y_v}{m - Y_{\dot{v}}} < 0 \\ a_{22} &= \frac{N_r}{I_z - N_{\dot{r}}} < 0 \end{aligned} \tag{5.20}$$

and the first of the stability conditions (5.19) are fulfilled. The second of the conditions (5.19) results in the following

$$
\begin{aligned}
&\left[\left(I_z - N_{\dot r}\right)Y_v + \left(Y_{\dot r} - mx_G\right)N_v\right]\left[-\left(N_{\dot v} - mx_G\right)\left(mU - Y_r\right) - \left(m - Y_{\dot v}\right)\left(mx_G U - N_r\right)\right] \\
&+\left[\left(I_z - N_{\dot r}\right)\left(mU - Y_r\right) + \left(Y_{\dot r} - mx_G\right)\left(mx_G U - N_r\right)\right]\left[\left(N_{\dot v} - mx_G\right)Y_v + \left(m - Y_{\dot v}\right)N_v\right] \\
&= -\left(I_z - N_{\dot r}\right)Y_v\left(N_{\dot v} - mx_G\right)\left(mU - Y_r\right) + \left(I_z - N_{\dot r}\right)\left(mU - Y_r\right)\left(N_{\dot v} - mx_G\right)Y_v \\
&-\left(I_z - N_{\dot r}\right)Y_v\left(m - Y_{\dot v}\right)\left(mx_G U - N_r\right) + \left(I_z - N_{\dot r}\right)\left(mU - Y_r\right)\left(m - Y_{\dot v}\right)N_v \\
&-\left(Y_{\dot r} - mx_G\right)N_v\left(N_{\dot v} - \mathrm{m}x_G\right)\left(mU - Y_r\right) + \left(Y_{\dot r} - mx_G\right)\left(mx_G U - N_r\right)\left(N_{\dot v} - mx_G\right)Y_v \\
&-\left(Y_{\dot r} - mx_G\right)N_v\left(m - Y_{\dot v}\right)\left(mx_G U - N_r\right) + \left(Y_{\dot r} - mx_G\right)\left(mx_G U - N_r\right)\left(m - Y_{\dot v}\right)N_v \\
&= \left(I_z - N_{\dot r}\right)\left(m - Y_{\dot v}\right)\left[Y_v\left(N_r - mx_G U\right) + \left(mU - Y_r\right)N_v\right] \\
&-\left(Y_{\dot r} - mx_G\right)\left(N_{\dot v} - mx_G\right)\left[Y_v\left(N_r - mx_G U\right) + \left(mU - Y_r\right)N_v\right] > 0.
\end{aligned}
\tag{5.21}
$$

The first part of the expression (5.21) is obviously much bigger than the second one because

$$\left(I_z - N_{\dot r}\right)\left(m - Y_{\dot v}\right) >> \left(Y_{\dot r} - mx_G\right)\left(N_{\dot v} - \mathrm{m}x_G\right)$$

As the term

$$\left(I_z - N_{\dot r}\right)\left(m - Y_{\dot v}\right)$$

is positive and large, the second condition of straight line stability can be simplified by

$$Y_v\left(N_r - mx_G U\right) + \left(mU - Y_r\right)N_v > 0. \tag{5.22}$$

The expression (5.22) is called the vessels stability criterion. If the ship's centre of gravity G is located very close to mid-ship then $x_G \approx 0$ and the second stability condition simplifies further to

$$Y_v N_r + \left(mU - Y_r\right)N_v > 0. \tag{5.23}$$

As already stated, Y_v and N_r are both large negative values so their product is positive. From (5.22) we can see that locating the centre of gravity bow-wards of mid-ship (which means that $x_G > 0$) increases directional stability. The term N_v is usually negative. The surface area aft in a form of the keel or projected hull area increases N_v, improving the directional stability.

5.4 Non-linear model of ship maneuvering

When expressing the external forces dependent upon the motion variables, the expansion factorials (1/2 and 1/6) of (5.5) are usually dropped. It is assumed that the external hull forces are independent of the initial speed U. Moreover, the symmetry properties are used. These for the X, that is for the x-directional force component mean that it is (Triantafyllou et al, 2004):

a. a symmetric function of v when r=0 and δ=0, that is

$X(u,v,r = 0, \delta=0) = X(u,-v,r = 0, \delta=0)$ and $X_{vvv}=0$.

b. a symmetric function of r when v=0 and δ=0,

c. a symmetric function of δ when v=0 and r=0.

Thus as a result this force can be expressed as follows:

$$\begin{aligned} X = {} & X_{\dot{u}}\dot{u} + X_u u + X_{uu}u^2 + X_{uuu}u^3 + X_{vv}v^2 + X_{rr}r^2 + X_{\delta\delta}\delta^2 \\ & + X_{vr}vr + X_{v\delta}v\delta + X_{r\delta}r\delta + X_{vvu}v^2u + X_{rru}r^2u + X_{\delta\delta u}\delta^2 u \\ & + X_{r\delta u}r\delta u + X_{rvu}rvu + X_{v\delta u}v\delta u + X_{r\delta v}r\delta v. \end{aligned} \tag{5.24}$$

In the case of the Y-force, hull symmetry implies that it has to be anti-symmetric in respect to v when $r=\delta=0$; and likewise for r and δ, i.e. (Triantafyllou et al, 2004) and thus for instance

$Y(u,v,r = 0, \delta=0) = -Y(u,-v,r = 0, \delta =0)$. The even derivatives of Y in respect to v, r and δ must be zero, that is:

$$Y_{vv} = 0,\ Y_{vvu} = 0,\ Y_{rr} = 0,\ Y_{rru} = 0,\ Y_{rru} = 0,\ Y_{\delta\delta} = 0, Y_{\delta\delta u} = 0. \tag{5.25}$$

As a result the following expression for the Y-force is obtained:

$$\begin{aligned} Y = {} & Y_{uu}u^2 + Y_{\dot{v}}\dot{v} + Y_{\dot{r}}\dot{r} + Y_v v + Y_r r + Y_\delta \delta + Y_{\delta u}\delta u + Y_{vu}vu + Y_{ru}ru + Y_{vuu}vu^2 \\ & + Y_{ruu}ru^2 + Y_{\delta uu}\delta u^2 + Y_{vvv}v^3 + Y_{rrr}r^3 + Y_{\delta\delta\delta}\delta^3 + Y_{rr\delta}r^2\delta + Y_{vrr}vr^2 \\ & + Y_{rvv}rv^2 + Y_{\delta vv}\delta v^2 + Y_{vr\delta}vr\delta + Y_{\delta\delta r}\delta^2 r + Y_{\delta\delta v}\delta^2 v. \end{aligned} \tag{5.26}$$

Following the same reasoning of the anti-symmetric form of the fluid moment *N*, the following expression is obtained:

$$\begin{aligned} N = {} & N_{uu}u^2 + N_{\dot{v}}\dot{v} + N_{\dot{r}}\dot{r} + N_v v + N_r r + N_\delta \delta + N_{\delta u}\delta u + N_{vu}vu + N_{ru}ru \\ & + N_{vuu}vu^2 + N_{ruu}ru^2 + N_{\delta uu}\delta u^2 + N_{vvv}v^3 + N_{rrr}r^3 + N_{\delta\delta\delta}\delta^3 \\ & + N_{rr\delta}r^2\delta + N_{vrr}vr^2 + N_{rvv}rv^2 + N_{\delta v}\delta v^2 + N_{r\delta}vr\delta + N_{\delta\delta r}\delta^2 r + N_{\delta\delta v}\delta^2 v. \end{aligned} \tag{5.27}$$

The *X, Y* and *N* terms marked with the subscripts are called slow motion derivatives. The indices of them depict the variable they apply to.

5.5 Non-dimensional form of the maneuvering equations

It is very common to use the equation of motions (5.1) in a non-dimensional form. In principle, the same equations and non-dimensional coefficients of them apply for ships of different sizes, and their models provided the geometrical form and mass properties are in scale. The variables in equations (5.1) are made non-dimensional as follows:

$$\begin{aligned} & u' = u/U, v' = v/U, \\ & \dot{u}' = \frac{\dot{u}L}{U^2}, \dot{v}' = \frac{\dot{v}L}{U^2}, \\ & r' = \frac{rL}{U}, \dot{r}' = \frac{\dot{r}L^2}{U^2}, \end{aligned} \tag{5.28}$$

where *L* is the ship length between perpendiculars. The remaining terms in (5.1) are made non-dimensional according to the so-called *'prime'* system as follows:

$$\begin{aligned} & m' = \frac{m}{\frac{\rho}{2}L^3}, I'_z = \frac{I_z}{\frac{\rho}{2}L^5} \\ & X' = \frac{X}{\frac{\rho}{2}L^2U^2}, Y' = \frac{Y}{\frac{\rho}{2}L^2U^2}, N' = \frac{N}{\frac{\rho}{2}L^3U^2}. \end{aligned} \tag{5.29}$$

As a result, with the origin located in the centre of gravity G, we obtain the non-dimensional form of the equations of motion:

$$
\begin{aligned}
m'\left(\dot{u}' - r'v'\right) &= X' \\
m'\left(\dot{v}' + r'u'\right) &= Y' \\
I'_z \dot{r}' &= N'.
\end{aligned}
\tag{5.30}
$$

The same equations are obtained using instead of L^2 a product of ship length and draft T that is LT. In the so-called *'bis'* system mass properties and forces are made non-dimensional using the actual ship mass $\rho\nabla$, with ρ being water density and ∇ being volumetric displacement.

5.6 Determination of the slow motion hydrodynamic derivatives

The knowledge of the hydrodynamic derivatives is crucial for a successful prediction of ship's manoeuvring. A normal approach in evaluating them relies on dedicated captive model tests. These are:

Straight-line test with a model set at a certain drift.

The so-called rotating arm test.

Planar motion mechanism tests (*PMM*).

In these tests, the model is set at a certain steady position or forced to conduct a prescribed regular (sinusoidal) motion. Propeller loading and rudder angle may belong to the varied parameters as well. Knowing these and measuring the forces acting on the model hull makes it possible to evaluate a set of hydrodynamic derivatives. The tests are tedious and require many test runs.

Last years' rapid development of Computational Fluid Dynamics (*CFD*) in evaluating the flows over the ships' hulls also makes possible (in principle) a numerical evaluation of the forces acting on the hull in a slow three-dimensional motion. However, for the time being, this approach is very limited and it is not used on a routine basis.

Tests with free-running radio-controlled models and sea-trial full-scale tests are sometimes used to evaluate some of the hydrodynamic derivatives with the aid of system identification techniques.

Regression analysis conducted using the experimentally (model tests) obtained data gives a first approximation of the linear hydrodynamic derivatives as a function of principal dimensions (Brix, 1993):

$$
\begin{aligned}
Y'_{\dot{v}'} &= -\pi (T/L)^2 \left[1 + 0.16 C_B B/T - 5.1 (B/L)^2 \right] \\
Y'_{\dot{r}'} &= -\pi (T/L)^2 \left[0.67 B/L - 0.00033 (B/T)^2 \right] \\
N'_{\dot{v}'} &= -\pi (T/L)^2 \left[1.1 B/L - 0.0003341 B/T \right] \\
N'_{\dot{r}'} &= -\pi (T/L)^2 \left[1/12 + 0.017 C_B B/T - 0.33 B/L \right] \\
Y'_{v'} &= -\pi (T/L)^2 \left(1 + 0.4 C_B B/T \right) \\
Y'_{r'} &= -\pi (T/L)^2 \left(-1/2 + 2.2 B/L - 0.08 B/T \right) \\
N'_{v'} &= -\pi (T/L)^2 \left(1/2 + 2.4 T/L \right) \\
N'_{r'} &= -\pi (T/L)^2 \left(1/4 + 0.039 B/T - 0.56 B/L \right),
\end{aligned}
\tag{5.31}
$$

where C_B is the volumetric block coefficient. The expressions (5.31) represent the linear approximation to the hull derivatives in the body-fixed co-ordinate system with the origin located at the mid-section. Formulas (5.31) are not very accurate ones. They can be used as such when evaluating stability derivatives for a new-building and can be applied when evaluating the effect of ship's main dimensions on the hydrodynamic derivatives. In other words, if we have the derivatives for a certain ship and want to use this knowledge for a similar ship, with a slightly changed main dimensions, we can use the above given expressions. Expressions 5.31 are derived for a ship with an even keel. For ships with trim t (positive bow up), correction factors to be applied to the linear even-keel velocity coefficients are (Brix, 1993):

$$
\begin{aligned}
Y'_{v'}(t) &= Y'_{v'} \left(1 + 0.67 t/T \right) \\
Y'_{r'}(t) &= Y'_{r'} \left(1 + 0.80 t/T \right) \\
N'_{v'}(t) &= N'_{v'} \left[1 - 0.27 (t/T) Y'_{v'} / N'_{v'} \right] \\
N'_{r'}(t) &= N'_{r'} \left(1 + 0.30 t/T \right).
\end{aligned}
\tag{5.32}
$$

Another model of hull forces, which is particularly suitable for a drifting vessel, is based on the so-called cross-flow resistance concept (Bertram, 2000). In this model the resistance per unit ship length is evaluated by $0.5 \rho T_x v_x^2 C_D$, where subscript x depicts the longitudinal position of a ship

section, and T_x and v_x are the draft and transverse velocity at this section respectively. The latter is given by $v_x = v + xr$. The forces and moments exerted on the hull due to the cross-flow resistance can be obtained by the integration of the sectional contributors as follows (Bertram, 2000)

$$\begin{Bmatrix} X \\ Y \\ K \\ N \end{Bmatrix} = \frac{1}{2}\rho \int_L \begin{Bmatrix} 0 \\ -1 \\ z_D \\ -x \end{Bmatrix} (v + xr)|v + xr| T_x C_D dx, \tag{5.33}$$

where z_D is the z coordinate (measured downward from the centre of gravity G of ship's mass m) of the action line of the cross-flow resistance. For typical cargo ship hull forms, this force acts about 65% of the draft above the keel line (Bertram, 2000). Thus a constant (mean) value over ship length of:

$$z_D = z_G - 0.65T. \tag{5.34}$$

Note that the above model makes allowance for roll as a degree of freedom in the manoeuvring simulation.

5.7 Ship resistance and propeller thrust

There are two ways to model ship resistance and propulsor action. The simplest way is to assume that resistance and thrust are of the same magnitude and do not change. If there is a change in a ship's speed during the manoeuvres, it is caused by the cross-coupling term *r'v'* of Equation 5.30 and by Equation 5.24. Another model, the modular model, takes into account the resistance with an operating propeller using the following formula

$$X_{\text{resistance}} = -R_T/(1-t) = -0.5\rho u^2 S C_T/(1-t) \tag{5.33}$$

where R_T is total resistance and C_T its coefficient, ρ water density, S wetted surface of ship hull, t thrust deduction factor, and u depicts the ship's velocity in x-direction. The total resistance coefficient C_T can be given in tabular form as a function of a Froude number.

5.7.1 Hull resistance

If there is no information on the resistance coefficient available but propulsion power P_D at a certain speed is known, the following way of evaluating the resistance can be used. The relation between the propulsion power and the resistance

$$P_D = P_E / \eta_D = R_T V / \eta_D \tag{5.36}$$

is used, yielding

$$R_T = P_D \eta_D / V \tag{5.37}$$

where the propulsive efficiency (Matusiak, 1993) is given by a product of open water, rotational and hull efficiencies i.e.

$$\eta_D = \eta_0 \eta_R \eta_H = \eta_0 \eta_R \frac{1-t}{1-w}. \tag{5.38}$$

If there is no better data available, the following can be assumed. The open water and the rotational efficiencies of the propeller are assumed to be η_0=0.65 and η_R=1 respectively. The wake coefficient w and thrust deduction factor t can be assumed to be as presented in Table 5.1 below

Table 5.1 Approximate values of the propulsion coefficients.

	Single screw vessel	Multi-screw vessel
Wake fraction w	0.25	0.05
Thrust deduction factor t	0.25	0.15

For small variations of forward speed u, ship's resistance can be evaluated using the expression 5.35 with the assumption of constant resistance coefficient C_T. If large ship speed variations are investigated than the

resistance coefficient as a function of speed or Froude number should be used instead.

5.7.2 Propeller thrust

There are two simple models representing the thrust developed by a propeller. The first one is appropriate for a fixed pitch propeller. Total thrust is evaluated from a known open water characteristic of the propeller (K_T-J curve) as follows

$$X_{\text{prop}} = Z\rho n^2 D^4 K_{\text{T}} \tag{5.39}$$

where Z is the number of propellers, n is the propeller revolutions per second, and D is the propeller's diameter. The initial value of propeller revolutions should be adjusted so that a desired ship velocity is obtained for the condition of still water and constant forward speed with no drift angle. In other words the propeller revolutions should be derived from the condition $X_{\text{prop}} = -X_{\text{resistance}}$. Depending on the type of propulsion machinery, the revolutions are kept constant or adjusted to keep the advance coefficient $J=V(1-w)/(nD)$ constant.

For the controllable pitch propellers ("CPP"), the following simplifying procedure can be used. The assumption of constant delivered power and constant propulsive efficiency is made. The latter implies good control of propeller pitch and disregards the efficiency losses for the off-design operational conditions (approx. 10%). The above assumptions and Equation (5.37) result in the following relation of thrust X_{prop} and ship's speed

$$X_{prop} = \frac{P_D \eta_0 \eta_R}{V(1-w)}. \tag{5.40}$$

The relation 5.40 may lead to unrealistically high thrust values at low speeds. The limiting value is known as the *bollard pull*.

5.7.3 Bollard pull estimate

The bollard pull of the propeller can be derived from the theory of ideal propulsor (Matusiak, 1993). In this theory, the thrust developed by a stationary propeller is given by

$$T = \frac{1}{2}\rho A_0 U_{A0}^2 = \frac{1}{2}\rho \frac{\pi D^2}{4} U_{A0}^2, \tag{5.41}$$

where U_{A0} is the flow velocity induced by the propeller far downstream. The propulsion power is related to U_{A0}^2 by the following formula

$$P_D = \frac{1}{4}\rho A_0 U_{A0}^3 = \frac{1}{16}\rho \pi D^2 U_{A0}^3. \tag{5.42}$$

Solving the induced velocity U_{A0} from formula 5.42 yields

$$U_{A0} = \left(\frac{16 P_D}{\rho \pi D^2}\right)^{1/3}, \tag{5.43}$$

which substituted into the thrust expression 5.41 yields the bollard pull that is the maximum attainable thrust

$$T = \frac{1}{2}\rho \frac{\pi D^2}{4}\left(\frac{16 P_D}{\rho \pi D^2}\right)^{2/3} = \frac{\sqrt[3]{\pi\rho}}{\sqrt{2}}\left(P_D D\right)^{2/3}. \tag{5.44}$$

Alternatively for an open propeller (no duct), the semi-empirical expression

$$T = 7.8\left(P_D D\right)^{2/3} \tag{5.45}$$

can be used when evaluating the maximum thrust delivered by the propeller.

5.8 Rudder action

The effect of a rudder on the forces acting on a ship is shown in Fig. 5.2. A rudder set at angle δ develops a positive y-directional force, which when approximated by a linear model is

$$Y_R = Y_\delta \delta. \tag{5.46}$$

As this force acts at a ship's stern, approximately half a length astern from the origin *0*, a negative turning moment $N_\delta \delta$ develops as well. This moment causes the ship to turn and sets it at a certain drift angle β. The turning motion initiated by the rudder is greatly amplified by the turning moment $N_v v$ developed by a hull set in the inclined flow. (See Fig. 5.2)

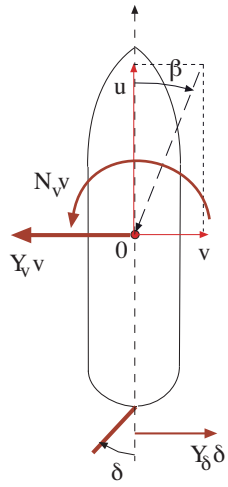

Fig. 5.2 Rudder causing a ship to turn.

The rudder forces may be modelled in two different ways. The first one is through a direct representation of the hull forces as dependent on the rudder angle as presented in equations 5.24-27. Another, more sophisticated model, called a modular one, attempts to use a mathematical model of the flow at the rudder. This one is presented in the following.

5.8.1 Kinematics of the inflow into rudder

It is important to note that the rudder angle and the angle at which the flow enters the rudder, the angle of attack, are not the same. Both the inflow velocity and the angle of attack are affected by the yaw and sway motion of the ship. If the rudder is located in the propeller slipstream this will also affect the inflow. Inflow to the rudder may be also changed significantly due to the flow velocity in the surface wave. Thus the rudder force model given by expression (5.46) can be regarded as a first linear approximation.

In order to evaluate rudder forces the flow velocities at the rudder location have to be evaluated first. A definition of the positive rudder angle is presented in Fig. 5.2 along with the definition of rudder forces.

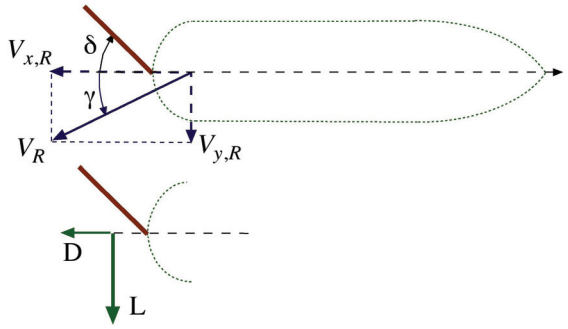

Fig. 5.3 Flow velocities at rudder.

Flow velocities at the rudder can be expressed as follows

$$\begin{Bmatrix} V_{x,R} \\ V_{y,R} \\ V_{z,R} \end{Bmatrix} = \begin{Bmatrix} V_x - V_{x,wave} \\ -v + V_{y,wave} \\ -w + V_{z,wave} \end{Bmatrix} - \begin{bmatrix} -i & j & k \\ p & q & r \\ x_R & y_R & z_R \end{bmatrix}, \tag{5.47}$$

or explicitly as

$$\begin{aligned} V_{x,R} &= V_x - V_{x,wave} + qz_R - ry_R \\ V_{y,R} &= -v + V_{y,wave} - rx_R + pz_R \\ V_{z,R} &= -w + V_{z,wave} - py_R + qx_R, \end{aligned} \tag{5.48}$$

where V_x is the x-component of flow velocity in the slipstream of propeller. This velocity can be evaluated as $V_x = u/(1-w)$ knowing ship instantaneous speed u and wake fraction w. Terms with subscript *wave* depict flow velocities due to the wave action (Eq. 5.48). $(x_R y_R z_R)$ depicts the rudder position in the body-fixed co-ordinate system. Note that the wave action is seldom included in the manoeuvring modelling. It is included here for the sake of completeness of the problem.

It is seen from Figure 5.3 that the effect of ship motion and the wave motion is to change the angle of attack of the rudder by the amount

$$\gamma = \arctan\left(V_{y,R} / V_{x,R}\right) \tag{5.49}$$

so that the total angle of attack is $\alpha=\delta+\gamma$.

Rudder forces are evaluated according to Söding (1982) and Brix (1993). Lift L and drag D forces are given by

$$L = \frac{1}{2}\rho C_L A_R V_R^2,\ D = \frac{1}{2}\rho C_D A_R V_R^2, \tag{5.50}$$

where lift coefficient is given by

$$C_{\mathrm{L}} = \frac{2\pi\Lambda\left(\Lambda+1\right)}{\left(\Lambda+2\right)^2}\sin\left(\delta+\gamma\right), \tag{5.51}$$

Here, $\Lambda = b^2/A_{\mathrm{R}}$ is the aspect ratio, where b denotes the rudder length. Note that the rudder area is not a wetted area. It is defined as a projected area of the side view of the rudder. The drag coefficient of the rudder is given by

$$C_{\mathrm{D}} = 1.1\frac{C_{\mathrm{L}}^2}{\pi\Lambda} + C_{\mathrm{D0}}, \tag{5.52}$$

where C_{D0} is the viscous drag coefficient. It can evaluated according to ITTC-57 frictional resistance coefficient as follows

$$C_{\mathrm{D0}} = 2.5C_{\mathrm{F}} = 2.5\frac{0.075}{\left(\log Rn - 2\right)^2}, \tag{5.53}$$

where Reynold's number is defined as

$$Rn = \frac{V_{\mathrm{rudder}}c}{\nu}, \tag{5.54}$$

with c being the mean value of the rudder chord and ν being the kinematic viscosity coefficient.

5.8.2 The effect of propeller action on the rudder flow

A rudder operates usually in the propeller slipstream. As a result, the forces developed by a rudder are substantially higher than the ones generated by a rudder placed outside the slipstream. The flow velocity in the propeller slipstream can be evaluated as follows.

According to the potential flow theory and considering the momentum conservation (ideal propulsor model), the mean axial flow velocity far downstream of the propeller is (Matusiak, 2005)

$$V_\infty = V_A + U_{A0} = V_A\sqrt{1 + C_T}, \tag{5.55}$$

where V_A is the advance velocity in the propeller plane, and the thrust loading coefficient is given by

$$C_T = \frac{Thrust}{0.5\rho V_A^2 \pi D^2/4} = \frac{8}{\pi}\frac{K_T}{J^2}. \tag{5.56}$$

Propeller diameter is denoted by D. According to this simple ideal propulsor model, the radius of the slipstream far behind the propeller is given by

$$r_\infty = r_0\sqrt{\frac{1}{2}\left(1 + \frac{V_A}{V_\infty}\right)}, \tag{5.57}$$

where r_0 is the propeller radius. The limited distance x of the propeller and rudder results in a smaller contraction of the slipstream radius r and a smaller value of the axial velocity V_x in the slipstream at the position of the rudder. These can be approximated by the following expressions

$$\begin{aligned}\frac{r}{r_0} &= \frac{0.14\left(r_\infty/r_0\right)^3 + \left(r_\infty/r_0\right)\left(x/r_0\right)^{1.5}}{0.14\left(r_\infty/r_0\right)^3 + \left(x/r_0\right)^{1.5}} \\ \frac{V_x}{V_\infty} &= \left(\frac{r_\infty}{r}\right)^2.\end{aligned} \tag{5.58}$$

Equations (5.57) are approximations based on potential flow theory. Turbulent mixing of the water jet and surrounding flow increases the radius of the slipstream by Δr. This effect is taken into account by the formula

$$\Delta r = 0.15x\frac{V_x - V_A}{V_x + V_A} \tag{5.59}$$

and the corresponding, corrected axial velocity of flow in the slipstream is

$$V_{corr} = (V_x - V_A)\left(\frac{r}{r + \Delta r}\right)^2 + V_A . \tag{5.60}$$

The limited radius of the slipstream has a diminishing effect on the rudder lift. This can be taken into account by multiplying the lift by the factor

$$\lambda = \left(V_A / V_{corr}\right)^f \text{ with } f = 2\left(\frac{2}{2 + d/c}\right)^8, \tag{5.61}$$

where

$$d = \sqrt{\pi/4}\left(r + \Delta r\right). \tag{5.62}$$

5.9 Azimuth thruster as the main propulsor

Azimuth thruster units used as the main propulsion means have become very popular in a variety of ship types within the last two decades. Very often they are called podded propellers. There are several benefits in using them. Apart from good manoeuvring qualities, ships equipped with this kind of propulsor are claimed to be free of vibration and noise problems. The the overall propulsion characteristics are also good, thanks to the absence of propeller shafts and supporting brackets.

Perhaps the biggest difference in the action of podded propellers when compared with traditional propellers is that they operate frequently in oblique inflow. The knowledge of the forces developed by a propeller in an oblique inflow is very important in order to evaluate ship's manoeuvring. In particular, stopping a vessel may be conducted quite differently and faster than in the case of the traditional propulsion arrangement.

The model of the forces acting on the azimuth type thruster in the oblique flow as outlined below is relatively simple. It addresses the problem of the forces acting on a propeller only. It does not attempt to deal with the hydrodynamic forces acting on the pod, strut and fins. A more elaborate model, which includes all the elements of the podded propulsor, is presented in Ruponen (2003) and Ruponen & Matusiak (2004). Oblique inflow to the propeller disk involves a radical change in the forces acting on a propulsor. Steady force components change. In particular, a significant in-plane component F_{py} of the total force develops (Matusiak, 2003b)

$$F_{py} = \rho A_p \left(V_A + U_A\right) V_{py}, \tag{5.63}$$

where A_p is the propeller disk area,

$$V_A = V_{x,R} \cos\delta - V_{y,R} \sin\delta \tag{5.64}$$

is propeller advance velocity,

$$V_{py} = V_{x,R} \sin\delta + V_{y,R} \cos\delta \tag{5.65}$$

is flow velocity in-plane of the propeller plane, and U_A is the propeller-induced velocity in this plane. Refer to the Figure 5.4 for definitions of flow kinematics and the definition of the forces.

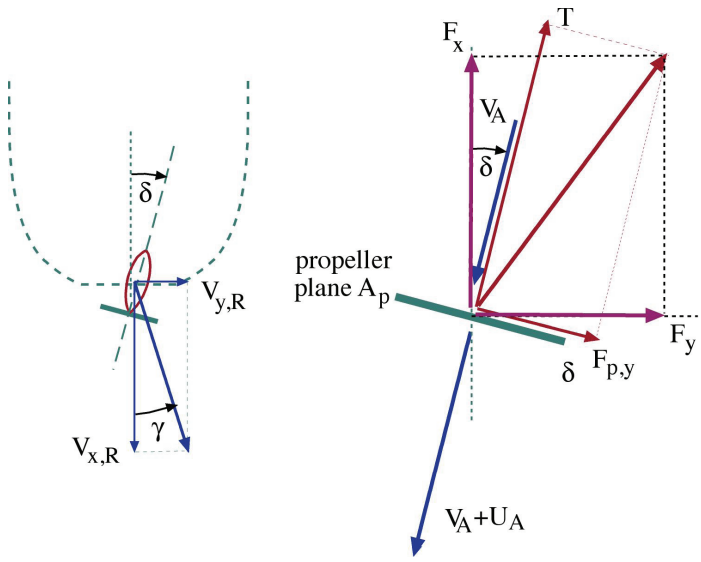

Fig. 5.4 Flow kinematics and forces acting on the propeller in an oblique flow.

The propeller-induced velocity U_A can be evaluated from the actuator disk approximation of the propeller as follows

$$U_A = V_A\left(-1+\sqrt{1+C_T}\right)/2, \tag{5.66}$$

where the thrust loading coefficient C_T is given by Formula (5.56).

The thrust of the propeller is evaluated from the known thrust coefficient K_T as a function of the advance ratio $J=V_A/(nD)$, where n and D are propeller revolutions and diameter, respectively. Having both the thrust T and the in-plane component F_{py} of the total force evaluated, the force propelling the ship F_x and rudder-like force F_y can be evaluated as follows:

$$\begin{aligned} F_x &= T\cos\delta - F_{py}\sin\delta \\ F_y &= T\sin\delta + F_{py}\cos\delta. \end{aligned} \tag{5.67}$$

A more profound discussion of rudder forces and propeller-rudder interaction can be found in Molland&Turnock (2007). Luukkainen (2011) has developed a model particularly suitable to simulate the manoeuvring of cruise and RoPax vessels.

5.10 Autopilot steering

A simple, *PD*-controller based autopilot can be used to steer a ship or to keep it on a straight course given by a heading ψ_0. The control function for the target value of the so-called rudder angle is given by

$$\delta_T = C_1\left(\psi - \psi_0\right) + C_2\dot{\psi}, \tag{5.68}$$

where C_1 and C_2 are the gain factors of the autopilot. The rate of turn of the rudder is given and equal to the prescribed value ω_δ. The actual rudder angle can be evaluated by a simple linear differential equation

$$\dot{\delta} = \mathrm{sgn}\left(\delta_T - \delta\right)\omega_\delta. \tag{5.69}$$

5.11 Aerodynamic forces acting on a ship

When considering ship dynamics, the hydrodynamic forces, which are the forces due to the interaction of the ship hull with the surrounding water, are obviously the most important ones. However, the aerodynamic loads may also play an important role. A strong side wind may disturb ship berthing. As we have already learned from the ship stability part, a gusty side wind may cause large dynamic heeling. A strong head wind may increase resistance. But even in calm weather, the aerodynamic load may be important. For example, a fast catamaran or trimaran having a large and bulky superstructure suffers from an aerodynamic load increasing its resistance. For a well-designed hull with relatively low hydrodynamic resistance, this aerodynamic resistance may be quite high and cannot be disregarded. Aerodynamic loads play an important role in simulations of the manoeuvring qualities of a ship.

Evaluation of the loads acting on a vessel requires information about them in a non-dimensional form as the aerodynamic force coefficients. These are given in the body-fixed co-ordinate system. If the in-plane horizontal motion of a ship is considered only, then two force components (x- and y-directional ones) and the yawing moment coefficient are required. An example of the aerodynamic force coefficients is given in Figure 5.5.

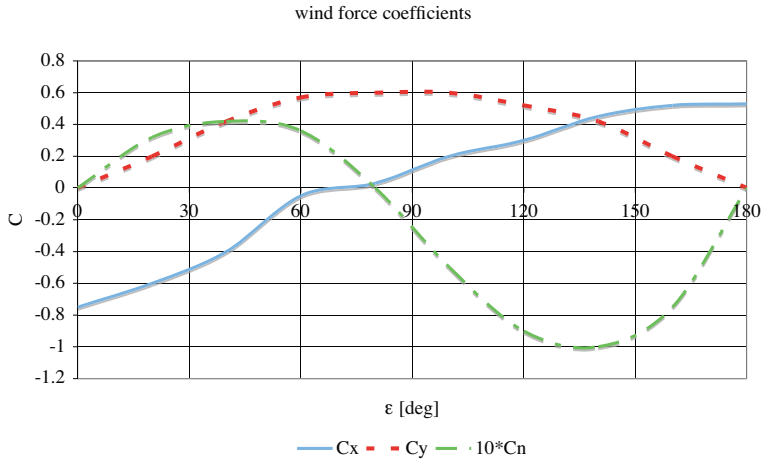

Fig. 5.5 Aerodynamic force coefficients and their dependence upon the angle of the apparent wind.

When evaluating aerodynamic loads acting on a moving vessel one has to take into account the varying orientation and velocity of the resulting airflow. Figure 5.6 presents the components of the airflow components making up the resulting wind vector V_{wres}.

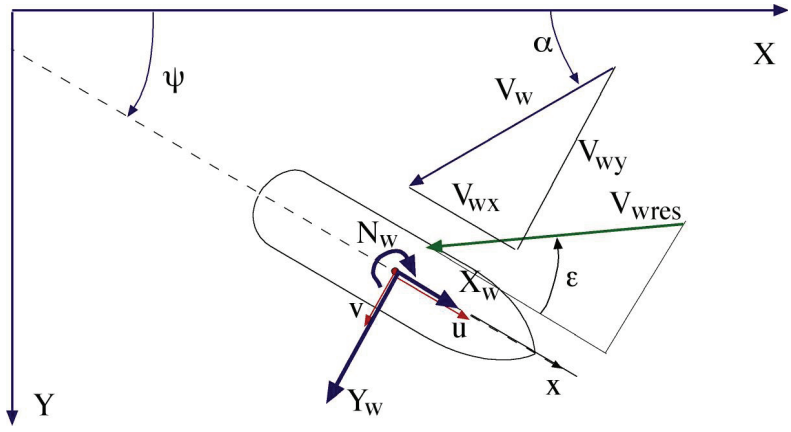

Fig. 5.6 Air velocity components and aerodynamic force vectors acting on a ship.

The wind blows with a velocity V_w from the direction making the angle α with the X- axis of the inertial co-ordinate system. The projections of this velocity vector on the body-fixed co-ordinate system x-y are

$$V_{wx} = V_w \cos(\alpha + \psi)$$
$$V_{wy} = V_w \sin(\alpha + \psi). \tag{5.70}$$

The resultant airflow velocity felt by a moving ship is given by the speed

$$V_{wres} = \sqrt{(V_{wx} + u)^2 + (V_{wy} - v)^2} \tag{5.71}$$

and the angle ε made with the symmetry plane of a ship

$$\varepsilon = \tan^{-1} \frac{V_{wy} - v}{V_{wx} + u}. \tag{5.72}$$

The aerodynamic forces and moment are finally given by

$$X_{wind} = 0.5 \rho_{air} A_T C_X V_{wres}^2$$
$$Y_{wind} = 0.5 \rho_{air} A_L C_Y V_{wres}^2 \tag{5.73}$$
$$N_{wind} = 0.5 \rho_{air} A_L L C_N V_{wres}^2.$$

5.12 Numerical implementation of the maneuvering simulation

A modular simulation model using the linear hydrodynamic derivatives 5.31, ship resistance, propeller thrust and rudder models, as given in sections 5.6 and 5.7, is implemented in the form of the computer program *ohjailu.f*. An allowance is made for autopilot steering and modelling the wind loads. The origin is located in the mid-ship and the mass moment of inertia is related to the Centre-Of-Gravity. The following equations of ship in-plane motion are used

$$
\begin{aligned}
&\frac{du}{dt} \equiv \dot{u} = \left(mrv + mx_G r^2 + X_{\text{resistance}} + T + X_w\right) / \left(m - X_{\dot{u}}\right) \\
&\frac{dv}{dt} \equiv \dot{v} = \left(-mru + Y_v v + Y_r r + Y_{\dot{r}} \dot{r} - mx_G \dot{r} + L + Y_w\right) / \left(m - Y_{\dot{v}}\right) \\
&\frac{dr}{dt} \equiv \dot{r} = \left[-mx_G \left(\dot{v} + ur\right) + N_v v + N_r r + N_{\dot{v}} \dot{v} + Lx_R + N_w\right] / \left(I_z + mx_G^2 - N_{\dot{r}}\right) \\
&\frac{dX_0}{dt} \equiv \dot{X}_0 = u\cos\psi - v\sin\psi \\
&\frac{dY_0}{dt} \equiv \dot{Y}_0 = u\sin\psi + v\cos\psi \\
&\frac{d\psi}{dt} \equiv \dot{\psi} = r.
\end{aligned}
\tag{5.74}
$$

The first three equations represent the modular nonlinear model of ship in-plane motion based on equations 5.1a. Hydrodynamic hull forces are represented by the linear approximation. The equations, as presented above, are coupled through the components of hull forces dependent upon the accelerations. This is visible as yaw and sway acceleration terms being present in the second and third equations. In order to solve the equations, they have to be de-coupled. This is done numerically as follows. The second and third of the equations (5.71) can be put in a matrix form as follows:

$$
\begin{bmatrix}
1 & \dfrac{mx_G - Y_{\dot{r}}}{m - Y_{\dot{v}}} \\
\dfrac{mx_G - N_{\dot{v}}}{I_z + mx_G^2 - N_{\dot{r}}} & 1
\end{bmatrix}
\begin{Bmatrix} \dot{v} \\ \dot{r} \end{Bmatrix}
=
\begin{Bmatrix}
\dfrac{-mru + Y_v v + Y_r r + L + Y_w}{m - Y_{\dot{v}}} \\
\dfrac{-mx_G ur + N_v v + N_r r + Lx_R + N_w}{I_z + mx_G^2 - N_{\dot{r}}}
\end{Bmatrix}
\tag{5.75}
$$

At each time step, the state vector $\begin{Bmatrix} \dot{v} \\ \dot{r} \end{Bmatrix}$ is solved numerically from the system of two linear algebraic equations (5.75) as:

$$
\begin{Bmatrix} \dot{v} \\ \dot{r} \end{Bmatrix}
=
\begin{bmatrix}
1 & \dfrac{mx_G - Y_{\dot{r}}}{m - Y_{\dot{v}}} \\
\dfrac{mx_G - N_{\dot{v}}}{I_z + mx_G^2 - N_{\dot{r}}} & 1
\end{bmatrix}^{-1}
\begin{Bmatrix}
\dfrac{-mru + Y_v v + Y_r r + L + Y_w}{m - Y_{\dot{v}}} \\
\dfrac{-mx_G ur + N_v v + N_r r + Lx_R + N_w}{I_z + mx_G^2 - N_{\dot{r}}}
\end{Bmatrix}
\tag{5.76}
$$

Numerical integration is performed by the Runge-Kutta integration method of fourth order. The solution of the first equation in 5.74 and the result of integrating equations 5.76 is the velocity vector $\mathbf{U}=u\mathbf{i}+v\mathbf{j}$ of the ship's origin 0 and yaw velocity r.

Integration of the three last equations of the set 5.74 yields ship's position $X_0(t),Y_0(t),\Psi(t)$ in the inertial co-ordinate system X-Y. An example of the simulated zigzag manoeuvre of Mariner ship is presented in Figure 5.7.

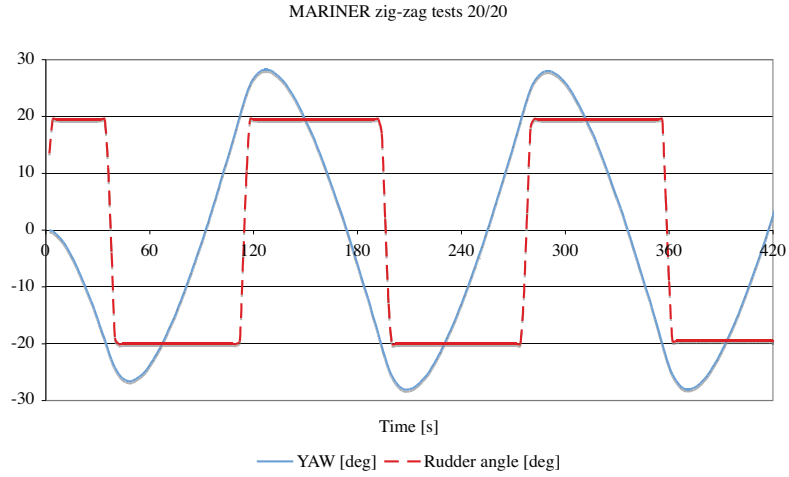

Fig. 5.7 Zigzag test of Mariner simulated with the program ohjailu.f. Initial speed is 15 knots.

The result of the simulated turning circle manoeuvre is shown in Figure 5.8 below.

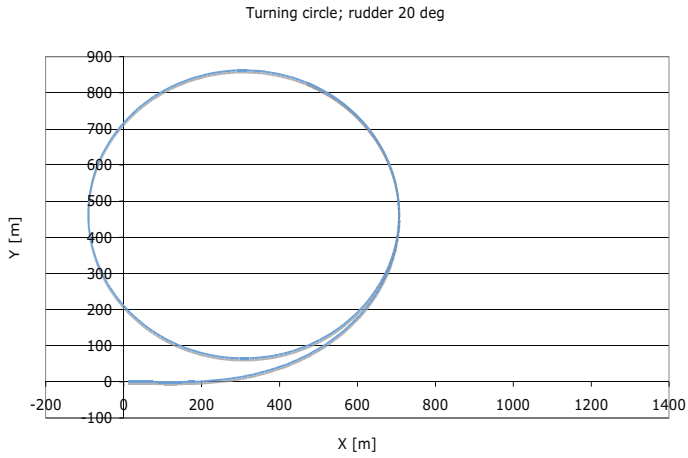

Fig.5.8 Turning circle test of Mariner simulated with the program ohjailu.f. Initial speed is 15 knots.

Speed drop during a turning circle manoeuvre is presented in Figure 5.9.

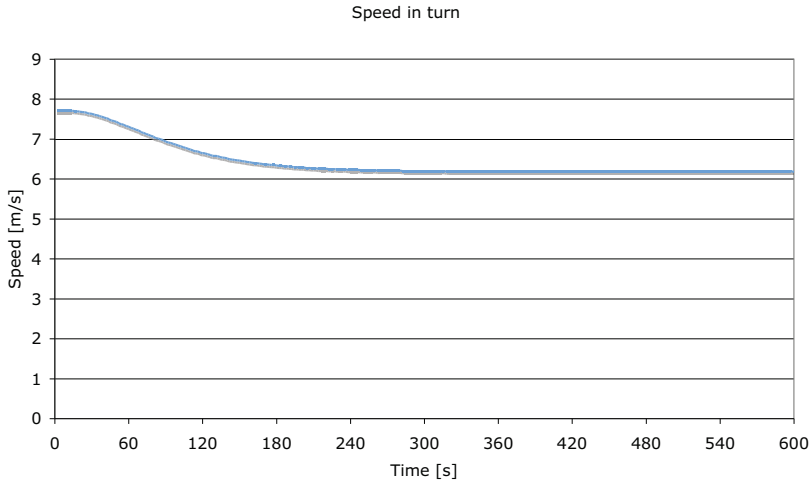

Fig. 5.9 Speed drop during a turning circle test of Mariner simulated with the program ohjailu.f. Initial speed is 15 knots. Propeller revolutions are kept constant.

6. Sea surface waves

The water sea surface is seldom (if ever) completely still and flat. It is mainly the interaction of wind and water that causes the free surface to deform. As a result, surface waves form. We shall not deal with the mechanism of generation of surface waves that is, we shall not treat the physical mechanism of wave evolution. This can be found for instance in Young (1999). Instead we shall present the classical, but still very much applicable, small amplitude that is the linear theory of surface waves as first presented by Airy.

Surface waves starting from the length of a few metres up to approximately the length of 1 km are of interest in ship and offshore structural dynamics. Apart these surface waves, there are much slower internal waves caused by density stratification. Tides, caused by a change of the position of heavenly bodies with respect to the Earth, are usually not important when considering periodic loads and motions acting on ships. Capillary waves and ripples are high frequency phenomena, which can be disregarded when dealing with ship dynamics problems.

6.1 Plane progressive linear regular waves

The pattern of waves observed from a travelling ship is very complex. Apart from the waves generated by the vessel itself, a large number of waves of different length and height can be observed, each progressing in a different direction. When we travel by air over the ocean and especially in the vicinity of the coastal line, we observe that the wave pattern exhibits certain regularities. The prevailing direction of wave progression is noticed, and the length of the waves does not vary so much anymore. This observation justifies modelling the sea surface waves as plane progressive ones. This is

done quite often in the model tests (see Fig. 6.1) and also in computational methods.

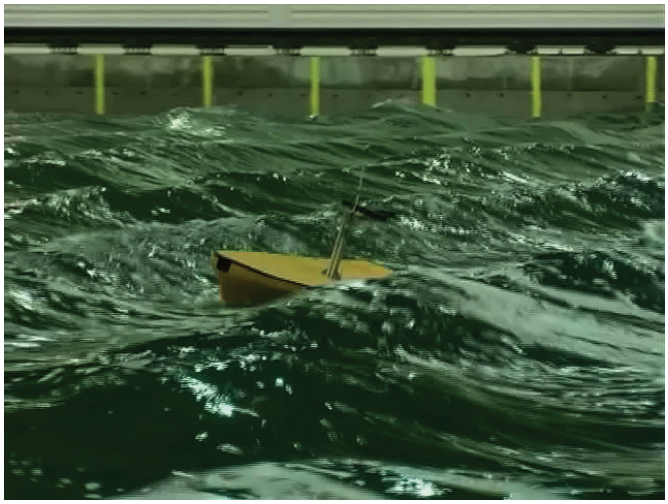

Fig. 6.1 Model of a pilot boat in the steep regular unidirectional waves generated in the multifunctional model basin of the Aalto University.

6.1.1 Assumptions and boundary conditions

The most common assumptions made when dealing with surface waves is that the associated flow is ideal. This means that the flow is assumed to be inviscid and irrotational. Thus the flow may be fully described by the velocity potential $\phi = \phi(X_0, Y_0, Z_0)$. Evaluation of this velocity potential rests on fulfilment of the mass continuity equation, which is of the form of Laplace equation

$$\frac{\partial^2 \phi}{\partial X_0^2} + \frac{\partial^2 \phi}{\partial Y_0^2} + \frac{\partial^2 \phi}{\partial Z_0^2} = 0 \tag{6.1}$$

and on satisfying the boundary conditions of the flow in question. The most important boundary conditions are these set by a free deforming surface.

When describing progressive waves we use a Cartesian co-ordinate system with the origin 0 fixed in space and located on the undisturbed water surface. The X_0-axis points in the direction of waves propagation, while the Z_0-axis points vertically upwards. The vertical elevation of the free surface is defined by

$$Z_0 = \zeta(X_0, Y_0, t). \tag{6.2}$$

Kinematic boundary condition at the free surface

The so-called kinematic boundary condition can be obtained by requiring that the substantial derivative of the quantity $F(X_0, Y_0, Z_0, t) \equiv Z_0 - \zeta(X_0, Y_0, t)$ is zero:

$$\begin{aligned} \frac{DF}{Dt} &= \frac{\partial F}{\partial t} + \mathbf{v} \cdot \nabla F = \frac{\partial}{\partial t}[Z_0 - \zeta(X_0, Y_0, t)] + \mathbf{v} \cdot \nabla[Z_0 - \zeta(X_0, Y_0, t)] \\ &= -\frac{\partial \zeta}{\partial t} - u_0 \frac{\partial \zeta}{\partial X_0} - v_0 \frac{\partial \zeta}{\partial Y_0} + w_0 \end{aligned} \tag{6.3}$$

Here u_0, v_0 and w_0 are X_0-, Y_0- and Z_0- directional flow components respectively. For the waves progressing in the X_0-direction we can write (6.3) as follows

$$w_0 = \frac{\partial \zeta}{\partial t} + u_0 \frac{\partial \zeta}{\partial X_0}. \tag{6.4}$$

The meaning of expression 6.4 is illustrated in Figure 6.2.

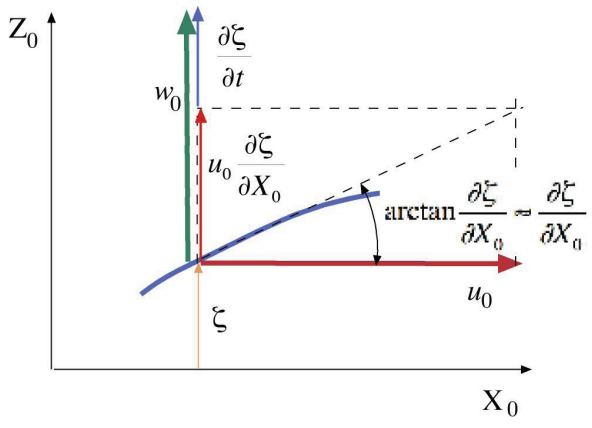

Fig. 6.2 Flow tangency condition at the free surface.

It is clearly seen that with the free surface being frozen, ($\partial\zeta/\partial t = 0$) (6.4) means the tangency condition of the flow at the free surface. For the unsteady free surface motion the vertical flow velocity also takes into account the vertical velocity component of the free surface deformation. In both cases the kinematic boundary condition implies the tangency of the flow velocity at the free surface. It is worth noting that the equation of the kinematic condition derived above also applies to the viscous and rotational flows as well.

Making use of the fact that the slopes of the surface water waves are small, the linearized kinematic boundary condition can be obtained by dropping the terms involving spatial derivatives of wave elevation and evaluating it approximately at Z_0=0. Using the velocity potential the linearized kinematical boundary condition is

$$\frac{\partial\zeta}{\partial t} = \frac{\partial\phi}{\partial Z_0} \text{ at } Z_0 = 0. \tag{6.5}$$

Dynamic boundary condition at the free surface

Neglecting surface tension, the dynamic boundary condition states that the pressure in water at the free surface equals the atmospheric pressure p_a. This can be expressed using Bernoulli's equation as follows

$$\frac{\partial\phi}{\partial t} + \frac{1}{2}\nabla\phi \bullet \nabla\phi + g\zeta = -(p - p_a)/\rho = 0, \tag{6.6}$$

which yields the wave elevation

$$\zeta = -\frac{1}{g}\left(\frac{\partial\phi}{\partial t} + \frac{1}{2}\nabla\phi \bullet \nabla\phi\right). \tag{6.7}$$

In the linear surface wave theory the second term in parentheses is neglected and the condition is expressed approximately at Z_0=0, yielding the linear version of the dynamic boundary condition

$$\zeta = \frac{1}{g}\frac{\partial \phi}{\partial t} \text{ at } Z_0 = 0. \tag{6.8}$$

The linearization of the kinematic boundary condition, that is the assumption of small slopes, means also that we apply the linearized equations (6.5 and 6.8) on the plane $Z_0=0$, rather than on the actual water free surface $Z_0=\zeta$.

Differentiation of Equation 6.8 with respect to time and substituting it into (6.5) yields a single linear equation to be satisfied in order to have both boundary conditions at the free surface fulfilled. This equation is

$$\frac{\partial \phi}{\partial Z_0} + \frac{1}{g}\frac{\partial^2 \phi}{\partial t^2} = 0 \text{ at } Z_0 = 0. \tag{6.9}$$

6.1.2 Velocity potential for regular progressive waves in deep water

For the two-dimensional X_0Z_0-flow domain restricted by the free surface only, the solution to Laplace's equation is given by the velocity potential

$$\phi = \frac{gA}{\omega} e^{kZ_0} \sin\left(kX_0 - \omega t\right), \tag{6.10}$$

where A is the wave amplitude, $k=2\pi/\lambda$ the wave number, λ the wave length and ω the wave angular frequency. It can be easily shown that velocity potential (6.10) also satisfies the linearized free surface condition (6.9). Differentiation of velocity potential (6.10) with respect to time yields

$$\frac{\partial \phi}{\partial t} = -gAe^{kZ_0} \cos\left(kX_0 - \omega t\right), \tag{6.11}$$

which substituted into the (6.8) yields the wave elevation of the form

$$\zeta = -\frac{1}{g}\frac{\partial \phi}{\partial t} = Ae^{kZ_0} \cos\left(kX_0 - \omega t\right)\Big|_{Z_0=0} = A\cos\left(kX_0 - \omega t\right). \tag{6.12}$$

As a result, we have obtained a simple regular progressive wave of a cosine form. The length of the wave, defined as the horizontal distance between

two successive crests or troughs, is $\lambda=2\pi/k$. It is interesting to notice that the cosine function applies both to the spatial (X_0-directional) and to the time dependence. Thus the spatial form of the wave is that of a cosine function, and the time dependency of the water elevation at the fixed position $X_0 = X_i$ is also of the same form. Quantities used in describing the regular progressive wave are shown in Fig. 6.3 below.

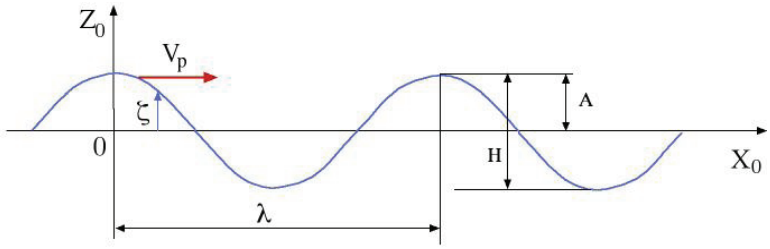

Fig. 6.3 Progressive regular wave at a certain instant of time.

In Figure 6.3, V_p is the wave celerity, also called the phase velocity, and H is the wave height.

6.1.3 Dispersion relation for the deep water

There is a relation between the wave frequency and length. This dependence, called the dispersion relation, for the deep water is obtained substituting (6.10) in (6.9):

$$\frac{\partial\phi}{\partial Z_0}+\frac{1}{g}\frac{\partial^2\phi}{\partial t^2}=\frac{kgA}{\omega}e^{kZ_0}\sin(kX_0-\omega t)-A\omega e^{kZ_0}\sin(kX_0-\omega t)=0 \qquad (6.13)$$

yielding

$$k=\frac{2\pi}{\lambda}=\frac{\omega^2}{g}\,. \qquad (6.14)$$

6.1.4 Fluid velocity and pressure below progressive regular waves in deep water

The flow velocities can be readily obtained from the velocity potential as follows

$$u_0 = \frac{\partial \phi}{\partial X_0} = \frac{gAk}{\omega} e^{kZ_0} \cos(kX_0 - \omega t)$$
$$w_0 = \frac{\partial \phi}{\partial Z_0} = \frac{gAk}{\omega} e^{kZ_0} \sin(kX_0 - \omega t). \tag{6.15}$$

The pressure can be evaluated from Bernoulli's equation (6.6) and using the velocity potential 6.10 as follows

$$p - p_a = -\rho g Z_0 - \rho \frac{\partial \phi}{\partial t} - \frac{1}{2} \rho \nabla \phi \bullet \nabla \phi \tag{6.16}$$
$$= \rho g \left[A e^{kZ_0} \cos(kX_0 - \omega t) - Z_0 \right] - \frac{1}{2} \rho \left(\frac{gAk}{\omega} \right)^2 e^{2kZ_0}.$$

It is quite usual to disregard the last term as a nonlinear and having little significance. Thus the pressure in the fluid domain, that is for $Z_0 \leq 0$, is given by

$$p_t = p - p_a = \rho g \zeta e^{kZ_0} - \rho g Z_0 \equiv p_d + p_h, \tag{6.17}$$

where p_d is the so-called dynamic and p_h the hydrostatic part of the pressure.

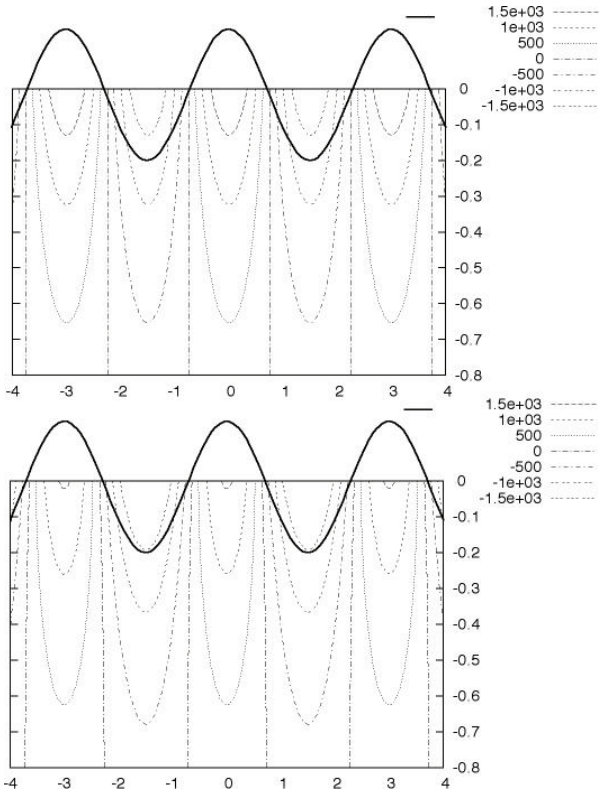

Fig. 6.4 Iso-lines of dynamic pressure due to a linear progressive wave of a length 3 m and amplitude 0.2 m. At the upper figure the linear term (the first bracketed term of Equation 6.16) is presented. The bottom figure includes also the nonlinear, third term of Equation 6.16.

As is clearly seen from Figure 6.4, the nonlinear term does not have much effect on the absolute value of the pressure, even in this very steep wave case. Actually so a steep wave is not of a cosine form. An increase in wave steepness is associated with the sharpening of the crests while the troughs get flatter. Steep waves are shown in Figure 6.1. The steepest possible waves are usually represented by a trochoid, as shown in Figure 6.5 below.

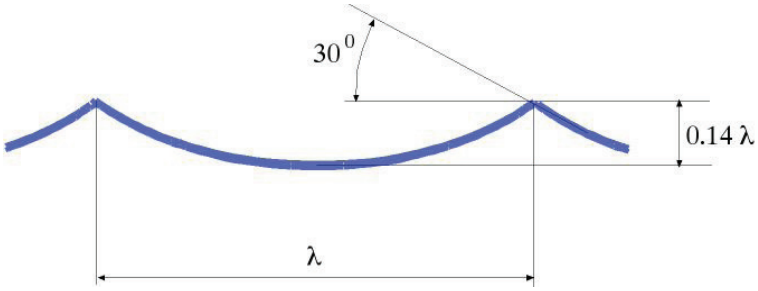

Fig. 6.5 Trochoidal steepest wave.

The nonlinear effects in water surface waves are further discussed in Section 6.2.

6.1.5 Wave celerity

Let us imagine an observer travelling at speed V_p along the X-axis so that its position is given by

$$X_0 = X_{INIT} + V_p t. \tag{6.18}$$

Using (6.12), the velocity of the wave surface elevation felt by the observer is given by

$$\begin{aligned} \frac{\partial \zeta}{\partial t} &= A\frac{d}{dt}\cos\left[kX_{INIT} + \left(kV_p - \omega\right)t\right] \\ &= -A\left(kV_p - \omega\right)\sin\left[kX_{INIT} + \left(kV_p - \omega\right)t\right]. \end{aligned} \tag{6.19}$$

The observer will see the wave as a stationary one if the following holds

$$kV_p - \omega = 0, \tag{6.20}$$

which infers that the velocity of wave profile travel in deep water, the so-called phase velocity (refer to Figure 6.3) or the wave celerity, is

$$V_p = \omega / k. \tag{6.21}$$

6.1.6 Encounter frequency

Let us next consider the case when an observer is no longer riding on a wave crest but is located on a ship that is moving at a constant speed V in the direction x making the heading angle μ with the direction of waves' propagation X_0 (Fig. 6.6).

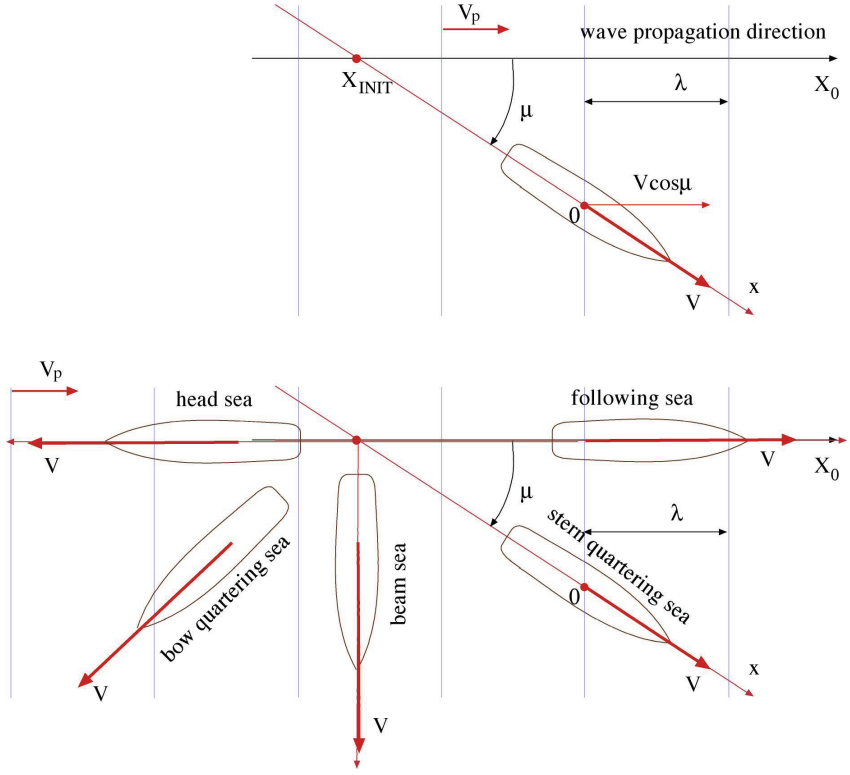

Fig. 6.6 Definition of heading.

The position of ship measured along the direction of waves' propagation (see upper part of Figure 6.6) is given by

$$X = X_0 + V\,t\cos\mu \tag{6.22}$$

and the wave elevation at the position of the ship's origin 0 where the observer is located is

$$\zeta = A\cos\left(kX_0 + kVt\cos\mu - \omega t\right) = A\cos\left[kX_0 - \left(\omega + kV\cos\mu\right)t\right]. \qquad (6.23)$$

Using (6.14) the last term in parenthesis

$$\omega_e = \omega - kV\cos\gamma = \omega\left(1 - \frac{V\omega}{g}\cos\mu\right) \qquad (6.24)$$

is called the *frequency of encounter*. It is the angular frequency the waves are felt by the ship. Different heading angles and their definitions are given in the lower part of Figure 6.6. From the form of expression 6.24, it is clearly seen that:

For the head sea (μ=180^0), that is heading into waves and swell, the encounter frequency is higher than the wave frequency and the difference increases with ship speed.

For beam seas (μ =90^0), heading 90^0 across the seas, the encounter frequency equals the wave frequency.

For following seas (μ =0^0), heading with the seas, the encounter frequency is lower than the wave frequency and the difference increases with ship speed. The encounter frequency is zero if the ship speed projected in the direction of wave propagation equals the wave celerity, i.e. $V\cos\mu=V_p$. A further decrease in ship speed or increasing wave length yields the situation where waves propagate faster than the ship and they start to overtake it.

6.2 The effects of shallow water

Shallow water affects the free surface deformation and the creation of surface waves. The velocity potential has to satisfy in addition to the free surface boundary condition (6.9), also the impermeability condition at the sea bottom:

$$w_0 = \frac{\partial\phi}{\partial Z_0} = 0 \text{ at } Z_0 = -h, \qquad (6.25)$$

where h is the water depth. It can be shown that the velocity potential satisfying these conditions is of the form

$$\phi = \frac{gA}{\omega}\frac{\cosh k(Z_0 + h)}{\cosh kh}\sin(kX_0 - \omega t). \tag{6.26}$$

The dispersion relation following from the satisfaction of the free surface boundary conditions gets more complicated and is given by the expression

$$k\tanh kh = \omega^2 / g. \tag{6.27}$$

The phase velocity for the limited water depth is given by

$$V_p = \omega / k = \sqrt{g\frac{\tanh kh}{k}}. \tag{6.28}$$

The Taylor series expansion of hyperbolic tangent of 6.28 yields

$$V_p = \sqrt{g\frac{kh - (kh)^3/3 + ...}{k}} \tag{6.29}$$

giving an approximate expression

$$V_p \approx \sqrt{gh} \tag{6.30}$$

for the phase velocity when $kh = 2\pi h / \lambda << 1$. In this case the phase velocity does not depend on the wave length.

6.3 Nonlinear models of surface waves

As will be discussed in the next sections, the linear wave model is very useful. The advantages are that it is easy to use, complies well with the linear modelling of ship motions in waves and makes it possible to model the sea condition consisting of waves of different lengths and heights. However, in some cases, certain nonlinear effects have to be considered. For instance, if we are dealing with an evaluation of local wave pressure loads on a ship's side shell, it is important to consider the pressures up to the actual instantaneous water free surface. The information provided by the

linear wave model just up to the still water level is not sufficient. As already mentioned, an increase in wave steepness results in wave profiles that differ from the ideal cosine form (Figure 6.5). An elegant and efficient way of dealing with steep regular waves is provided by the so-called *Stokes' expansion* (Newman, 1977). However, this will be not discussed here because this wave model is seldom used in ship dynamics. Moreover, it can be found in a number of books dealing with surface waves. Instead, in the following, we shall discuss two simplified heuristic models. Both models retain the regular cosine form of surface wave. What distinguishes them from the linear model is the fact that they attempt to evaluate the pressures up to the actual water surface.

6.3.1 The Faltinsen's model of pressure

In the model of Faltinsen (Faltinsen, 1990) both the hydrostatic and the dynamic pressure part are calculated from the still water level being the reference. In this sense, the method is in agreement with the linear wave theory. For the wave crest, the dynamic pressure is extended as a uniform distribution from the still water level up to the actual water surface (see Fig. 6.7). For a wave trough, the hydrodynamic pressure is disregarded in the region located between the actual water surface and the still water level. As a result, a small non-zero total pressure p_t at the actual water surface is obtained. Thus the dynamic boundary condition is not fully fulfilled for the wave trough.

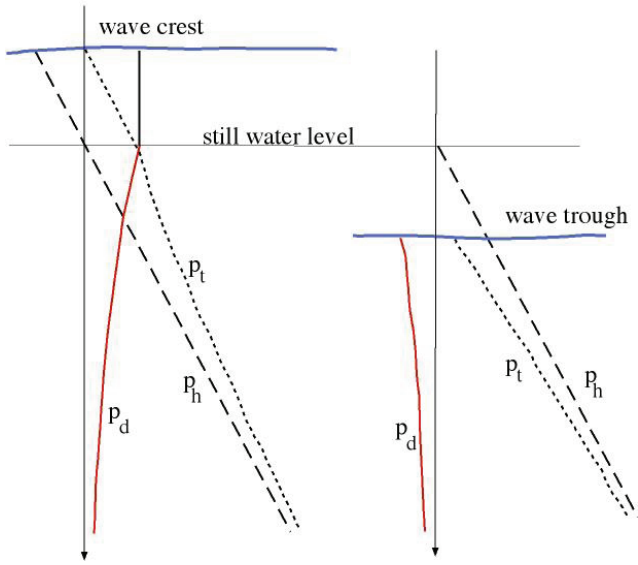

Fig. 6.7 Extrapolation of the hydrodynamic pressures above and below the still water level (Faltinsen, 1990).

6.3.2 Stretching approximation of pressure distributions

The so-called stretching for the pressure distributions stems from the desire to have the dynamic boundary condition fulfilled on the water free surface. For the deep water condition, this technique is given by the following formula

$$p_t = p - p_a = \rho g \zeta e^{k(Z_0 - \zeta)} - \rho g Z_0 = p_d + p_h . \tag{6.31}$$

Stretched pressures are presented in Fig. 6.8 below.

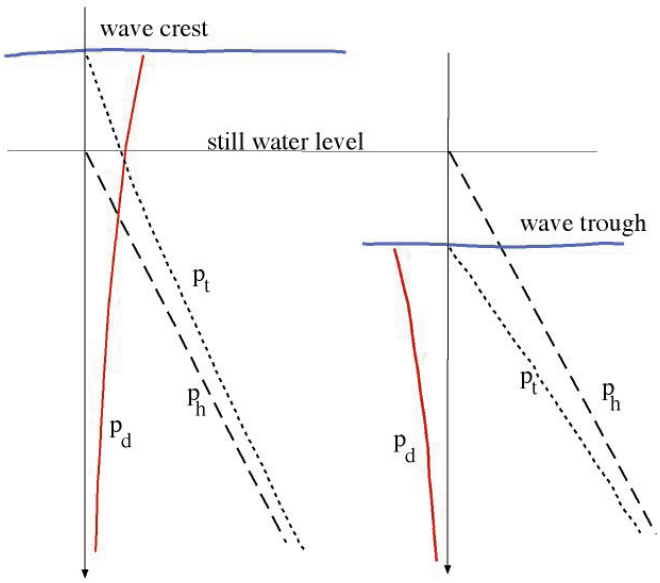

Fig. 6.8 Stretched pressure distributions.

6.4 Wave group

The concept of a wave group can be explained by considering waves resulting from the superposition of two cosine form wave trains having the same amplitude A but slightly different angular frequencies ω_1 and ω_2. The resulting water surface elevation is

$$\begin{aligned}\zeta &= A\cos\left(k_1X_0-\omega_1t\right)+A\cos\left(k_2X_0-\omega_2t\right)\\ &= 2A\cos\left[\frac{\left(k_1+k_2\right)X_0-\left(\omega_1+\omega_2\right)t}{2}\right]\cos\left[\frac{\left(k_1-k_2\right)X_0-\left(\omega_1-\omega_2\right)t}{2}\right]\\ &= 2A\cos\left(k_{mean}X_0-\omega_{mean}t\right)\cos\left(\frac{\delta k}{2}\ X_0-\frac{\delta\omega}{2}\ t\right).\end{aligned} \tag{6.32}$$

The resulting wave is shown in Figure 6.9. It consists of the so-called carrier frequency wave with angular frequency $\omega_{mean}=(\omega_1+\omega_1)/2$ and slowly varying component with frequency $\delta\omega/2=(\omega_1-\omega_2)/2$.

The group velocity, which is the velocity of propagation of a group of carrier waves, is obtained by setting the observer of the waves following the group with the velocity V_g. The X-directional position of the observer is given by

$$X_0 = X_{INIT} + V_g t. \tag{6.33}$$

Thus,

$$\begin{aligned} \zeta &= 2A\cos\left(k_{mean}X_0 - \omega_{mean}t\right)\cos\left[\frac{\delta k}{2}\left(X_{INIT} + V_g t\right) - \frac{\delta\omega}{2}t\right] \\ &= 2A\cos\left(k_{mean}X_0 - \omega_{mean}t\right)\cos\left[\frac{\delta k}{2}X_{INIT} + \left(\delta k V_g - \delta\omega\right)t/2\right]. \end{aligned} \tag{6.34}$$

Following the reasoning of frequency of encounter, the wave group velocity in the deep water case is

$$V_g = \frac{\delta\omega}{\delta k} \approx \frac{d\omega}{dk} = \frac{1}{2}\sqrt{\frac{g}{k}} = \frac{1}{2}\frac{\omega}{k} = \frac{1}{2}V_p. \tag{6.35}$$

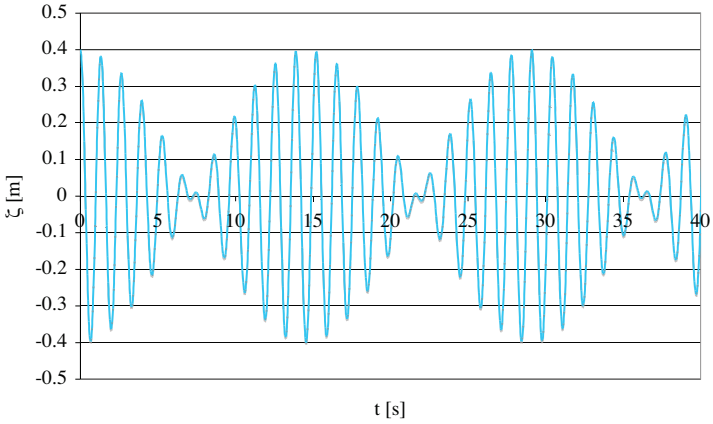

Fig.6.9 Wave groups as the result of a superposition of two wave trains. A_1=A=0.2 m and ω_1= 4.53 rad/s and ω_2= 4.96 rad/s.

From (6.35) we see that in the deep water, the group velocity is half of the phase velocity. If we conduct model tests in a tank and create the waves at one end of the basin, the group velocity rules the time required by the waves to arrive at the measuring position.

6.5 Spectral representations of sea surface waves

It is quite obvious that sea surface waves are far more complex than the ones described above. What we observe is a variety of waves with different

frequencies and different heights. Fortunately, there is a dispersion relation giving a connection between the wave frequency and length. Moreover, the waves propagate in different directions, although usually most of them follow the wind direction. Thus there is a prevailing course of their motion. This nearly unidirectional propagation of waves makes it possible to use a simplified model of irregular waves, the so-called *long-crested waves* model.

6.5.1 Long-crested irregular waves

Let us consider three regular waves propagating in the positive X_0-direction having amplitude A_i and frequency ω_i (i=1,2,3). The component waves and the resulting irregular combination of them are shown in Figure 6.10 with the phase of each of them being selected at random.

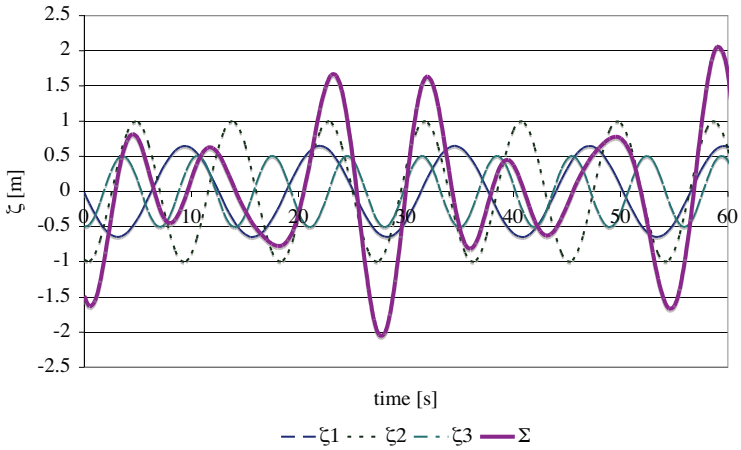

Fig. 6.10 Irregular wave as a sum (denoted by Σ) of the three regular wave components.

Spectral representation of the wave train of Figure 6.10 is shown in Figure 6.11.

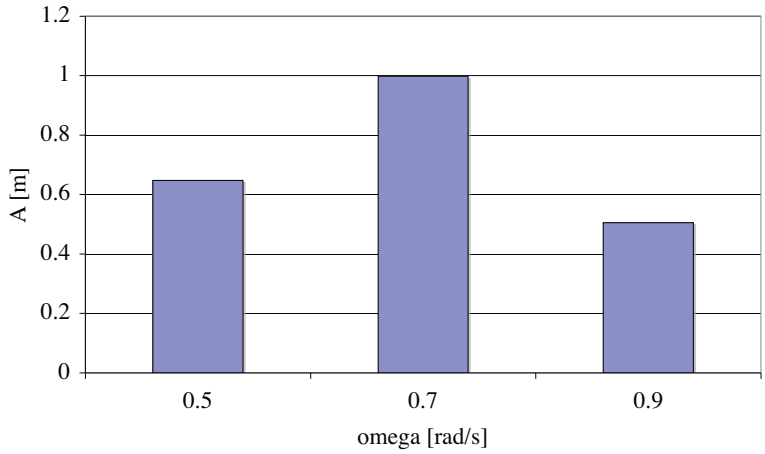

Fig. 6.11 A discrete amplitude spectrum of the wave train of Figure 6.10.

In Figure 6.11, co-ordinates are the frequencies and ordinates the amplitudes of the component waves. In order to describe wave trains comprising of an infinite number of regular components, another type of spectral representation is used. The so-called power spectral density is used instead of a discrete amplitude spectrum. This is a continuous function of wave angular frequency ω, which gives information on the wave amplitude related to a certain frequency. An example of the wave spectrum is presented in Figure 6.12.

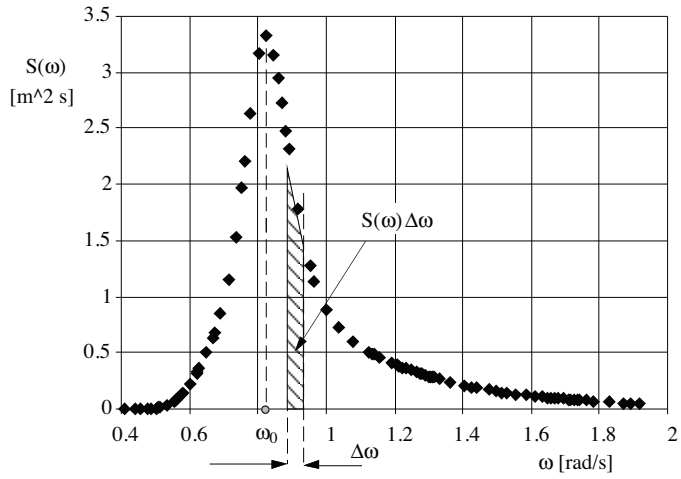

Fig. 6.12 Power spectral density of wave amplitude represented by N=100 frequency components.

The area under the curve represented by dots is a measure of the energy density of water surface motion. This energy given by

$$\bar{E} = \rho g \int_0^\infty S(\omega) d\omega = \frac{\rho g}{2N} \sum_1^N A_i^2 = \rho g \sigma^2, \tag{6.36}$$

where σ^2 is variance of the wave signal. An amplitude of a single wave component having the angular frequency ω_i can be evaluated by the integration of the wave spectrum as follows:

$$A_i = \sqrt{2S(\omega_i)\Delta\omega}. \tag{6.37}$$

Note that frequency differential $\Delta\omega$ can be selected freely. Quite often, in order to secure a generation of non-repeatable wave trains from the given wave spectrum, the sample angular frequencies ω_i are random numbers covering the frequency range of interest ($\omega_{min} \leq \omega \leq \omega_{max}$). In this case, the frequency increments $\Delta\omega_i$ are also random numbers governed by the adjacent frequencies ω_i and ω_{i+1}. The wave train from the given wave spectrum is obtained as

$$\zeta(t) = \sum_{i=1}^N a_i \sin\omega_i t + b_i \cos\omega_i t = \sum_{i=1}^N A_i \cos(\omega_i t - \delta_i), \tag{6.38}$$

where $-\pi \leq \delta_i \leq \pi$ is a random number representing the phase angle of the *i*th wave component. Wave elevation given by formula (6.38) can be understood as measured at the origin of the co-ordinate system, that is $X_0=0$. This wave generation is based on the so-called *Deterministic Spectral Amplitude* model. In the so-called *Non-deterministic Spectral Amplitude* model the a_i and b_i coefficients of the series (6.38) are taken as a normally distributed uncorrelated variables (Naito, 1995). This results in the wave amplitude component evaluated with the aid of (Matusiak, 2000)

$$A_i = \sqrt{2S(\omega_i)\frac{\chi_2^2}{2}\Delta\omega}, \tag{6.39}$$

where χ^2_2 is a chi-squared distribution with two degrees of freedom that results from the normal distribution of a_i and b_i coefficients. Randomness of wave amplitudes is observed in nature. If we took a number of relatively short records of waves at sea, we should notice that the power spectrum based on each of them is very irregular and different at each time. The common feature would be the area made up by each spectrum, which is nearly the same. The ensemble average of these spectra yields the smoothed wave spectrum as the one in Figure 6.12. This smoothed spectrum can be also understood as the spectrum obtained by processing a very long time record.

Other parameters describing in general terms the wave spectra are spectrum moments and periods. The *k*th moment of spectrum is evaluated by the following form integral

$$m_k = \int_0^\infty \omega^k S(\omega) d\omega. \tag{6.40}$$

The so-called significant wave height is defined by

$$H_S = 4\sqrt{m_0}. \tag{6.40a}$$

Another symbol frequently used for the significant wave height is $H_{1/3}$. This stems from the fact that the significant wave height is the mean of one-third of the highest observed waves. As a rule of thumb we can take that the highest wave encountered at sea is approximately twice the significant wave height. The latter number is roughly what is observed visually as the wave height.

There are many wave spectra used to describe wave conditions at sea. In seakeeping the most often used is the spectrum recommended by the ISSC (International Ship and Offshore Structures Congress) and the so-called Jonswap wave spectrum. The ISSC (two-parameter) wave spectrum is appropriate to describe developed ocean waves; it is given by

$$S(\omega) = 171.44 \frac{H_{1/3}^2}{T_1^4 \omega^5} \exp\left(\frac{-685.76}{T_1^4 \omega^4}\right) \text{ [m}^2\text{s]}, \tag{6.41}$$

where T_1 is the average wave period. T_1 is related to the spectral moments by

$$T_1 = 2\pi m_0 / m_1. \tag{6.42}$$

The Jonswap spectrum can be evaluated either from the significant wave height and from the average period or from wind velocity U and fetch X. In the first case, the spectrum is given by

$$S(\omega) = 155 \frac{H_{1/3}^2}{T_1^4 \omega^5} \exp\left(\frac{-944}{T_1^4 \omega^4}\right) (3.3)^{\gamma} \text{ [m}^2\text{s]}, \tag{6.43}$$

where

$$\gamma = \exp\left[-\left(\frac{\omega/\omega_0 - 1}{\sqrt{2}\sigma}\right)^2\right] \tag{6.44}$$

and

$\sigma = 0.07$ for $\omega \le 5.24 T_1$
$\sigma = 0.09$ for $\omega > 5.24 T_1$.

In the second case, the Jonswap spectrum is given by

$$S(\omega) = \frac{\alpha g^2}{\omega^5} \exp\left[-\frac{5}{4}\left(\frac{\omega_0}{\omega}\right)^4\right] (3.3)^{\gamma} \text{ [m}^2\text{s]}, \tag{6.45}$$

where the so-called Philip's number is

$$\alpha = 0.076 \left(\frac{gX}{U^2}\right)^{-0.22}, \tag{6.46}$$

with U [m/s] and X [m] being the wind velocity and fetch respectively. Fetch means the sea distance over which wind blows. The so-called modal angular frequency is denoted by ω_0 and given by the relation

$$\omega_0 = 7\pi \frac{g}{U}\left(\frac{gX}{U^2}\right)^{-0.33}. \tag{6.47}$$

This frequency is related to the modal period by the expression $\omega_0=2\pi/T_0$ For the Jonswap spectrum, the following relation for the spectral periods holds (Faltinsen, 1990)

$$T_1 = 0.834T_0. \tag{6.48}$$

Both wave spectra are presented in Figure 6.13.

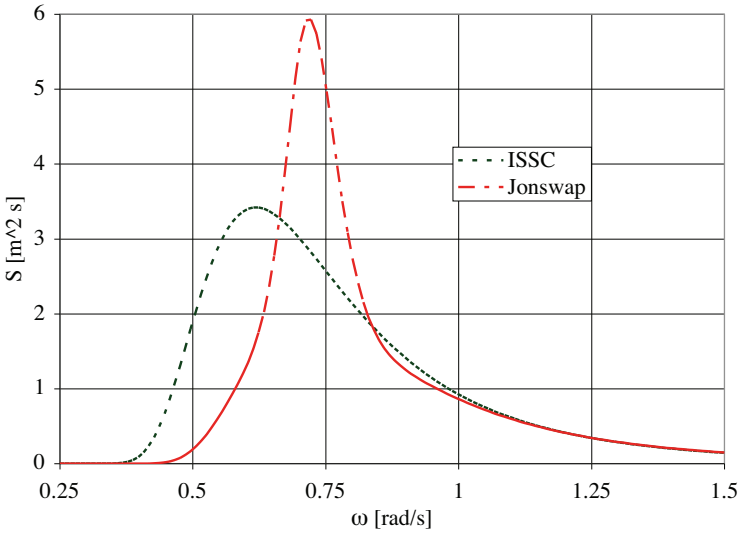

Fig. 6.13 ISSC and Jonswap wave spectra. T_1=7.5 [s] and H_S=4.5 [m].

As can be seen from the spectra comparison, the frequency content of Jonswap spectrum is more concentrated and located more towards higher frequencies, i.e. shorter waves. This means that this spectrum is usually better suited for a raising storm and for a limited fetch than the other one.

6.5.2 Short-crested irregular waves

An extension of Fourier representation (6.38) of surface waves allowing for wave propagation at angle μ with respect to axis X of the co-ordinate system fixed with Earth of the form

$$\zeta(X_0,Y_0;t)=\sum_{i=1}^{N}A_i\cos\left[k_i\left(X_0\cos\mu_i+Y_0\sin\mu_i\right)-\omega_i t+\delta_i\right] \tag{6.49}$$

can in principle be used. Similarly as for the long-crested waves, a spectral representation of directional spectrum $S(\omega,\mu)$ can be derived such that

$$\sigma^2=\int_0^{2\pi}\int_0^{\infty}S(\omega,\mu)d\omega d\mu. \tag{6.50}$$

The feature of multi-directional wave propagation, if at all taken into account, is modelled by introducing the so-called spreading function $f(\mu)$ such that the directional spectrum is presented as a product of two functions

$$S\left(\omega,\mu\right)=S\left(\omega\right)f(\mu). \tag{6.51}$$

ITTC recommends a spreading function of the form

$$f(\mu)=\frac{2}{\pi}\cos^2\mu,\ \text{where}\ -\pi/2<\mu<\pi/2. \tag{6.52}$$

7. Hydrodynamic forces acting on a rigid body in waves

7.1 Velocity potential due to ship oscillatory motion and caused by wave action

We assume that the flow associated with the motion of a ship hull in waves is well represented by the potential flow approximation. That is, we disregard the viscous effects. A ship is a rigid body moving in six degrees of freedom. The action of regular sinusoidal form waves of frequency ω is felt by a moving ship as the oscillatory excitation with the encounter frequency ω_e. We disregard initial transients and assume linearity of the ship's response to wave action. This motion in the *j*-th degree of freedom is denoted by ξ_j and it is given by the formula

$$\xi_j(x,y,z,t) = \xi_{0j} e^{i\omega_e t}, \tag{7.1}$$

where ξ_{0j} is the complex amplitude of the *j*-th displacement component. Note that for the sake of convenience, we use exponential function notation rather than trigonometric functions for representing the oscillatory motion. The real part of (7.1) can be taken in order to have an instantaneous value of displacement.

Moreover, at least at the beginning, we assume that the amplitudes ξ_{0j} of this oscillatory motion are small. This assumption means that the waves affecting ship are of small amplitude, too. Another important fact resulting from the small amplitude assumption is that we do not have to take into account complicated relations (3.4) and (3.6) between the inertial and body-fixed coordinate systems when describing ship motions.

This means that the following simplified relations hold:

$$\dot{\xi}_1 = u = \dot{X}_G,\ \dot{\xi}_2 = v = \dot{Y}_G,\ \dot{\xi}_3 = w = \dot{Z}_G,\ \dot{\xi}_4 = p,\ \dot{\xi}_5 = q,\ \dot{\xi}_6 = r. \tag{7.2}$$

The assumption of linearity substantially simplifies equations of motion (4.4) and (4.7).

Velocity of any point P of the body can be presented in the following form

$$\mathbf{V} = \mathbf{V}_0 + \Omega \times \mathbf{r}, \tag{7.3}$$

where $\mathbf{V}_0$ is the velocity of the origin, $\mathbf{\Omega}=p\mathbf{i}+q\mathbf{j}+r\mathbf{k}$ is the angular velocity, and $\mathbf{r}$ is the position vector of point P. The velocity normal to the body surface is given by

$$\begin{aligned} v_n &= \mathbf{V}_0 \bullet \mathbf{n} + (\Omega \times \mathbf{r}) \bullet \mathbf{n} = \mathbf{V}_0 \bullet \mathbf{n} + \Omega \bullet (\mathbf{r} \times \mathbf{n}) \\ &= \dot{\xi}_1 n_1 + \dot{\xi}_2 n_2 + \dot{\xi}_3 n_3 + \dot{\xi}_4 (\mathbf{r} \times \mathbf{n})_1 + \dot{\xi}_5 (\mathbf{r} \times \mathbf{n})_2 + \dot{\xi}_6 (\mathbf{r} \times \mathbf{n})_3 \\ &= \sum_{j=1}^{3} \dot{\xi}_j n_j + \sum_{j=4}^{6} \dot{\xi}_j (\mathbf{r} \times \mathbf{n})_{j-3}, \end{aligned} \tag{7.4}$$

where $\mathbf{n}$ is the unit normal to the body surface directed into the body and n_j is projection of it in the j-th direction.

As the motion is oscillatory, with constant amplitude, this means that we disregard the transients and concentrate on the fully developed responses caused by regular linear waves, such as the ones given by formula (6.12) or (6.23). The small amplitude assumption makes it possible to use the benefits of the model's linearity. The biggest advantage is in using the superposition principle. This allows us to construct the total flow model and the ship response to waves as the sums of simple sub-models. Thus, for instance, the responses in irregular sea waves can be easily computed using the spectral representation of surface waves presented in Section 6.5.

A linearity assumption makes it also possible to present the total flow due to the ship oscillatory motion and caused by waves as a sum of velocity potentials

$$\phi(x,y,z,t) = \mathrm{Re}\left\{\left[\sum_{j=1}^{6}\xi_{0j}\phi_j(x,y,z) + A\phi_A(x,y,z)\right]e^{i\omega_e t}\right\}. \tag{7.5}$$

The flow disturbance produced by a ship's motion in still water is represented by the first term (sum-term) in the brackets. An oscillatory motion of a ship in the *j*-th degree of freedom with unit amplitude is represented by the velocity potential ϕ_j. The action of waves is represented by the second term in the brackets. This term comprises the amplitude of the velocity potential of an oncoming wave having an amplitude of 1 m (see Eq. 6.10) and denoted in the following by ϕ_0, and the amplitude of the so-called diffraction potential ϕ_7. The latter takes into account the disturbance effect of the ship on the oncoming wave. Thus the amplitude of the velocity potential describing the action of a wave having amplitude equal to 1 m can be written as the sum of both potentials:

$$\phi_A = \phi_0 + \phi_7. \tag{7.6}$$

7.2 Boundary conditions

The boundary conditions for the oncoming waves were dealt with in Section 6.1. The boundary condition for the diffraction velocity potential stems from the fact that there is no flow through the hull surface S_B. This means that the normal velocity component of flow due to oncoming waves and that of the diffracted waves must be of the same magnitudes but of the opposite sign, that is

$$\frac{\partial\phi_7}{\partial n} = -\frac{\partial\phi_0}{\partial n} \tag{7.7}$$

at the body surface S_B. This is equivalent to the requirement that the normal component of the total to hull flow velocity due to waves is zero that is

$$\frac{\partial\phi_A}{\partial n} = 0. \tag{7.8}$$

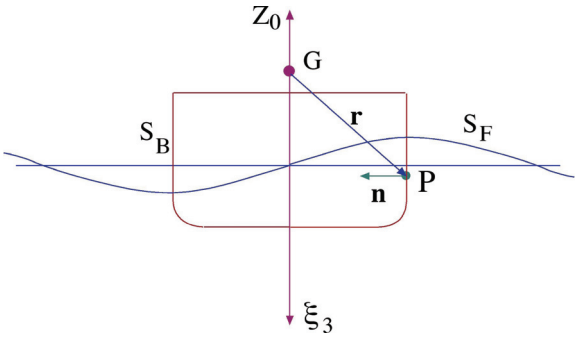

Fig. 7.1 Cross section of a ship in beam seas

An assumption of linearity makes it possible to apply boundary condition (7.8) for a stationary that is a non-oscillating ship.

The velocity potentials of flow due to the body motion have to also fulfil the no-penetration boundary condition. This means that the normal component of the fluid velocity at each point on the hull surface has to be the same as the corresponding body velocity component in the direction normal to the body surface. This requirement applies to each degree of freedom *j*. According to Formula 7.4 the velocity of any point P at the hull surface associated with the *j*-th degree of freedom motion and oriented in the *j*-th direction is

$$\begin{aligned} &\frac{\partial \xi_j(t)}{\partial t} n_j = i\omega_e \xi_{0j} e^{i\omega_e t} n_j, \text{ for } j = 1,2,3 \\ &\frac{\partial \xi_j(t)}{\partial t} \left(\mathbf{r} \times \mathbf{n}\right)_{j-3} = i\omega_e \xi_{0j} e^{i\omega_e t} \left(\mathbf{r} \times \mathbf{n}\right)_{j-3}, \text{ for } j = 4,5,6, \end{aligned} \tag{7.9}$$

while the corresponding flow velocity is

$$\frac{\partial \left[\xi_{0j} \phi_j(x,y,z) e^{i\omega_e t}\right]}{\partial n} = \frac{\partial \phi_j(x,y,z)}{\partial n} \xi_{0j} e^{i\omega_e t}. \tag{7.10}$$

Equating expressions 7.9 and 7.10 yields the boundary conditions for the velocity potential components corresponding to the oscillatory motion of the rigid body (Newman, 1977)

$$\begin{aligned}\frac{\partial \phi_j}{\partial n} &= i\omega_e n_j, \text{ for } j = 1,2,3 \\ \frac{\partial \phi_j}{\partial n} &= i\omega_e (\mathbf{r} \times \mathbf{n})_{j-3}, \text{ for } j = 4,5,6.\end{aligned} \tag{7.11}$$

7.3 Linear hydrodynamic forces in general

Hydrodynamic forces acting on a ship's hull can be evaluated using Bernoulli's equation

$$\rho \frac{\partial \phi}{\partial t} - \rho g Z_1 + \frac{1}{2}\rho |\mathbf{v}|^2 + p = C, \tag{7.12}$$

where Z_1 is the vertical distance measured from the still water level downwards. Using the velocity potential (7.5) and retaining in Bernoulli's equation only the linear terms, the following expression for the total pressure is obtained

$$p = -\rho \frac{\partial \phi}{\partial t} + \rho g Z_1 = -\rho \,\mathrm{Re}\left\{ \left[\sum_{j=1}^{6} \xi_{0j} \phi_j(x,y,z) + A(\phi_0 + \phi_7) \right] i\omega_e e^{i\omega_e t} \right\} + \rho g Z_1. \tag{7.13}$$

The total force **F** and moment **M** due to this pressure are obtained by

$$\begin{aligned}\begin{pmatrix} \mathbf{F} \\ \mathbf{M} \end{pmatrix} &= \int_S \begin{pmatrix} p\mathbf{n} \\ p(\mathbf{r} \times \mathbf{n}) \end{pmatrix} dS = \rho g \int_S \begin{pmatrix} \mathbf{n} \\ \mathbf{r} \times \mathbf{n} \end{pmatrix} Z_1 dS \\ &- \rho \,\mathrm{Re}\left[\sum_{j=1}^{6} i\omega_e \xi_{0j} e^{i\omega_e t} \int_S \begin{pmatrix} \mathbf{n} \\ \mathbf{r} \times \mathbf{n} \end{pmatrix} \phi_j dS \right] - \rho \,\mathrm{Re}\left[i\omega_e A e^{i\omega_e t} \int_S \begin{pmatrix} \mathbf{n} \\ \mathbf{r} \times \mathbf{n} \end{pmatrix} (\phi_0 + \phi_7) dS \right],\end{aligned} \tag{7.14}$$

where integrals are taken over the wetted surface of the hull. Using the boundary conditions 7.11, the k=1,2,3 component of force or moment (with k=4,5,6 for x,y and z-directional component respectively) can be presented as

$$F_k = \rho g \int_S \begin{pmatrix} n_k \\ (\mathbf{r} \times \mathbf{n})_{k-3} \end{pmatrix} Z_1 dS - \rho \mathrm{Re}\left[\sum_{j=1}^{6} \xi_{0j} e^{i\omega_e t} \int_S \frac{\partial \phi_k}{\partial n} \phi_j dS \right]$$
$$-\rho A \mathrm{Re}\left[e^{i\omega_e t} \int_S \frac{\partial \phi_k}{\partial n} (\phi_0 + \phi_7) dS \right]. \tag{7.15}$$

The first term in (7.15) depicts the hydrostatic load. The second term describes the radiation forces while the third term represents the wave loading. The name radiation forces stems from the fact that these are the fluid reaction forces to the oscillatory motion with a finite acceleration. Radiation and wave forces are solved separately and they are evaluated for a ship moving steadily without wave-induced motions being taken into account. In other words, wetted surface S does not change.

7.4 Hydrostatic forces

Hydrostatic forces and moments depict the reactions of water acting in calm water on a hull subjected to a very slow motion. Note that these forces are dependent on the geometry of only the submerged part of the hull. As the hydrostatics were covered in the Ship Buoyancy and Stability course, only a brief summary is presented in the following of what was dealt with earlier. Instead, we shall elaborate on a three-dimensional model of evaluating the nonlinear hydrostatic loads.

7.4.1 Linear approximation

In case of the hydrostatic forces, a linearity assumption means that they are dealt with using the initial stability model. This model yields a linear relation between hull slow sinkage z_L, heel ϕ_L and trim θ_L motions and the corresponding restoring vertical force $Z_{\text{restoring,L}}$ and two corresponding moments $K_{\text{restoring,L}}$ and $M_{\text{restoring,L}}$. These relations are:

$$\begin{aligned} Z_{\text{restoring L}} &= -\rho g A_W z_L + \rho g A_W x_F \theta_L \\ K_{\text{restoring L}} &= -\mathrm{mg}\overline{GM}_T \phi_L \\ M_{\text{restoring L}} &= \rho g A_W x_F z_L - \mathrm{mg}\,\overline{GM}_L \theta_L , \end{aligned} \tag{7.16}$$

where A_W is the waterplane area, x_F is the longitudinal position of the centre of floatation and GM_T and GM_L are the transversal and longitudinal metacentric heights, respectively.

7.4.2 Nonlinear models

In principle there is no obstacle to use a fully nonlinear representation of the restoring forces and moments. Two nonlinear models are normally used when evaluating them. The first one is known from classical hydrostatics. In this model the restoring force $Z_{restoring}$ and moments $K_{restoring}$ and $M_{restoring}$ are based on the global geometrical properties of the immersed part of the hull, such as volumetric buoyancy, water-plane area and static levers of the restoring moments. This method is particularly suitable for ships.

The second model, used in the LaiDyn method, is based on a discrete representation of the hull using panels. In this model the restoring force and moment are evaluated by summing up discrete pressure forces acting at each panel in contact with water. In other words the wetted surface S takes into account an instantaneous position of ship in waves. This model can be used for ships and for offshore structures of a general shape. It is also very suitable when evaluating the so-called Froude-Krylov part of a wave load. For this reason this model is discussed here in a more detail.

Triangular flat panels cover the hull surface including the weather deck. Three points $P_1(x_1,y_1,z_1)$, $P_2(x_2,y_2,z_2)$ and $P_3(x_3,y_3,z_3)$ in a three-dimensional space described by the body-fixed co-ordinate system xyz define a single panel. The so-called control point of this panel is given by

$$\begin{aligned} x_c &= (x_1 + x_2 + x_3)/3 \\ y_c &= (y_1 + y_2 + y_3)/3 \\ z_c &= (z_1 + z_2 + z_3)/3 \end{aligned} \tag{7.17}$$

and as a result, the position of a panel in the body-fixed co-ordinate system is given by

$$\mathbf{r} = x_c\mathbf{i} + y_c\mathbf{j} + z_c\mathbf{k} \tag{7.18}$$

while its surface area is

$$\Delta S = \frac{1}{2}\sqrt{\begin{vmatrix} y_1 & z_1 & 1 \\ y_2 & z_2 & 1 \\ y_3 & z_3 & 1 \end{vmatrix}^2 + \begin{vmatrix} z_1 & x_1 & 1 \\ z_2 & x_2 & 1 \\ z_3 & x_3 & 1 \end{vmatrix}^2 + \begin{vmatrix} x_1 & y_1 & 1 \\ x_2 & y_2 & 1 \\ x_3 & y_3 & 1 \end{vmatrix}^2} \,. \tag{7.19}$$

Components of the normal vector at the control point can be evaluated from the following expressions derived from the definition of the vector product

$$\mathbf{c} = \mathbf{a} \times \mathbf{b} = \begin{vmatrix} \mathbf{i} & \mathbf{j} & \mathbf{k} \\ a_x & a_y & a_z \\ b_x & b_y & b_z \end{vmatrix}, \tag{7.20}$$

where

$$\begin{aligned} \mathbf{a} &= a_x\mathbf{i} + a_y\mathbf{j} + a_z\mathbf{k} = (x_1 - x_3)\mathbf{i} + (y_1 - y_3)\mathbf{j} + (z_1 - z_3)\mathbf{k} \\ \mathbf{b} &= b_x\mathbf{i} + b_y\mathbf{j} + b_z\mathbf{k} = (x_2 - x_3)\mathbf{i} + (y_2 - y_3)\mathbf{j} + (z_2 - z_3)\mathbf{k}. \end{aligned} \tag{7.21}$$

The normal to the panel is given by

$$\mathbf{n} = \mathbf{c}/|\mathbf{c}|. \tag{7.22}$$

Note that two co-ordinate systems are used when evaluating the hydrostatic loads. The position of the panel (given by the co-ordinates of its control point) and the components of the normal vector **n** are given in the body-fixed co-ordinate system (*xyz* of Fig. 1). The depth Z_c of each control point is measured in the global inertial co-ordinate system (*XYZ* in figures 3.1 and 7.2). The following relation, being derived from expression (3.4), can be used when transforming the control or other ship's points (x_c,y_c,z_c) from the moving body-fixed co-ordinate system to the Earth-fixed inertial system

$$\begin{Bmatrix} X_c \\ Y_c \\ Z_c \end{Bmatrix} = \begin{Bmatrix} \delta X_G \\ \delta Y_G \\ \delta Z_G \end{Bmatrix} + \begin{bmatrix} \cos\psi\cos\theta & \cos\psi\sin\theta\sin\phi & \cos\psi\sin\theta\cos\phi \\ & -\sin\psi\cos\phi & +\sin\psi\sin\phi \\ \sin\psi\cos\theta & \sin\psi\sin\theta\sin\phi & \sin\psi\sin\theta\cos\phi \\ & +\cos\psi\cos\phi & -\cos\psi\sin\phi \\ -\sin\theta & \cos\theta\sin\phi & \cos\theta\cos\phi \end{bmatrix} \begin{Bmatrix} x_c \\ y_c \\ z_c \end{Bmatrix}. \tag{7.23}$$

In the above formula, δX_G, δY_G and δZ_G are surge, sway and heave displacements of the ship's centre of gravity G. Using the Formula 7.23, the one can evaluate the depth Z_c of any panel of a rigid ship having 6 degrees-of-freedom motion as follows

$$Z_c = \delta Z_G - x_c \sin\theta + y_c \cos\theta \sin\phi + z_c \cos\theta \cos\phi. \tag{7.24}$$

As could be expected, the panel's depth does not depend on surge, sway and yaw motions.

7.5 Nonlinear hydrostatic and Froude-Krylov forces

The Froude-Krylov pressures are the pressures in an undisturbed surface wave. For a linear (the so-called Airy) wave, this pressure is given by Expression 6.17. Moreover, the linearity assumption of the Froude-Krylov forces means that they are evaluated for a ship without taking into account wave-induced motions. Thus the pressure is evaluated at the stationary (non-oscillating) hull location without taking the disturbances to the waves caused by the ship into account. If we want to take into account the nonlinearities of the hydrostatic and Froude-Krylov forces we can integrate the pressure (6.17) or (6.31) given by

$$p = \rho g \left[\zeta e^{-k(Z_c+\zeta)} + Z_c \right] \tag{7.25}$$

over the instantaneous wetted surface S with Z_c given by 7.24 and for an instantaneous hull position. This is illustrated in Figure 7.2.

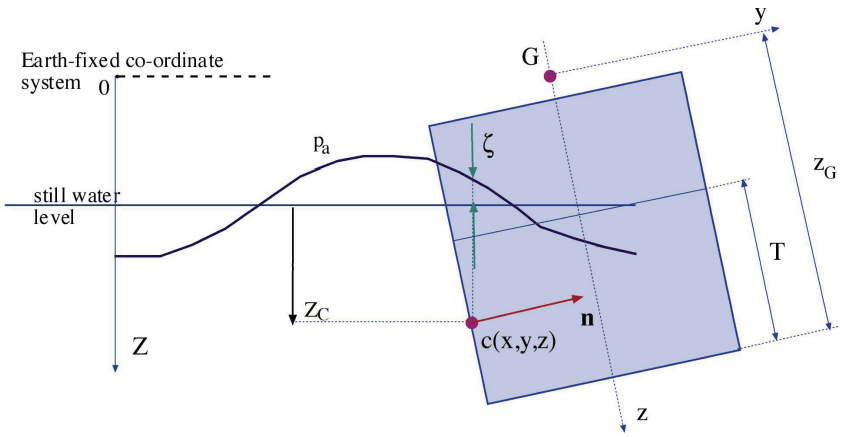

Fig. 7.2 Hydrostatic and Froude-Krylov pressure.

Wave elevation is given by

$$\zeta(t) = -\frac{1}{g}\frac{\partial \phi_0}{\partial t}\bigg|_{z_1=0} = A\cos\left[k\left(X_c\cos\mu - Y_c\sin\mu\right) - \omega t\right], \tag{7.26}$$

where ϕ_0 is the velocity potential of an oncoming wave given by (6.10), X_c and Y_c are the control points of the hull surface given in the Earth-fixed co-ordinate system *XYZ* evaluated with the aid of a transformation (7.23). This transformation and evaluation of wave height is illustrated in Figure 7.3 below.

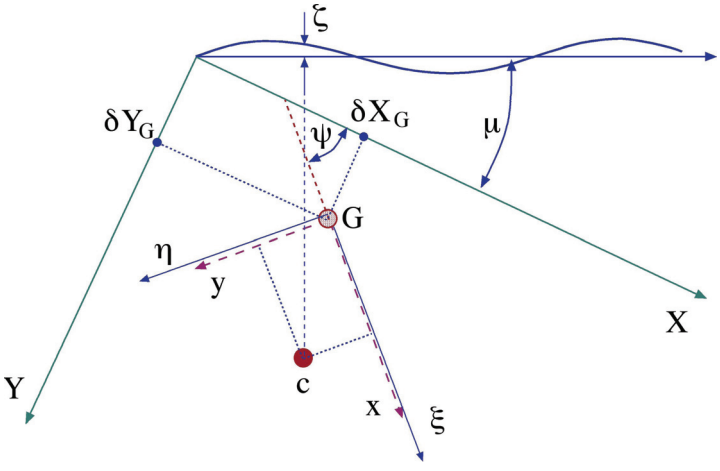

Fig. 7.3 Evaluation of wave height for a control point c.

The force **F** and moment **M** are obtained by integrating the pressure (7.24) in the body fixed co-ordinate system. This integration is performed numerically by summing up the contribution from each wetted panel using

$$\begin{aligned}\mathbf{F}_{\mathrm{F.K}}^{\mathrm{total}} &= \sum_{i}^{N} \mathbf{F}_{\mathrm{F.K;i}}^{\mathrm{total}} = \sum_{i}^{N} p_{\mathrm{i}} \Delta S_{\mathrm{i}} \mathbf{n}_{\mathrm{i}} \\ \mathbf{M}_{\mathrm{F.K}}^{\mathrm{total}} &= \sum_{i}^{N} \mathbf{r}_{\mathrm{i}} \times \mathbf{F}_{\mathrm{F.K;i}}^{\mathrm{total}},\end{aligned} \tag{7.27}$$

where N is the wetted panel number, ΔS_{i} is the panel area, $\boldsymbol{n}_{\mathrm{i}}$ is the unit vector normal to panel and $\boldsymbol{r}_{\mathrm{i}}$ is the position vector of the control point in the body fixed co-ordinate system xyz.

7.6 Radiation forces

The second term in (7.15) depicts the so-called radiation forces. As already stated, these are the forces acting on an oscillating body in still water. The k-th component of this force (moment for k=4,5,6) can be written as (Newman, 1980)

$$F_{rad,k} = -\rho \,\mathrm{Re}\left[\sum_{j=1}^{6} \xi_{0j} e^{i\omega_e t} \int_S \frac{\partial \phi_k}{\partial n} \phi_j dS\right] = \mathrm{Re}\left[\sum_{j=1}^{6} \xi_{0j} e^{i\omega_e t} f_{kj}\right], \tag{7.28}$$

where

$$f_{kj} = -\rho \int_S \frac{\partial \phi_k}{\partial n} \phi_j dS = -\rho \int_S \phi_j n_k dS \tag{7.29}$$

is a complex force in the k-th direction, due to a sinusoidal motion of unit amplitude in the direction j. In the unbounded liquid, radiation forces are the forces related to the acceleration of small amplitude oscillations with angular frequency ω. For the oscillations in the liquid bounded by a free surface, radiation force is not in-phase with acceleration only. It is a complex quantity, which is customarily presented as

$$f_{kj} = \omega^2 a_{kj} - i\omega b_{kj} \tag{7.30}$$

with a_{kj} and b_{kj} being the so-called added mass and damping coefficients, respectively. The k-th component of the radiation force can be expressed in terms of the added mass and damping coefficients as follows:

$$F_{rad,k} = -\sum_{j=1}^{6}\left(a_{kj}\dot{U}_j + b_{kj}U_j\right), \tag{7.31}$$

where U_j and $\dot{U}_j$ are velocity and acceleration of the oscillatory motion with the j-th motion component. It can be shown (Newman, 1980) that for a body in an unsteady motion and in an unbounded in-viscid fluid, radiation force is in-phase with the body's acceleration. In other words, the damping terms b_{kj} are zero. Moreover, the added mass coefficients are constant and they are dependent only on the body geometry.

Using the added mass definition 7.29 and applying the free surface boundary condition 6.9 to the velocity potential ϕ_j yields the conclusion that in the presence of a free surface, added mass and damping coefficients are dependent upon the angular frequency of the oscillatory motion. This dependency and the existence of the added damping stems from the free surface. There is a direct relation between damping and the amplitude of waves generated by the oscillating body (Newman, 1980). Thus the damping term can be attributed to wave-making due to the oscillatory motion of a body in the presence of a free surface. Newman (1980) also presents proof that both the added mass and damping coefficients are symmetrical so that

$$a_{kj} = a_{jk} \text{ and } b_{kj} = b_{jk}. \tag{7.32}$$

The details of evaluating the coefficients of added mass and damping are given by Newman (1980), Ohkusu (1996) and Lloyd (1989), among others. Added mass and damping coefficients are usually evaluated using a co-ordinate system with the origin located at the water-plane. The equations of motion are normally derived with the origin located in the centre of gravity. For this reason, the coefficients obtained have to be transferred to the body-

fixed co-ordinate system *x,y,z*. This transformation is presented in Appendix A.

7.6.1 Radiation forces and nonlinear models of ship dynamics

Added mass and damping terms (7.30) are normally derived for a small amplitude oscillatory motion. This means that their use is in principle restricted to the linear model of ship dynamics, where the wetted surface of the hull is constant and does not change in time. Moreover, this model of radiation forces is good for monochromatic oscillatory ship motion that is sinusoidal motion with a single frequency. The latter restriction is relaxed with the use of the so-called retardation function dealt with in the next section. There are two linear approximate approaches of defining the radiation forces in the nonlinear models of ship dynamics. The one, used in the following, is based on the assumption that the linear radiation forces are fixed with a ship hull. This is illustrated in Figure 7.4a. Another approach is to assume that they are primarily ruled by the free surface and thus their orientation is given by the inertial Earth-fixed co-ordinate system, Figure 7.4b.

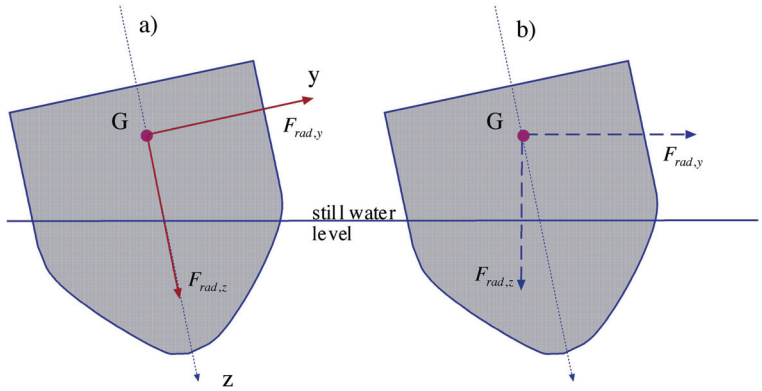

Fig. 7.4 Two definitions of radiation forces orientation.

7.6.2 Memory effect of the radiation forces

In the time domain simulations radiation forces have to take into account the history of the previous motion. The time domain approach requires the so-called convolution integral representation of the radiation forces (Cummins,

1962; Johansson, 1986). In this time-domain approach radiation forces vector $\boldsymbol{X}_{\text{rad}}$ is represented by the expression:

$$\mathbf{X}_{rad}(t) = -\mathbf{a}_{\infty}\ddot{\mathbf{x}}(t) - \int_{-\infty}^{t} \mathbf{k}\left(t-\tau\right)\dot{\mathbf{x}}(\tau)d\tau, \tag{7.33}$$

where $\boldsymbol{a}_{\infty}$ is the matrix comprising the added mass coefficients for an infinite frequency and $\boldsymbol{x}$ is the response vector. Matrix function $\boldsymbol{k}$ is the so-called retardation function, which takes into account the memory effect of the radiation forces. This function can be evaluated as:

$$\mathbf{k}(t) = \frac{2}{\pi}\int_{0}^{\infty} \mathbf{b}(\omega)\cos(\omega t)d\omega, \tag{7.34}$$

where $\boldsymbol{b}$ is the frequency dependent added damping matrix. The $\boldsymbol{k}(t)$ functions have to be evaluated before the simulation. The Fast Fourier Transform algorithm can be used when evaluating the retardation functions. The procedure is described in Appendix B.

7.7 Diffraction forces

The k-th component of the diffraction force is a second part of the wave loading given by

$$F_{Wave,k} = -\rho A \,\mathrm{Re}\left[e^{i\omega_e t}\int_{S}\frac{\partial\phi_k}{\partial n}\left(\phi_0+\phi_7\right)dS\right]. \tag{7.35}$$

The no-penetration boundary condition at the hull surface S implies that the following holds:

$$\frac{\partial\left(\phi_0+\phi_7\right)}{\partial n} = 0, \tag{7.36}$$

that is

$$\frac{\partial \phi_7}{\partial n} = -\frac{\partial \phi_0}{\partial n} \tag{7.37}$$

at the hull surface.

The knowledge of the wave potential ϕ_0 and condition 7.36 makes it possible to evaluate the diffraction potential in a similar way as the potential of the radiation problem.

8. Single degree of freedom linear system

For the sake of simplicity, we shall first consider a simple case of a heaving conical shape buoy like the one presented in Fig. 8.1.

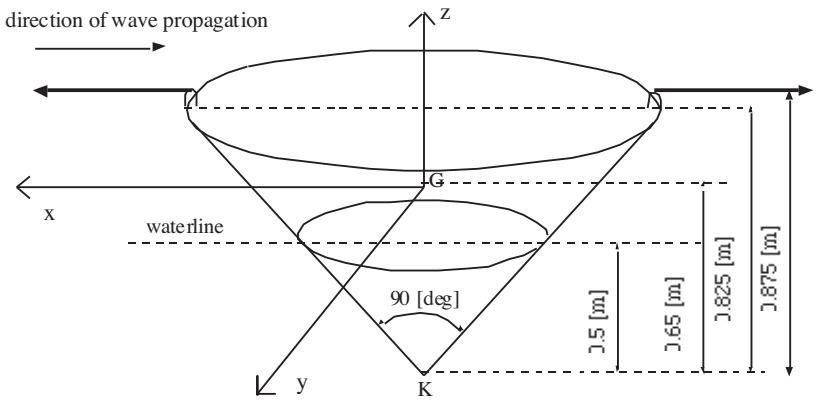

Fig. 8.1 Conical buoy.

Note that a single degree of freedom linear representation of ship rolling motion was presented in the textbook on ship buoyancy and stability (Matusiak, 1995). The heave motion z of a conical buoy in regular waves can be approximated by the formula

$$\left(m + a_{zz}\right)\ddot{z} + b_{zz}\dot{z} + kz = F_{Wave,z}\left(t\right), \tag{8.1}$$

where m is buoy mass, a_{zz} is added mass associated with the harmonic heave motion, b_{zz} is the damping coefficient, k is the restoring coefficient and $F_{\mathrm{Wave},z}$ is the excitation force caused by the action of regular waves (6.12).

Note that both the added mass and damping coefficients depend upon the motion frequency ω. Coefficients a_{zz} and b_{zz} (added mass and damping) represent the radiation force acting on a buoy in a heaving harmonic motion. Coefficients a_{zz} and b_{zz} are presented in Figure 8.2 below in a non-dimensional form as $a_{zz}/(\rho D^3)$ and $b_{zz}/(\rho D^3 \omega)$, where D is a diameter of the water-plane area.

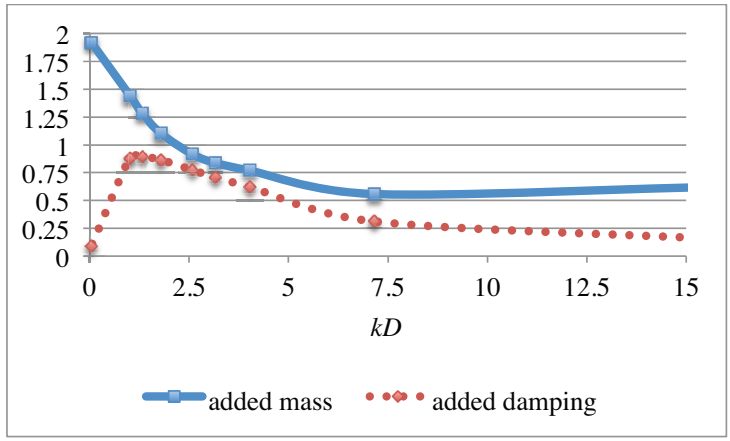

Fig. 8.2 Non-dimensional coefficients of added mass and damping of a conical buoy as a function of non-dimensional wave number kD.

These coefficients were obtained using the three-dimensional diffraction problem solving method of Garrison (1974).

In Equation 8.1, the first term on the left side depicts the inertia force of the heaving buoy, including the added mass of water following this motion. The second term describes the damping force associated with this motion. This is mainly caused by the wave-making effect of the heaving motion. The third term is the restoring force known from the hydrostatics i.e. $k=\rho g A_W$, where A_W is the water-plane area (refer to Eq. 7.16). Thus the left side of Equation 8.1 represents the forces acting on the heaving buoy without taking into account the wave effect. In other words the water surface remains still (flat). Linearity assumption implies small amplitude motion. This makes it possible to assume that coefficients a_{zz} and b_{zz} are constant for harmonic motion with a fixed frequency ω. The action of waves is represented by the right side of Equation (8.1). The linear model of it means that it is linearly

related to the wave amplitude *A* (refer to sections 7.6 and 7.7) and that it can be evaluated for a stationary buoy in a water domain limited by the still water level.

The natural angular frequency and damping ratio of the Single-Degree-Of-Freedom system 8.1 are given by

$$\omega_z = \sqrt{k/(m + a_{zz})} \tag{8.2}$$

and

$$\xi_z = \frac{b_{zz}}{2\omega_z (m + a_{zz})}. \tag{8.3}$$

8.1 Outline of the solution method

The solution of Equation 8.1 is normally sought in the frequency domain. This means that the solution is derived for a number of discrete frequency values covering a relevant range of waves' lengths. The linearity of the model makes it possible to seek solution for the waves of unit amplitude.

8.1.1 Hydrodynamic problem

For floating bodies possessing a general three-dimensional form there are no simple closed form solutions for added masses, damping coefficients and diffraction forces. However, there are numerical methods, based on panel discretization of the body surface and on a special Green function fulfilling the free surface conditions, capable of solving the problem stated by equations 7.28 and 7.36 (Ohkusu, 1996; Garrison, 1974). The solution is sought for a single frequency at a time. Usually these methods do not allow for a forward speed of a body, and thus they are not fully capable of solving the problem of ship hydrodynamics in waves.

8.1.2 Heave response of a buoy in waves of unit amplitude

The linear wave excitation model yields the right hand side of equation 8.1 of the form

$$\frac{F_{Wave,z}(t)}{m+a_{zz}} = \frac{F^0_{Wave,z}}{m+a_{zz}}\cos(\omega t+\delta). \tag{8.4}$$

where $F^0_{Wave,z}$ is the amplitude of the wave force and δ is the phase angle referred to the situation where a wave crest is passing the origin G in Fig. 8.1.

For a lightly damped case (ξ_z<1), Equation 8.1 has a particular solution of the form (Kreyszig, 1993)

$$\frac{z(t)}{A} = \frac{F^0_{Wave,z}/A}{\sqrt{(m+a_{zz})^2\left(\omega_z^2-\omega^2\right)^2+b_z^2\omega^2}}\cos(\omega t+\delta-\varepsilon), \tag{8.5}$$

where ε is the phase angle of the response referred to the wave excitation force given by

$$\varepsilon = \arctan\frac{\omega b_z}{(m+a_z)\left(\omega_z^2-\omega^2\right)}. \tag{8.6}$$

Taking the particular solution 8.5 as the only response component implies that the transients due to the initial conditions have died out and the response has achieved a steady state. Moreover, the linearity of Equation 8.1 is assumed. The form of response 8.5 as related to wave amplitude A is a very convenient non-dimensional form making it possible to use a very efficient and useful concept of transfer function.

The form 8.5 of response z suggests that for a wave of unit amplitude, response amplitude is dependent upon the frequency of wave excitation only. In other words Eq. 8.5 can be written as

$$\frac{z(t)}{A} = \frac{z_0}{A}(\omega)\cos(\omega t+\delta-\varepsilon) = \frac{z_0}{A}(\omega)\cos(\omega t+\gamma), \tag{8.7}$$

where

$$\frac{z_0}{A}(\omega) = \frac{F^0_{Wave,z} / A}{\sqrt{\left(m + a_{zz}\right)^2 \left(\omega_z^2 - \omega^2\right)^2 + b_z^2 \omega^2}} \tag{8.8}$$

is called Response-Amplitude-Operator (abbrev. RAO) and γ is the phase angle referred to in the situation where a wave crest is passing the origin. Both RAO and phase angle γ define the transfer function of a linear dynamic system. The response amplitude operator of a heaving buoy, as computed by the three-dimensional panel method of Garrison (1974), is shown in Fig. 8.3. Note that the frequency axis is also made non-dimensional. It is customary to use the ratio of wave length λ related to characteristic length of the body instead of frequency. In case of the buoy its diameter D at the water-plane is used as the characteristic measure.

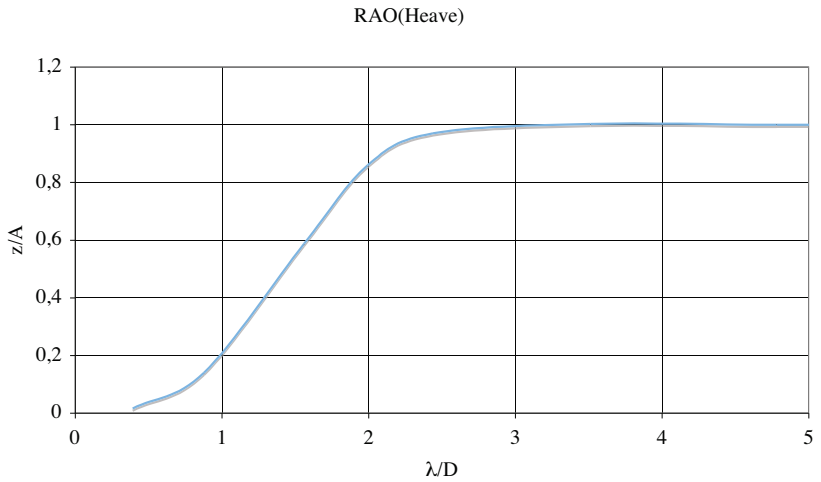

Fig. 8.3 Response amplitude operator of the heaving buoy presented in Figure 8.1.

As seen from the Figure 8.3, for wave lengths below two times the water-plane diameter of the cone, the heaving motion of the body is smaller than the wave elevation. For longer waves, heaving motion follows very closely the wavy water surface. Note that for waves' lengths in excess of three times the diameter D, RAO is very close to unity. Unlike the transfer function of roll motion, the RAO of heave does not exhibit motion amplification at

resonance. This is mainly due to a substantial damping associated with wave-making caused by a heaving body. The non-dimensional form of presentation allows a fast evaluation of the scale-free responses both for model- and full-scale. For instance, a buoy with a water-plane diameter of 10 m in a wave of 10 m in length and 0.5 m amplitude will have a heaving motion of 0.1 m amplitude.

9. Linear approximation to ship motion in waves

A linear approximation of a ship motion in waves disregards all the nonlinear terms of the general equations of motion (4.4) and (4.7). With this simplification, the equations of motion are of the form

$$\begin{aligned} m\dot{u} &= X \\ m\dot{v} &= Y \\ m\dot{w} &= Z \\ I_x\dot{p} - I_{xy}\dot{q} - I_{xz}\dot{r} &= K \\ I_y\dot{q} - I_{yx}\dot{p} - I_{yz}\dot{r} &= M \\ I_z\dot{r} - I_{zx}\dot{p} - I_{zy}\dot{q} &= N. \end{aligned} \tag{9.1}$$

The left-hand sides of Equations 9.1 represent inertia forces and moments of a ship without the contribution of added masses. The right-hand sides of the equations 9.1 are comprised of the restoring, radiation and wave excitation (Froude-Krylov and diffraction) forces. These are also simplified in the linear models given in paragraph 7.4.1 and sub-chapters 7.6 and 7.7. Equation of surge motion component, that is x-directional equation, does not include hull resistance or propeller. Usually the forward speed of the vessel is assumed to be nearly constant with small oscillatory variations caused by the wave action. Harmonic surge motion, as well as other motion components, occurs with the encounter frequency.

Linearization of the equations precludes simulation of ship manoeuvring. The equations 9.1 are very suitable to evaluate linear, that is small amplitude, motions in not too steep waves.

9.1 Solution to the hydrodynamic problem of ship motions in waves

When evaluating hydrodynamic forces on a hull, different methods and discretization types of hull geometry are used. Because of the general form three-dimensional nature of a hull form, numerical methods are used when evaluating radiation and diffraction forces. The most common is the so-called strip-method. The slenderness of a ship hull makes it possible to discretize the hull in the longitudinal direction, that is divide it into a number (from 10 to 20) strips as shown in Figure 9.1 below.

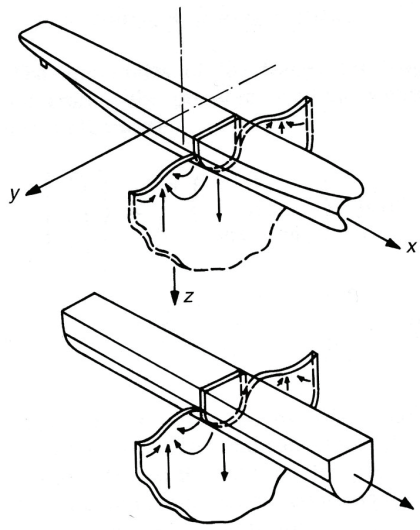

Fig. 9.1 Strip-representation of a ship hull when evaluating hydrodynamic forces (Bertram 2000).

The radiation/diffraction problem is solved on each of the strips separately, either by a simple two-dimensional panel method or by using conforming mapping techniques (Journee, 1992). Thus the concerned problem is handled with a two-dimensional approximation in which each hull frame (strip) is represented by a cylinder having the same cross section and an infinite length. Added mass and damping coefficients, hydrodynamic and hydrostatic forces are evaluated for an entire hull by summing-up partial (strip-wise) solutions. In the radiation problem the cylinder is oscillating in a still water. Diffraction forces are solved by setting the cylinder in regular waves and imposing the boundary condition 7.37. A simple model taking

into account the forward speed of the vessel is usually utilized. The methods based on this approach are called strip methods. Details of the algorithms will be not given in this textbook. The reader interested in them should refer to the books and publications of Makoto Ohkusu, Johan Journee and A.R.J.M. Lloyd.

There are also the 3-dimensional methods capable of solving the radiation and diffraction problem without making the assumption of two-dimensional flow nature. These potential flow theory based, so-called panel or boundary element, methods can be divided into two classes in two different ways.

First, they can be divided according to computational domain. The solution can be sought in the frequency domain or in the time domain. The frequency domain means that a harmonic mono-chromatic small amplitude motion (radiation problem) or wave of small amplitude (for in diffraction problem) is considered at a time, and a solution is sought in in form of pressures in the discrete points representing the hull up to the still water level. The process is repeated for a number of frequencies covering the frequency range relevant for ship motions or for the investigated wave-lengths. The problem is linearized, which means that the wetted surface of a hull does not change and extends to the still-water level. The pressures are summed up (Eq. 7.27) and as a result of computations radiation forces for a unit ship motion added masses and damping coefficients are obtained. Same is done for a wave of unit amplitude and as a result diffraction forces are obtained.

Computation in the time domain makes it possible in principle to take different nonlinearities into account; that is, pressures are evaluated for an instantly wetted portion of the hull surface. In other words, in the latter case pressures may be computed taking into account ship motions and wave profile along the hull.

Another division of the methods is according to the type of Green function used when evaluating the flow. In the so-called *Green Function Method (GFM),* the flow domain is limited to the flat free surface level. Hull discretization may be either extend to the still water level or take into account variations in the wetted surface. A special, complicated form Green

function is used. This function automatically fulfils the boundary conditions at the free surface.

In the *Rankine Singularity Method (RSM),* the Green function is of a very simple form G=1/r, so the complicated, slowly converging oscillatory form of the function does not have to be used. The drawback of *RSM* is the fact that both ship hull surface and still water surface have to be discretized by panels in this case. A comprehensive review of the methods briefly described above is given for instance by Bertram (2000).

9.2 Outline of the solution of the linear ship motion in waves problem

The solution of equations 9.1 is usually sought in the frequency domain. Thanks to the system's linearity, the response to the regular that is monochromatic, linear waves occurs at the frequency of encounter ω_e which is related to the wave frequency according to the equation 6.24. The responses can be expressed in the non-dimensional form as

$$\begin{aligned}
&\frac{x(t)}{A}=\frac{x_0}{A}\cos\left(\omega_e t+\gamma_x\right),\ \frac{y(t)}{A}=\frac{y_0}{A}\cos\left(\omega_e t+\gamma_y\right),\\
&\frac{z(t)}{A}=\frac{z_0}{A}\sin\left(\omega_e t+\gamma_z\right),\frac{\phi(t)}{kA}=\frac{\phi_0}{kA}\cos\left(\omega_e t+\gamma_\phi\right),\\
&\frac{\theta(t)}{kA}=\frac{\theta_0}{kA}\cos\left(\omega_e t+\gamma_\theta\right),\ \frac{\psi(t)}{kA}=\frac{\psi_0}{kA}\sin\left(\omega_e t+\gamma_\psi\right).
\end{aligned} \tag{9.2}$$

Note that angular responses are made non-dimensional by dividing them by wave steepness *kA*. Equations 9.1 suggest that the determination of responses 9.2 is a straightforward task. However, it is not that easy and not unified because of the complexity and due to different approaches used to solve radiation and diffraction forces. It is customary to use the strip theory approach described in Section 8.1. That is the hydrodynamic forces are evaluated using a two-dimensional model for a finite number (10 to 20) of ship hull sections. These forces are summed up in the total forces acting on ship hull to be used in equations 9.1.

9.3 Transfer function of ship motion, response spectra

An example of the transfer functions of a modern passenger vessel is shown in Figure 9.2.

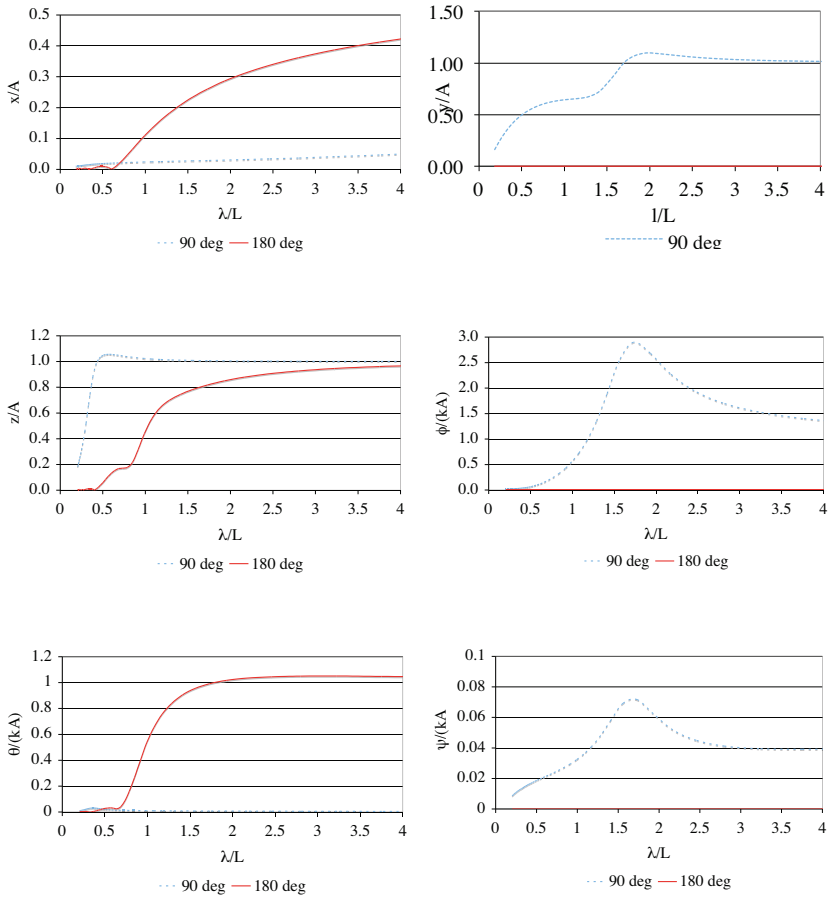

Fig. 9.2 Transfer function of motions in waves of a RoPax vessel; Fn=0.224.

For the sake of clarity, only RAOs of motion components are shown. It is worth noting that transfer functions depend upon the ship's speed and heading. Normally, roll is the only motion component that exhibits resonant behaviour. Sway, heave and pitch motion components are low for wave lengths well below a ship's length, and as expected, they are close to wave amplitude or steepness for the long waves. There is no clear resonant behaviour associated with them.

The linear ship dynamics model does not predict non-symmetric ship motions in the symmetrically acting waves. For this reason, for the head and the following waves, RAOs of roll, sway and yaw are zero.

Transfer functions of a ship, such as these presented in Figure 9.2, can be obtained using some of the linear approximation based strip theories or experimentally by conducting model tests in regular waves.

One of the benefits of using the linear wave and ship dynamics models is the possibility of evaluating, in a straightforward manner, spectra of ship motions in irregular waves given by spectrum $S(\omega)$. This is done by the following operation

$$S_r(\omega_e) = \left|H(\omega_e)\right|^2 S(\omega_e) = RAO^2 S(\omega_e), \tag{9.3}$$

where S_r is the power spectral density of the response in question and $H(\omega_e)$ is the transfer function comprising *RAO* and phase information. Operation 9.3 is presented in Figure 9.3 below.

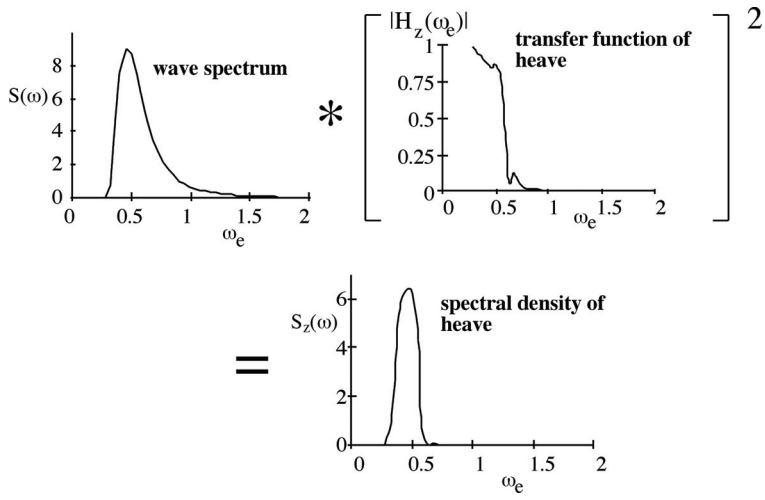

Fig. 9.3 Calculation of heave motion in irregular waves.

It should be noted that the frequency of encounter is used as an argument when evaluating response spectra. Sometimes another definition of *RAO* is used. In this definition, by *RAO,* the absolute value of transfer function squared is meant, that is $RAO=|H(\omega)|^2$. The spectrum of the encountered

waves can be derived assuming that the wave spectrum $S(\omega)$ is given and using the relation 6.24. The differential equation

$$\frac{d\omega_e}{d\omega} = 1 - \frac{2V\omega}{\mathrm{g}}\cos\mu \tag{9.4}$$

is obtained by differentiating equation 6.24. The wave energy contained within the frequency bandwidths $d\omega$ and $d\omega_e$ is not affected by ship motion. This means that the following holds

$$S(\omega_e)d\omega_e = S(\omega)d\omega \tag{9.5}$$

and as a result the wave spectrum in terms of the encounter frequency is given by

$$S(\omega_e) = S(\omega)\frac{d\omega}{d\omega_e} = S(\omega)\frac{\mathrm{g}}{\mathrm{g} - 2V\omega\cos\mu}. \tag{9.6}$$

Transformation 9.6 yields an increase in frequency and thus is visible as a shift of power density towards higher frequencies for head and bow waves (see Fig. 9.4).

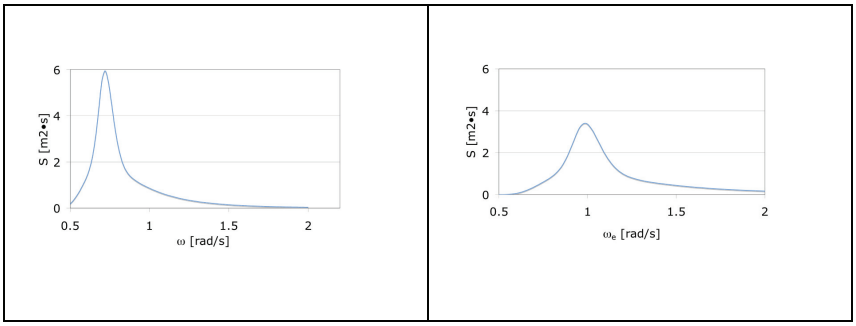

Fig. 9.4 Wave power spectrum of the Jonswap type (Hs=4.7 m, T1=7.5 s) as measured by a stationary buoy (left figure) and felt by a ship proceeding at a speed of 14 knots and heading angle of 135 [degrees] (right figure).

Having the power spectral density of the response in question evaluated with the aid of Equation 9.3, it is easy to derive the root-mean-square (rms) value from

$$\sigma_0 = \sqrt{m_0}, \tag{9.7}$$

where m_0 is zero-th spectral moment defined by Equation 6.40. The rms values of the time derivatives of the response in question are given by

$$\sigma_2 = \sqrt{m_2} \tag{9.8}$$

for the velocity and

$$\sigma_4 = \sqrt{m_4} \tag{9.9}$$

for the acceleration.

When evaluating the angular responses of a ship in irregular waves, it is feasible to use the spectrum of wave slopes instead of the spectrum of amplitudes. Knowing that for a deep water condition the slope of each wave component is $kA=A\omega^2/g$, the spectrum $S_\alpha(\omega)$ of wave slopes is

$$S_\alpha(\omega) = \frac{\omega^4}{g^2} S(\omega). \tag{9.10}$$

Another way of evaluating the responses in irregular waves is based on using the wave frequency rather than applying the frequency of encounter. In this approach the response spectra are obtained by the operation

$$S_r(\omega) = |H(\omega)|^2 S(\omega) \tag{9.11}$$

for the linear responses, and by

$$S_r(\omega) = |H(\omega)|^2 S_\alpha(\omega) \tag{9.12}$$

in case of angular responses. These spectral densities do not have much physical meaning but they can be transferred to the meaningful frequency of encounter equation 9.6. Using the wave frequencies ω when evaluating the responses in irregular waves is particularly useful for the following and

quartering waves, as it avoids the complexities of multi-valued spectral ordinates at the same encounter frequency (Lloyd, 1989).

10. Nonlinear model of ship motion in waves

If non-linear terms of the equations of motion (equations 4.4 and 4.7 and non-linear hydrodynamic terms discussed in Chapters 5 to 7) are to be included in the ship motion simulation than solution can not be sought in a frequency domain. Neither a powerfull and very usefull concept of transfer function can be used. Nonlinear mathematical model has to be solved in a time-domain instead. Ship motions in waves can be solved by integrating numerically the general non-linear equations of motions presented in Chapter 4 with the appropriate model of hydrodynamic reaction and excitation forces. When integrated, these equations yield velocitities $\mathbf{U}=u\mathbf{i}+v\mathbf{j}+w\mathbf{k}$ and $\boldsymbol{\Omega}=p\mathbf{i}+q\mathbf{j}+r\mathbf{k}$ in terms of their components expressed in the body-fixed, that is moving, co-ordinate system. In order to obtain the information on ship position in respect to the inertial Earth-fixed frame, these velocity components are projected on the Earth-fixed co-ordinate system and integrated into the position vector and Euler angles.

Ship resistance in still water, thrust of propeller(s), rudder forces and wind forces are evaluated as discussed in sub-chapters 5.6, 5.7 or 5.8 and 5.10. Hydrodynamic reaction forces due to the manoeuvring and excitation due to waves have to be taken into account when applying the models of Section 5.6 and Chapter 7. If manoeuvring in waves is of concern, there is the problem of different time scales and different hydrodynamic reaction forces associated with them. The so-called slow motion hydrodynamic derivatives of Section 5.6 were evaluated for the still water condition. Thus their application for the ship operating in waves may be questioned. A good compromise is to preserve only the terms related to velocities such as

Y_v, Y_r, N_v and N_r. The argument is that these terms include the effects that are related to slow motion, and they are mainly governed by the non-potential flow effects. The terms related to the accelerations are taken as added masses being related to the radiation forces (Sub-Section 7.6), with the flow memory effect being included.

10.1 Direct evaluation of ship responses in time domain used in the program LaiDyn

The equations of motion solved in time domain and resulting in a simulation of ship motions in waves are given below.

$$\begin{aligned}
\left(m+a_{11}\right)\dot{u}+a_{15}\dot{q} &= -\mathrm{mg}\sin\theta + X_{\text{resistance}} + X_{prop} + X_{rudder} + X_{wave} + X_{man} \\
&\quad -k_{15} + \left(m+a_{22}\right)\left(rv-qw\right) \\
\left(m+a_{22}\right)\dot{v}+a_{24}\dot{p}+a_{26}\dot{r} &= \mathrm{mg}\cos\theta\sin\phi + \left(m+a_{11}\right)\left(pw-ru\right) + Y_{man} \\
&\quad +Y_{rudder} + Y_{wave} - k_{22} - k_{24} - k_{26} \\
\left(m+a_{33}\right)\dot{w}+a_{35}\dot{q} &= mg\cos\theta\cos\phi + m\left(uq-vp\right) + Z_{wave} - k_{33} - k_{35} \\
a_{42}\dot{v}+\left(I_x+a_{44}\right)\dot{p}+a_{46}\dot{r} &= \left(I_y-I_z\right)qr - Y_{rudder}z_{rudder} + K_{man} + K_{wave} - k_{44} \\
&\quad -k_{42} - k_{46} + 2\xi p\omega_{\phi} \\
a_{15}\dot{u}+a_{53}\dot{w}+\left(I_y+a_{55}\right)\dot{q} &= \left(I_y-I_x\right)pr + X_{rudder}x_{rudder} + M_{wave} - k_{55} - k_{53} - k_{15} \\
a_{62}\dot{v}+a_{64}\dot{p}+\left(I_z+a_{66}\right)\dot{r} &= \left(I_x-I_y\right)pq + Y_{rudder}x_{rudder} + N_{man} + N_{wave} \\
&\quad -k_{66} - k_{62} - k_{64}
\end{aligned} \tag{10.1}$$

In principle, the above equations are the same as the ones discussed in Chapter 4 (equations 4.4 and 4.7). The difference is in an explicit inclusion of the hydrodynamic terms, which are discussed below.

Discussion of the terms included in the above equations of motion.

Radiation terms

The terms a_{ij} and k_{ij} are the added mass coefficients corresponding to the infinite frequency and elements of the memory function respectively, as described in Section 7.6.

Manoeuvring terms

The terms depicted by subscript ‘man’ are the manoeuvring forces and moments represented by hull forces related to yaw and sway velocities. When evaluating them one of the models used in a manoeuvring simulation

(such as the one given by expressions 5.31) is used. In other words, the effect of ship motions in waves is disregarded when evaluating the slower wave-induced motion of a ship. It is worth noting that the terms related to yaw and sway accelerations are included in the radiation model.

Resistance and thrust

Still water resistance for a vessel on a straight course with no drift is represented by the term $X_{\text{resistance}}$. Thrust generated by a propeller is depicted by X_{prop}. They are evaluated as described in Section 5.7.

Rudder

The subscript 'rudder' refers to rudder forces and to the location of the rudder in the body-fixed co-ordinate system. The forces are evaluated as presented in the Section 5.8.

Restoring forces and wave loads

Forces and moments depicted with subscript 'wave' are the ones incorporating the restoring forces and moments as well as the wave loads.

For the irregular waves nonlinear hydrostatic and Froude-Krylov pressures are evaluated as described in Section 7.5, but summing up the contributions of several wave components. That is, wave elevation above the control point C is given by

$$\zeta(t) = \sum_{i=1}^{N} A_i \cos\left[\mathrm{k}_i \left(X_\mathrm{c} \cos\mu - Y_\mathrm{c} \sin\mu\right) - \omega_i t + \delta_i\right], \tag{10.2}$$

where X_c and Y_c are the control points of the hull surface given in the Earth-fixed co-ordinate system XYZ given by the transformation 7.23. The co-ordinates X_c and Y_c take into account the ship's position in waves. $k_\mathrm{i}=\omega_\mathrm{i}/\mathrm{g}$ is the wave number corresponding to the i-th wave component. For the immersed panel, that is, for $Z_\mathrm{c}+\zeta(t)>0$, pressure is evaluated from the expression

$$p_c(t) = \rho g \left\{ Z_c + \sum_{i=1}^{N} A_i \exp\{-k_i[Z_c + \zeta(t)]\} \right.$$
$$\left. \bullet \cos\left[k_i \left(X_c \cos\mu - Y_c \sin\mu \right) - \omega_i t + \delta_i \right] \right\}. \tag{10.3}$$

The argument of the exponent function in (10.3) satisfies the dynamic boundary condition at the actual water surface. The pressure profile thus obtained is sometimes called as the stretched one. This approach is a kind of extension of the linear wave theory to incorporate nonlinear effects associated with the variation of a ship's wetted surface. Refer to figures 7.2 and 7.3 for the quantities used in evaluating hydrostatic and Froude-Krylov pressures. The position of the control point C in the inertial co-ordinate system *XYZ* is obtained from the transformation given by equation 7.23.

Diffraction part of the wave load is taken from the linear seakeeping theory.

Additional damping of roll

An allowance for a viscous damping of roll is incorporated in the fourth equation. In the second line of this equation, ζ stands for the critical damping ratio and ω_ϕ stands for the natural roll angular frequency.

The solution of nonlinear differential equations of motion 10.1 in the time-domain can be obtained by integrating them using an appropriate numerical procedure and applying a sufficiently small time step.

On the left-hand side of equations 10.1, several terms related to motion accelerations occur in each of the equations. This means that equations are coupled and cannot be solved as such. Before solving, equations 10.1 have to be de-coupled. This is done numerically at each time step as follows. The equations 10.1 can be expressed in the matrix form as

$$\mathbf{A} \bullet \ddot{\mathbf{x}} = \mathbf{B}, \tag{10.4}$$

where matrix

$$\mathbf{A}=\begin{bmatrix} m+a_{11} & 0 & 0 & 0 & a_{15} & 0 \\ 0 & m+a_{22} & 0 & a_{24} & 0 & a_{26} \\ 0 & 0 & m+a_{33} & 0 & a_{35} & 0 \\ 0 & a_{42} & 0 & I_x+a_{44} & 0 & a_{46} \\ a_{15} & 0 & a_{53} & 0 & I_y+a_{55} & 0 \\ 0 & a_{62} & 0 & a_{64} & 0 & I_z+a_{66} \end{bmatrix},$$

vector comprising accelerations is given by:

$$\ddot{\mathbf{x}}=\begin{Bmatrix} \dot{u} \\ \dot{v} \\ \dot{w} \\ \dot{p} \\ \dot{q} \\ \dot{r} \end{Bmatrix}=\left\{\dot{u},\dot{v},\dot{w},\dot{p},\dot{q},\dot{r}\right\}^T$$

and vector **B** is built-up by the right-hand sides of equations 10.1 as follows:

$$\mathbf{B}=\begin{Bmatrix} -\mathrm{m}g\sin\theta+X_{\text{resistance}}+X_{prop}+X_{rudder}+X_{wave}+X_{man}-k_{15}+\left(m+a_{22}\right)\left(rv-qw\right) \\ \mathrm{m}g\cos\theta\sin\phi+\left(m+a_{11}\right)\left(pw-ru\right)+Y_{man}+Y_{rudder}+Y_{wave}-k_{22}-k_{24}-k_{26} \\ mg\cos\theta\cos\phi+m\left(uq-vp\right)+Z_{wave}-k_{33}-k_{35} \\ \left(I_y-I_z\right)qr-Y_{rudder}z_{rudder}+K_{man}+K_{wave}-k_{44}-k_{42}-k_{46}+2\zeta p\omega_{\phi} \\ \left(I_y-I_x\right)pr+X_{rudder}x_{rudder}+M_{wave}-k_{55}-k_{53}-k_{15} \\ \left(I_x-I_y\right)pq+Y_{rudder}x_{rudder}+N_{man}+N_{wave}-k_{66}-k_{62}-k_{64} \end{Bmatrix}$$

Equation 10.4 can be written as

$$\mathbf{A}^{-1}\bullet\mathbf{A}\bullet\ddot{\mathbf{x}}=\ddot{\mathbf{x}}=\mathbf{A}^{-1}\bullet\mathbf{B}\,. \tag{10.5}$$

As a result we have obtained a set of six nonlinear normal second order differential equations with acceleration terms (vector $\ddot{\mathbf{x}}$) on the left-hand – side of the matrix equation 10.5. This set of equations 10.5 is integrated numerically using the Runge-Kutta fourth-order scheme yielding velocity vector $\dot{\mathbf{x}}=\left\{u,v,w,p,q,r\right\}^T$.

Next, at the same time step, the transformation given by expression 3.7 is used to project the velocities on the axes of Earth-fixed co-ordinate system. The projected velocities are integrated numerically using also the same

Runge-Kutta routine. The position of the ship, given by the vector $\mathbf{X} = \{X_G, Y_G, Z_G, \phi, \theta, \psi\}^T$ at each time step is obtained as a result.

10.2 Linear approximation to ship motions in irregular long-crested waves

Linear approximation to the global responses of a ship in irregular waves is evaluated in order to judge the effects of nonlinearity on the derived responses. Normally, in the linear seakeeping theory, a constant forward speed is assumed. In the *Laidyn* method, surge motion of a ship is evaluated in the time domain taking into account, amongst the others, propeller action and variations of the wetted surface. Thus in-plane motion of a ship is simulated in a time domain along with the other motion components. This results in ship position X_G, Y_G in the Earth-fixed co-ordinate system. This, in addition to the knowledge of transfer functions of the corresponding responses, makes it possible to evaluate the linear approximation of the responses using the expressions

$$
\begin{aligned}
x_L(t) &= \sum_{i=1}^{N} A_i x_{L0}(\omega_i,\mu)\cos\left[\mathrm{k}_i\left(X_G\cos\mu - Y_G\sin\mu\right) - \omega_i t + \delta_i - \gamma_{x,i}\right] \\
y_L(t) &= \sum_{i=1}^{N} A_i y_{L0}(\omega_i,\mu)\cos\left[\mathrm{k}_i\left(X_G\cos\mu - Y_G\sin\mu\right) - \omega_i t + \delta_i - \gamma_{y,i}\right] \\
z_L(t) &= \sum_{i=1}^{N} A_i z_{L0}(\omega_i,\mu)\cos\left[\mathrm{k}_i\left(X_G\cos\mu - Y_G\sin\mu\right) - \omega_i t + \delta_i - \gamma_{z,i}\right] \\
\phi_L(t) &= \sum_{i=1}^{N} \mathrm{k}_i A_i \phi_{L0}(\omega_i,\mu)\cos\left[\mathrm{k}_i\left(X_G\cos\mu - Y_G\sin\mu\right) - \omega_i t + \delta_i - \gamma_{\phi,i}\right] \\
\theta_L(t) &= \sum_{i=1}^{N} \mathrm{k}_i A_i \theta_{L0}(\omega_i,\mu)\cos\left[\mathrm{k}_i\left(X_G\cos\mu - Y_G\sin\mu\right) - \omega_i t + \delta_i - \gamma_{\theta,i}\right] \\
\psi_L(t) &= \sum_{i=1}^{N} \mathrm{k}_i A_i \psi_{L0}(\omega_i,\mu)\cos\left[\mathrm{k}_i\left(X_G\cos\mu - Y_G\sin\mu\right) - \omega_i t + \delta_i - \gamma_{\psi,i}\right],
\end{aligned}
\tag{10.6}
$$

where terms with subscripts *L0* depict gain factors of the transfer functions and γ the corresponding phase angles.

10.3 More on the numerical solution

The solution to the problem starts with the linear approximation 9.1 yielding the transfer functions 9.2. Added masses and damping coefficients and their

dependence upon the frequency are also evaluated by the linear strip theory based seakeeping method (Journee, 1992). These coefficients are transformed to the co-ordinate system having an origin in the ship's centre of gravity G as described in Appendix B. After that, the convolution integrals are evaluated with the aid of the Fast-Fourier-Transform algorithm yielding the retardation functions 7.34. The details are given in Appendix C

There are two options in the *Laidyn* method. In the first version, the responses are solved by a direct integration of the equations as discussed in the preceeding paragraph. An interesting option to the solution is the so-called *Two-stage approach* described in the following paragraph.

In both solution strategies, the zero initial conditions are used for all equations with the exception of surge velocity, which is set initially to a prescribed ship velocity in calm water. In order to damp spurious transients, the wave amplitude is gradually increased from zero to the prescribed final value A_{final} using the expression

$$A(t) = A_{final}\left[1-\left(\cos\frac{\pi t}{2T_f}\right)^2\right] \text{ for } t < T_f \qquad (10.7)$$
$$A(t) = A_{final} \text{ for } t \geq T_f,$$

with T_f= 50 seconds in full scale being used.

10.4 Two-stage approach

Instead of solving the nonlinear equations of motions directly, it is possible to apply the so-called two-stage approach to the non-linear set of equations of motion.

Illustration of the two-stage approach using a single-degree-of-freedom nonlinear system

For the sake of simplicity the two-stage approach is explained in this section using a single-degree-of-freedom model. Let us consider a single-degree-of-freedom system given by a nonlinear equation

$$m\ddot{X} + g(\dot{X}) + h(X) = F(X;t), \tag{10.8}$$

where m is the system mass and t is the time. The functions g and h are in general nonlinear functions of response velocity $\dot{X}$ and displacement X, respectively. Function F is also a nonlinear function of X describing the external excitation of the system. The linear version of the equation (10.8) is given by

$$m\ddot{x}_L + c\dot{x}_L + kx_L = F_L(t), \tag{10.9}$$

where F_L is a linear, independent of the response forcing function. The total response is decomposed into a linear part x_L and a nonlinear portion x as

$$X = x_L + x. \tag{10.10}$$

Subtracting linear approximation (10.9) from the general equation (10.8) yields an equation for the non-linear part x of the response

$$m\ddot{x} + \left[g(\dot{x}_L + \dot{x}) - c\dot{x}_L\right] + \left[h(x_L + x) - kx_L\right] = f, \tag{10.11}$$

where $f = F(X;t) - F_L(t)$ is the nonlinear part of the forcing function.

In the two-stage approach, nonlinear differential equation (10.8) is solved by solving first the linear version (10.9) of it. Next, the nonlinear part x of the response is derived by solving numerically (10.11) with a known linear solution x_L. The total solution is evaluated using a sum (10.10).

11. Some applications of the theory

11.1 Capsizing of a ship in steep regular waves

Two ship cases were used in the benchmark study initiated by the International Towing Tank Conference and presented in the 23rd ITTC (2002). The first vessel, ship A1, is a containership with a waterline length of L_{PP} = 150 m and a low metacentric height (GM_0 = 0.15 m). This low GM_0 value means that the static stability of the ship is poor. The second vessel ship A, is a model of a fishing vessel with the length L_{PP} = 35.68 [m]. Both models were run in regular waves, different headings and Froude numbers ($Fn = \frac{V_S}{\sqrt{gL_{PP}}}$). The summary of the model test results and simulation results are given in two Tables 11.1 and 11.2. Wavelength is denoted by λ and a_W is the wave amplitude.

Table 11.1 Summary of the results for the containership (Ship A1).

Case	λ/L_{pp}	$2A_W/\lambda$	Fn	Heading μ [deg]	Experiment	Computed
1	1.5	1/25	0.2	0	Parametric roll resonance, capsize	Parametric roll resonance, no capsizing
2	1.5	1/25	0.2	45	No capsizing	No capsizing
3	1.5	1/25	0.3	30	No capsizing	No capsizing
4	1.5	1/25	0.4	30	Capsize	Capsize

Table 11.2: Summary of the results for the fishing vessel (Ship A).

Case	λ/L_{pp}	$2A_W/\lambda$	Fn	Heading μ [deg]	Experiment	Computed
A	1.637	0.1	0.3	-30	No-capsizing	No-capsizing
B	1.637	0.1	0.43	-10	Surfing, capsize	Surfing
C	1.127	0.115	0.3	-30	No- capsizing	No- capsizing
D	1.127	0.115	0.43	-30	Capsize	Capsize

A reasonable agreement of the computed results with the experimental ones is noted. An example of computed angular motion prior to capsizing is shown in Figure 11.1 and the corresponding experimental result is presented in Figure 11.2.

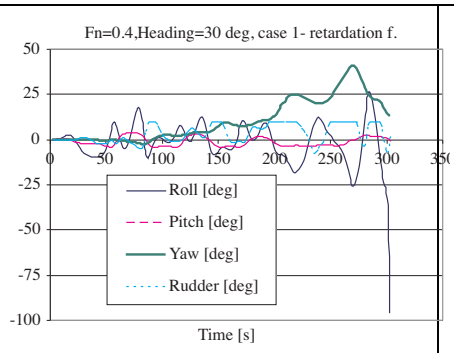

Figure 11.1: Containership (ship A1) running at Fn = 0.4 capsizes in regular quartering regular waves (heading 30 [deg]). Simulated result.

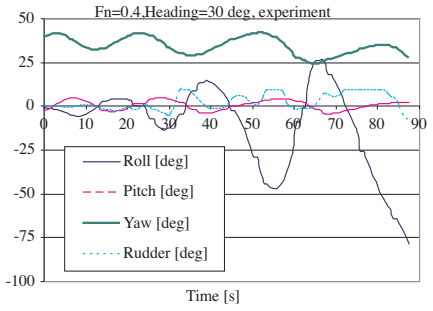

Figure 11.2: Model of ship A1 running at Fn = 0.4 capsizes in regular quartering regular waves (heading 30 [deg]). Model test result scaled to full-scale (Mattila, 1999).

Both time histories are similar. Capsizing is preceded by a couple of large heeling events. The surge motion and the position of the ship in waves seems to have an important influence on the development of a dangerous situation.

11.2 Parametric rolling in regular waves

Parametric roll resonance is an unexpected ship roll motion in head or following seas. The phenomenon is known to shipmasters. Linear seakeeping theory is not capable of predicting this roll motion; and for this reason, we can call it an unexpected response. The phenomenon is generally attributed to the parametric variation of the restoring moment of heel caused by a large variation in the water-plane area in waves. Thus, qualitatively, the phenomenon is often described by a single equation of the Mathieu type.

An extensive model test series of a modern, fast twin-screw Ro-Pax vessel was conducted at the Ship Laboratory of the Helsinki University of Technology. Tests were primarily concerned with the dynamic stability. In particular, a loss of stability on a crest of a following wave and parametric roll resonance were investigated both in regular and irregular waves for three KG values with a ship model without and with two different height bilge keels (450 mm and 900 mm in the full scale). Tests were run with the self-propelled model steered manually (Mattila, 1999). The main particulars of the vessel are given in Table 11.3.

The stability lever curve of the vessel is shown in Fig. 11.3

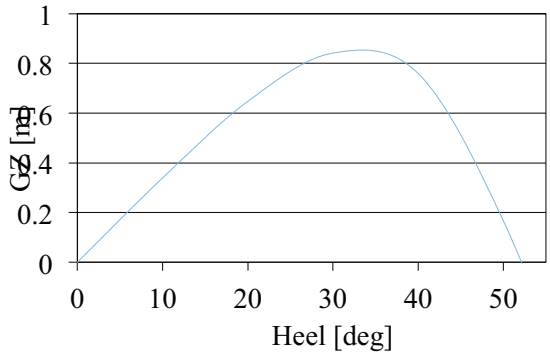

Fig. 11.3 Static stability lever curve of the investigated vessel for the height of the centre of gravity KG = 12 [m].

In the following figures 11.4 and 11.5, example time histories of motions corresponding to only a single test case are presented.

Table 11.3 Main particulars of the vessel Seatech-D

	Full scale	*Model Scale*
	1	39.024
L_{wl} [m]	158.6	4.064
L_{pp} [m]	158	4.049
D_p [m]	4.8	0.123
B [m]	25	0.641
B_{wl} [m]	25	0.641
T_a [m]	6.1	0.156
T_ϕ [m]	6.1	0.156
D [m]	15	0.384
∇ [m^3]	13766	0.232
M_m [kg]		231.40
S [m^2]	4356	2.860
C_B	0.571	0.571
L_{wl}/B_{wl}	6.344	6.344
B_{wl}/T_{wl}	4.098	4.098
$L_{wl}/\nabla^{(1/3)}$	6.618	6.618
KG [m]	11, 11.5, 12	0.282, 0.295, 0.307

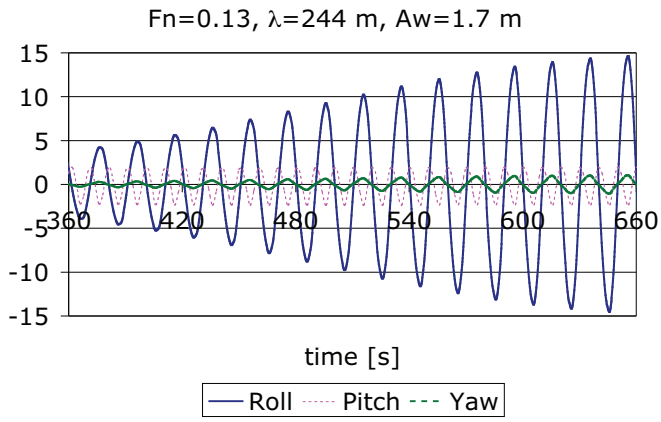

Fig. 11.4 Simulated angular motions for a ship with low bilge keels and KG = 12 m. Wave amplitude A=1.7 [m]. T_ϕ = 20 [s], ξ = 0.046. Ultimate roll amplitude is 16 [deg].

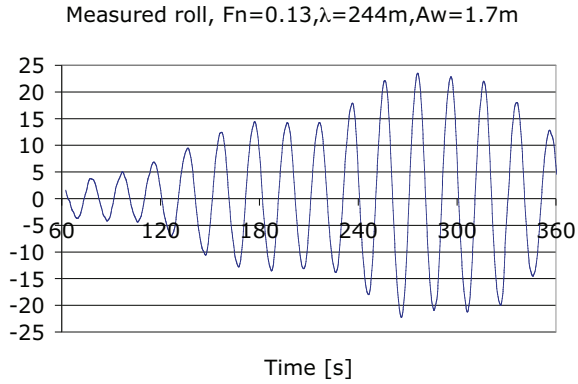

Fig. 11.5 Measured roll for a ship equipped with low bilge keels and KG = 12 m. Wave amplitude A=1.7 [m]. T_ϕ = 20 [s], ξ = 0.046.

Both the simulations and the model test experiments gave similar conclusion. In this case of a pure parametric resonance, where the ratio of an encounter period to roll natural period is 0.5, roll amplitude seems to be related to wave amplitude squared. Moreover, an increase of the wave amplitude results in a lower number of encounter periods required for a roll motion to start. Simulations indicated that there is a certain threshold value of wave amplitude below which parametric roll resonance does not develop.

Both the simulations and the tests indicated that an increase in damping, achieved by bilge keels, results in a somewhat lower roll amplitude. Damping also delays and slows the development of the parametric roll resonance (Matusiak, 2003).

11.3 Time-domain simulation of the weather criterion

In order to ensure the safety of a vessel in a 'dead ship condition', the so-called weather criterion was made mandatory for ships in 2005. The criterion takes into account resonant beam waves and gusty wind (IMO). As the origin of the criterion is quite old and there are a number of strong assumptions involved, its application to a modern large size passenger vessel can be questioned. In order to make it better-suited for modern ships, an allowance for the alternative assessment using model tests was made. Tests are believed to yield more realistic values of wind loading and better estimates of roll amplitude at the resonance. The first attempts to utilize model tests in validating fulfilment of the weather criterion were presented in Yon (2006) and Ishida (2006).

The LAIDYN method was used to evaluate the fulfilment of the weather criterion by an example passenger ship design (Matusiak&Hamberg, 2006). The original idea was to substitute the model tests of the alternative assessment with the appropriate numerical simulations. The interesting findings of this study were:

The so-called "effective" roll-back angle obtained by simulating a ship's behaviour in beam seas was very close to the one given by the rule (-5 [deg] in the considered case).

Weather criterion considers the resonant beam seas as a critical situation yielding an initial heel at which wind gust impacts the vessel. Wave action as such is disregarded when considering the transient response of the ship caused by heeling moment due gusty wind loading. Thus the fulfilment of the weather criterion can be simulated (numerically or with the aid of model tests) by investigating ship's transient heel response in still water with an

initial value set by a roll-back angle and step-wise heeling moment simulating gusty wind. The simulated result of this kind of response is shown in Figure 11.6 with ship heeling by 27 [deg]. The corresponding situation, as evaluated traditionally with the aid of the dynamic lever concept, is shown in Figure 11.7 and yields maximum heeling of 30 [deg].

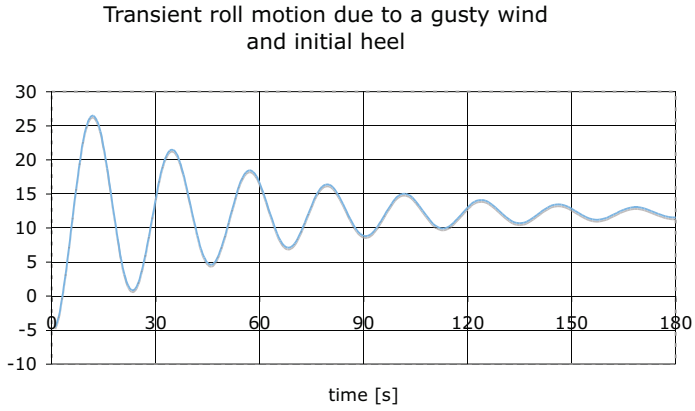

Fig. 11.6 Ship transient rolling caused by the gusty wind and initial heel. Gust loading is taken according to the weather criterion.

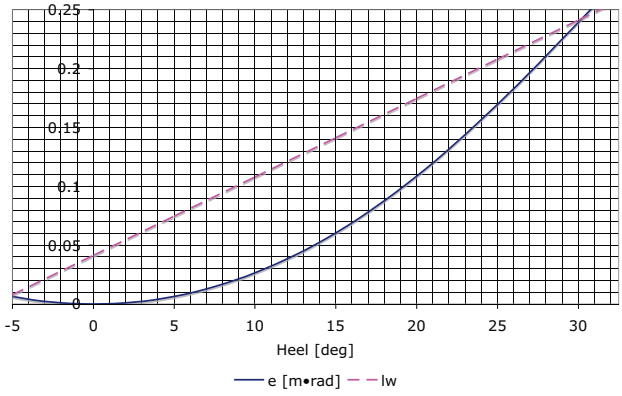

Fig. 11.7. Ship dynamic heeling according to the weather criterion. lw is dynamic lever of gusty wind loading and e is dynamic lever of the restoring moment (integral over the GZ curve).

If wind loading is represented by the horizontal force and the corresponding heeling moment then dynamic behaviour (taking sway motion into account) yields a still smaller maximum heel angle (see Figure 11.8).

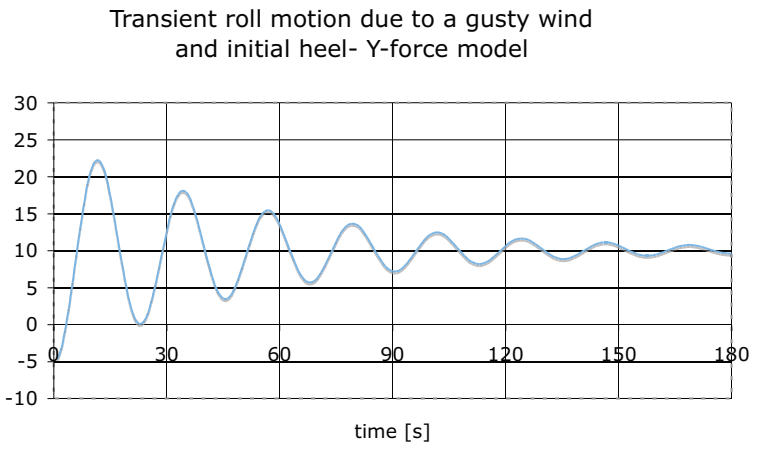

Figure 11.8. Ship dynamic heeling according to the loading model represented by a horizontal Y-force and model of dynamics including the sway motion component

The conclusion of the numerical simulation of the scenario set-up by the weather criterion is that it does not really pretend to evaluate capabilities of a ship in realistic sea conditions and with a sound model of ship dynamics. It is merely a simple measure of intact ship stability. However, the criterion contains important elements affecting ship safety and thus can be regarded as an important element of ship safety assessment.

11.4 The occurrence of roll resonance in stern quartering seas

In Chapter 9, when discussing the evaluation of ship responses in irregular waves, the concept of the spectrum of waves as felt by a ship was discussed (refer to Equation 9.6 and Figure 9.2 for the head seas condition). This spectrum is called the encountered wave spectrum. A dangerous situation for a ship travelling at relatively high speeds may occur in stern quartering seas. Let us examine a situation of the containership A1 travelling at speed V_s=17.7 [kn], that is Fn=0.235 at a heading μ=30 [deg]. The mean period of waves is T_1= 7.7 [s] and the significant wave height is H_S=4.6 [m]. Using the

expression 6.24 we evaluate an approximate value of the mean period of the encountered waves as

$$T_e = \frac{T_1}{1 - \frac{2\pi V}{gT_1}\cos\mu} = \frac{7.7}{1 - \frac{2\pi 9.1}{9.81 \bullet 7.7}\cos 30^0} = 22\ [s]. \qquad (11.1)$$

The result of (11.1) indicates that the action of waves felt by the ship will be slowed down. The Doppler effect that is a change of frequency will be in this case slowing down the wave loads and motions. Ship motions were computed for one hour of vessel operation in these sea conditions. The metacentric height of the ship was GM_0=1.2[m] yielding natural roll period T_ϕ=19 [s]. The main responses of the ship in terms of heave, pitch and roll motion along with the wave acting on a ship are presented in figures 11.9

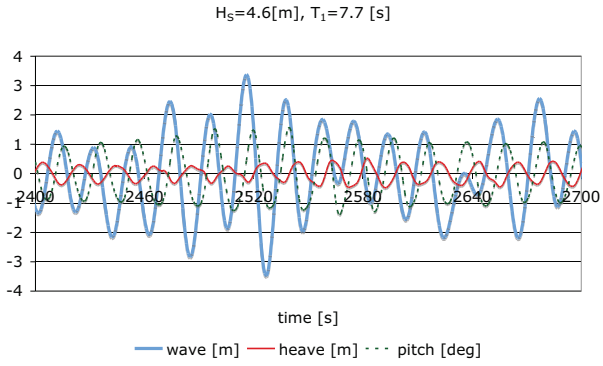

Fig. 11.9 Heave and pitch motion of ship A1 in the stern quartering irregular waves (Jonswap spectrum of H_s=4.6 m and T_1=7.7 s). Ship speed is Fn=0.235.

and 11.10 below. Only a short record (5 minutes long) of the responses is shown.

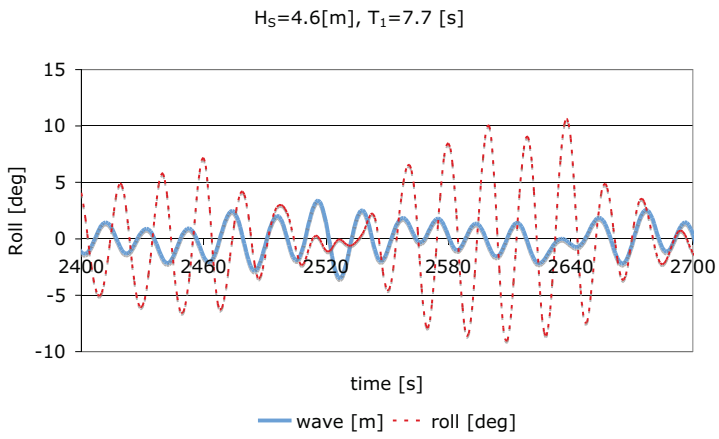

Figure 11.10 Ship A1 rolls in the stern quartering irregular waves (Jonswap spectrum of Hs=4.6 m and T1=7.7 s). Ship speed is Fn=0.235 and metacentric height GM_0=1.2 m.

An interesting feature of the encountered waves is noted. Although the amplitude of the waves changes, the period of the wave train seems to be nearly constant, at least for the selected record. The mean value of the encounter period is 20 [s], which is close both to the estimate given by formula 11.1 and to the natural roll period of ship. Fourier analysis of the encountered waves was conducted and the results of it are presented in Figure 11.11 below.

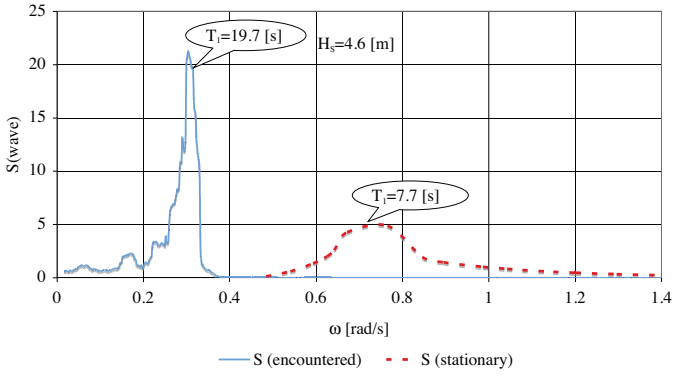

Figure 11.11 The effect of ship speed (Fn=0.235) and course in respect to wave propagation direction (μ=30^0) on the waves encountered by a ship.

Apart form a shift in frequency content towards lower values, a sharpening of the spectrum of the encountered waves is noted. This means that in this condition, waves of different lengths act on the ship with nearly the same frequency. As this frequency (encounter frequency) is close to the natural frequency of roll, a resonance of roll motion occurs.

Next we check what will be the effect of decreasing ship speed to 12 knots. The spectra of encountered and stationary waves are shown in Figure 11.12 below.

Lowering the ship speed to 12 knots decreases the mean value of the encounter period to T_1=13 [s]. This is sufficiently away from the natural roll period. As a result ship roll motion decreases radically.

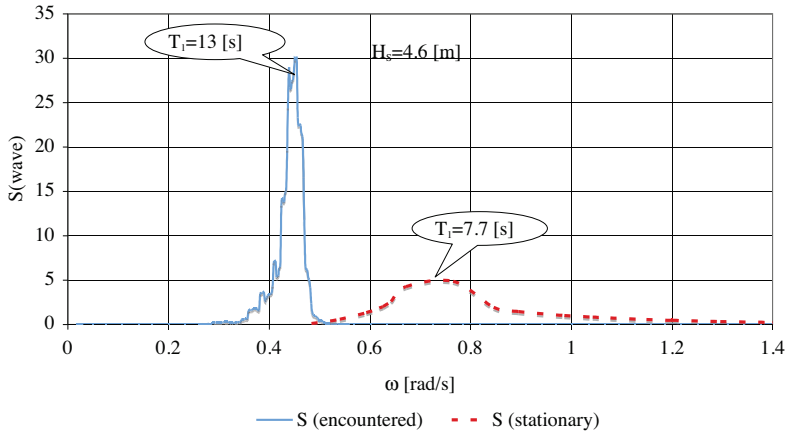

Figure 11.12 The effect of ship speed (Fn=0.16) and course with respect to wave propagation direction (μ=30^0) on the waves encountered by a ship.

In Figure 11.13 shows a record 5 minutes in length comprising the maximum roll motion experienced by the ship within an hour of operation.

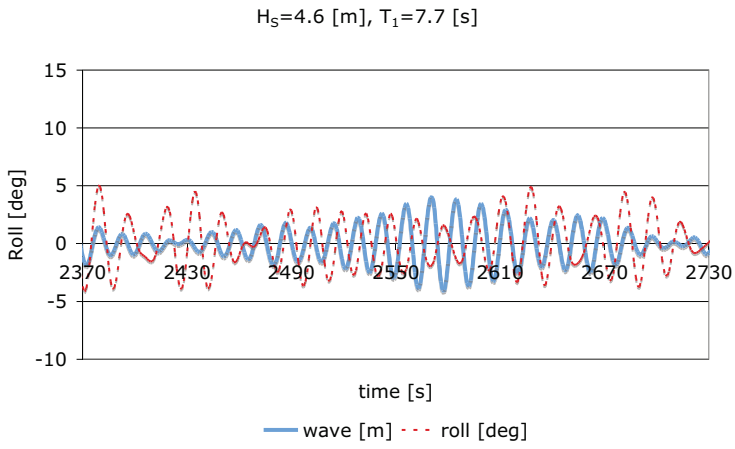

Figure 11.13 Ship A1 rolls modestly in the stern quartering irregular waves (Jonswap spectrum of H_s=4.6 m and T_1=7.7 s). Ship speed is Fn=0.16 and metacentric height GM_0=1.2 m.

It is clear that in the considered sea condition and ship's heading, the high speed of the vessel, may lead to a dangerous situation. The danger of running a ship at high speed in stern quartering seas is recognized by IMO, which has Revised Guidance to The Master For Avoiding Dangerous Situations in Adverse Weather and Sea Conditions (2007).

Claus Stigler (2012) has investigated the same phenomenon using the RoPax ship model (Seatech-D) presented in Chapter 11 and in Section 10.2. A self-propelled model was radio-controlled in tests conducted in the multifunctional model basin at Aalto University. The height of Centre-Of-Gravity was adjusted so that the natural roll period in the model scale was 3 s, that is, it corresponded to the full-scale value T_*=18.75 s. The turning circle tests were run in the basin in irregular waves given by the significant wave height H_S=4.8 m and an average period T_1=5.9 s. Speed of the model was controlled manually by adjusting the revolutions of propellers. The target value of it was V_S=16.5 kn full-scale. This creates a dangerous situation of roll resonance in stern quartering seas. A typical behaviour of a model in the resonance condition is presented in Figure 11.14 below.

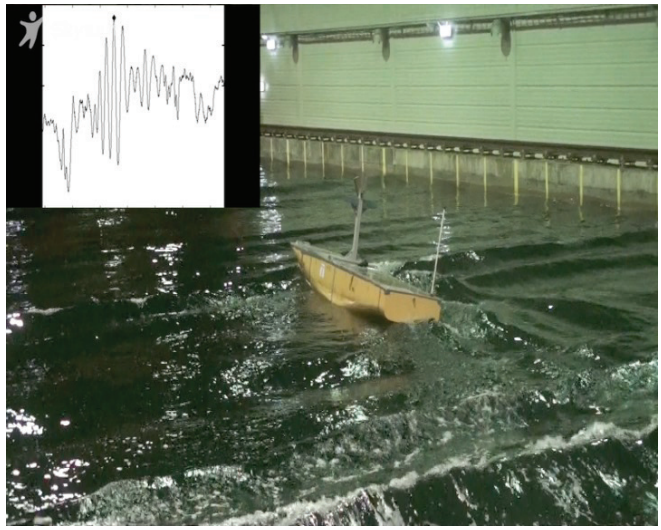

Figure 11.14 Model of a RoPax vessel in the multifunctional model basin of Aalto University. Instanteneous heel angle of 13 degrees.

Time history of the typical response is shown in Figure 11.15.

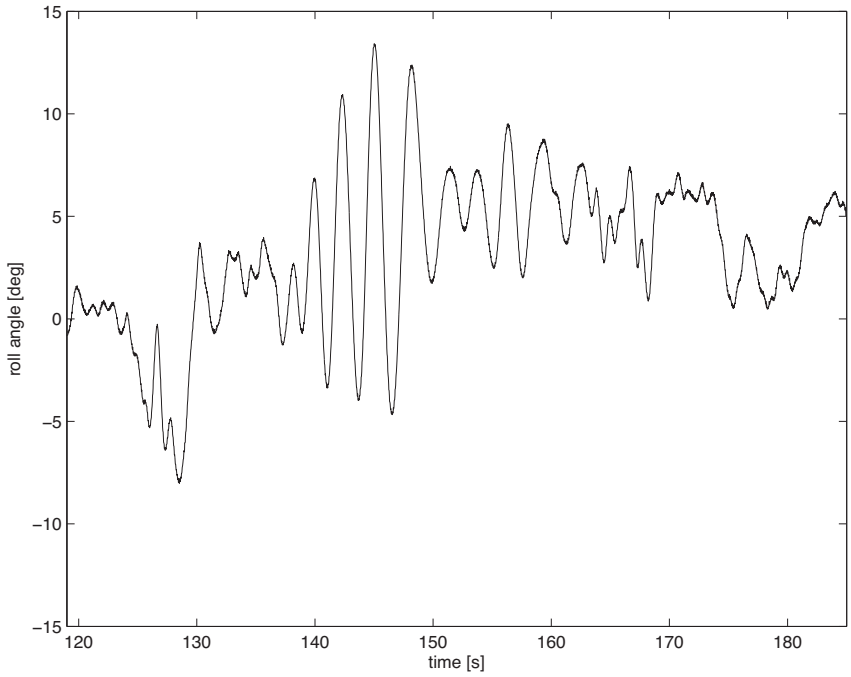

Figure 11.15 Time-history of roll motion recorded during a turning circle test in irregular waves of significant height H_S= 4.8 [m] full-scale. Time is given in model scale.

Simulated ship motion, corresponding to the conditions of the model test, is presented in Figure 11.16 below.

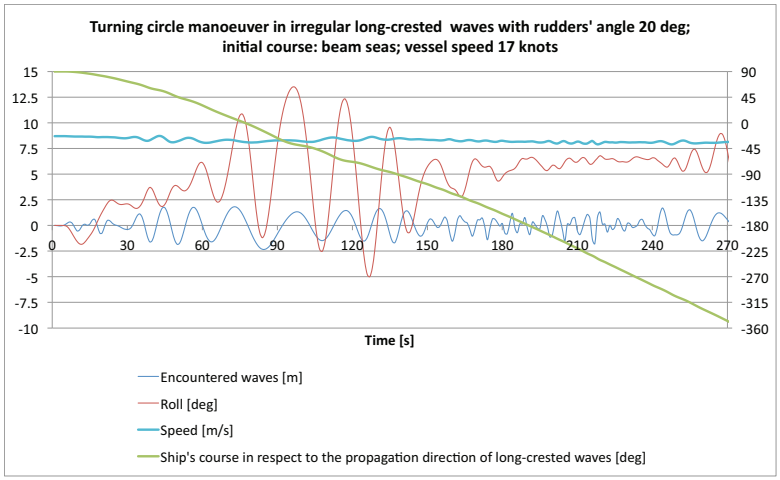

Figure 11.16 Simulated turning circle test in irregular waves of a significant wave height H_S= 4.8 [m].

Despite different wave trains of irregular waves realizations, measured and simulated roll motion are quite similar. The simulated maxima of roll amplitude are close to the measured ones. A steady heel caused by a centrifugal force effect is noted in both signals. As the simulated turning circle is somewhat smaller, the steady heel for a simulated test is slightly larger. Roll motion develops in stern quartering seas as an unfavourable effect of a change in frequency of encounter. This is clearly seen in the time-history of the simulated waves encountered by a ship. In critical conditions, short and long waves act on a ship with a period close to the natural roll period (T_φ=19 [s]). This is a primary reason for roll motion that may endanger ship operation. It is worth noting that reducing the speed of a ship or change in the heading suppresses the danger in this case.

12. Internal loads acting on a rigid hull girder

Apart from a ship's rigid body motion, it is important to know the internal forces and moments that act on a hull of a ship operating in waves. These forces are primarily composed of mass and hull/water interaction forces. In still water, the mass force (or its distribution) is simply the distributed ship weight. Hull/water interaction force, in this case, is the buoyancy or its distribution in the form of hydrostatic pressure. In waves, mass forces get an additional contributor associated with accelerations due to ship motions. As a result, the inertia component is added to the weight. Moreover, hull/water interaction gets more complicated. As described in Chapter 7, pressure acting on a hull surface in waves comprises, apart from the hydrostatic part, the radiation, Froude-Krylov and diffraction contributions.

The predictions of the wave-induced primary stresses are important in the ultimate strength assessment of the hull girder. If the hull girder has compression on deck, it is called a sagging condition. If there is compression on the bottom, it is called a hogging condition. (See Figure 12.1.)

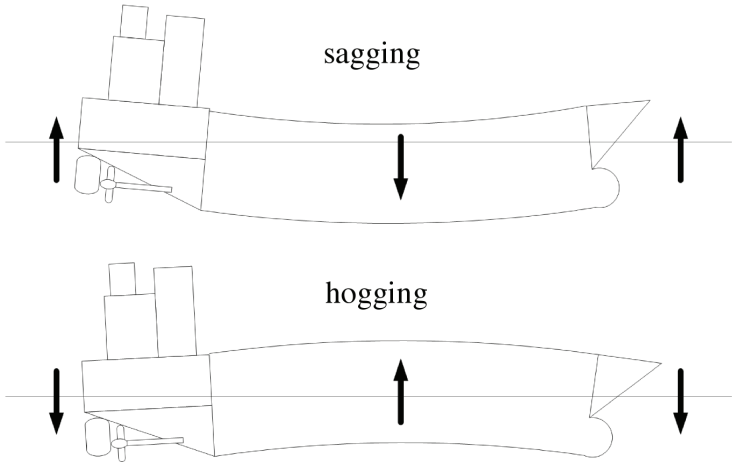

Figure 12.1 Hull sagging and hogging.

In waves, the sagging condition occurs if wave crests are at the bow and stern and hogging occurs if a wave crest is at mid-ship. The sagging increases if the ship has large bow flare and the ship motions are large with respect to waves. The stern form of the ship can have the same effect if the ship has a flat bottom stern close to the waterline. In the structural design of ships, a common practice is to express the extreme design loads by means of the sagging and hogging bending moments and shear forces. The sagging and hogging bending moments and shear forces are hull girder loads. The hull girder loads are internal forces and moments affecting a cross-section of the ship hull. The accurate prediction of the extreme wave loads is important in the ultimate strength assessment of the hull girder. For ships in a heavy sea, the sagging loads are larger than the hogging loads. The linear theories cannot predict the differences between sagging and hogging loads (Kukkanen, 2012).

12.1 Linear approach

We start discussion of internal loads with a simple linear model, which is normally a part of a linear strip-theory approach to a solution of ship

motions in waves (discussed in paragraph 9.1). We shall adopt the body-fixed co-ordinate system, which is often called 'the sea-keeping co-ordinate system as presented in Figure 12.2 below.

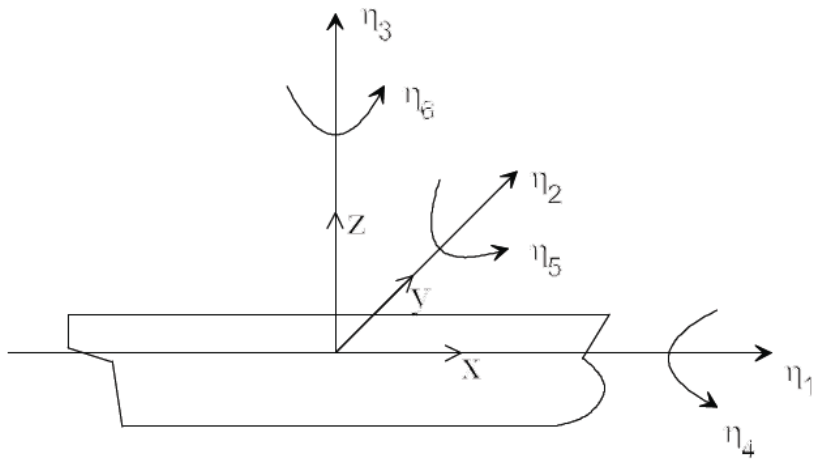

Figure 12.2 Definition of the ship-fixed co-ordinate system and the motion components used by Kukkanen (2012)

For the sake of simplicity, we shall limit the discussion to the global load in terms of vertical shear force and the bending moment acting on a hull regarded as a beam resting on a flexible foundation. First we consider a hull in still water. At each station, denoted by a position *x,* we have the vertical force per unit length given by a sum of weight and buoyancy at this section, that is

$$q(x) = -m(x)g + \rho g A(x), \tag{12.1}$$

where *m(x)* is mass of the hull per unit length and *A(x)* is the sectional frame area. With ship heaving η_3 and pitching η_5 motion, we have to also take inertia and hydrodynamic *F(x)* loads as well. As a result, the vertical force per unit length of a hull gets the form

$$q(x) = -m(x)g + \rho g A(x) - m(x)\left(\ddot{\eta}_3 - x\ddot{\eta}_5\right) + F(x) \qquad (12.2)$$

Total vertical shear force and bending moment at section x_p can be obtained by integrating load 12.2 along the ship length from the stern up to the section x'_p as follows

$$Q(x'_p) = \int_0^{x'_p} q(x')dx' \qquad (12.3)$$

$$M(x'_p) = \int_0^{x'_p} x'q(x')dx' \qquad (12.4)$$

It is worth noting that both the shear force and the bending moment are zero at the stem and at the stern. If we subtract from the expressions 12.3 and 12.4 the still water values of the shear force and the bending moment, respectively we get a linear approximation of the internal load distribution along the ship length related to wave action. As the model is linear, we can use the concept of transfer function or RAO in order to relate the internal loads to the wave and ship operating condition (wave length, heading and ship speed). That is, we can proceed similarly as we did with the other linear responses (section *Transfer function of ship motion, response spectra*) and derive a short time internal load prediction for a ship operating in irregular waves. The shortcoming of the linearity assumption is that the result does not distinguish between the sagging and the hogging condition except for the still water condition.

12.2 Example ship and linear load evaluation

In order to illustrate a wave loads evaluation for a modern form ship, we use a model of a roll-on roll-off passenger Ro-Pax vessel named as Seatech-D, which was investigated a great deal in Otaniemi (Mattila 1999; Kukkanen 2012).

The main dimensions and weight data of the RoPax are given in Table 11.3, and the line drawings are shown in Figure 12.3 below.

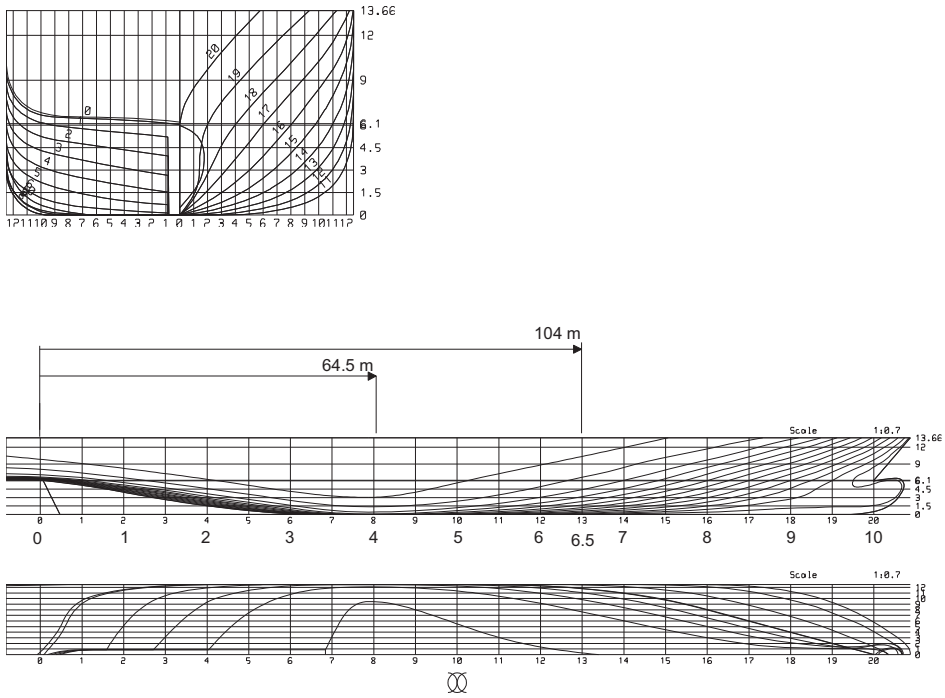

Figure 12.3. Line drawings of the RoPax. Internal loads were measured and computed for stations #4 and #6.5.

The weight distribution and the still water bending moment and shear force distribution along the length of the ship are presented in Figure 12.4.

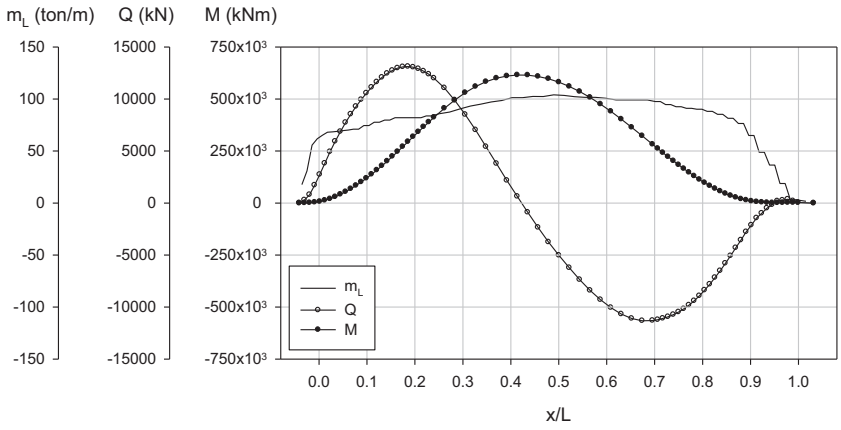

Figure 12.4. Weight distribution (m_L) and still water vertical shear force (Q) bending moment (M) (Kukkanen 2012).

Response amplitude operators of the vertical shear force Q and bending moment M for ship in head seas and velocity $Fn=0.25$ are presented in Figure 12.5. Transfer functions of internal loads were evaluated applying the linear strip-theory based computer program *sealoads*.

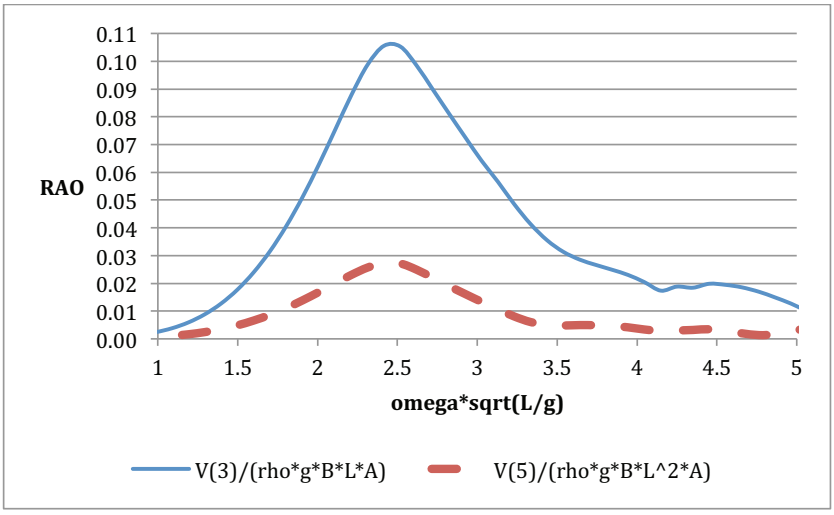

Figure 12.5 Response Amplitude Operators of the vertical shear force Q (station #6.5) and bending moment M (station #4) for RoPax in head seas at Fn=0.25.

Response amplitude operators are defined as the shear force divided by the factor $\rho gBLA$ and moment divided by ρgBL^2A, B and L are the ship's breadth and length between perpendiculars and A wave amplitude. The frequency axis is made non-dimensional by multiplying wave angular frequency (ω) by the factor $\sqrt{L/g}$. Different ways of presenting the frequency axis in non-dimensional form are used when presenting RAOs or transfer functions. Note that the previously used (paragraph 9.1.3) representation of the frequency domain as the lengths' ratio is related to the presentation of Figure 12.5, as follows $\omega\sqrt{L/g} = \sqrt{\frac{2\pi}{\lambda/L}}$.

12.3 The effect of nonlinearities on internal loads

Model tests disclose a certain nonlinear effect in internal wave loads. This is visible in terms of the analysed transfer functions of shear force and moment obtained with different wave amplitudes (Figures 12.6 and 12.7).

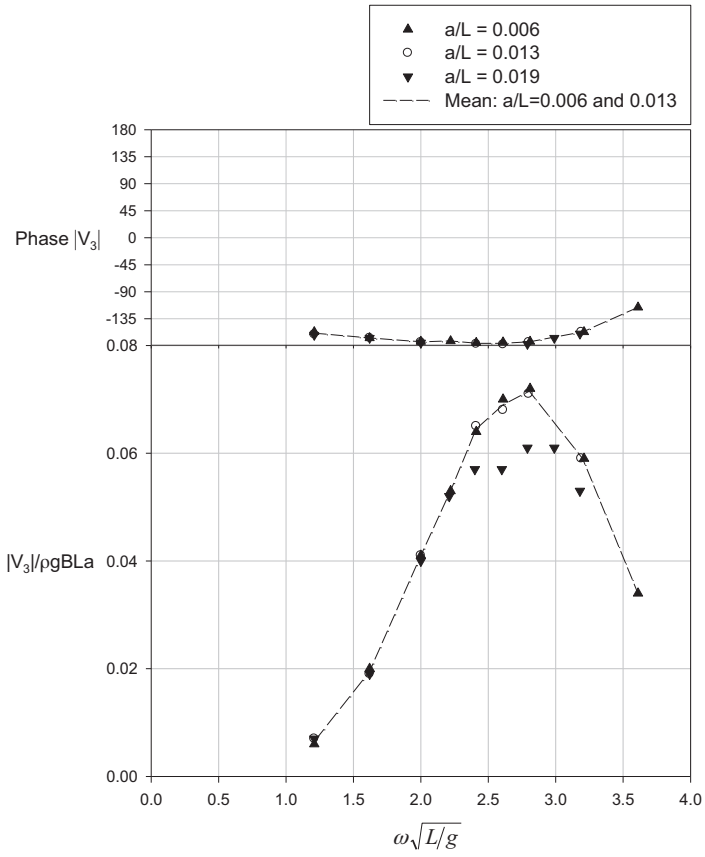

Figure 12.6. Model test results for vertical shear force at Fn = 0.25 in head seas at different wave amplitudes related to a ship's length a/L (Kukkanen 2012).

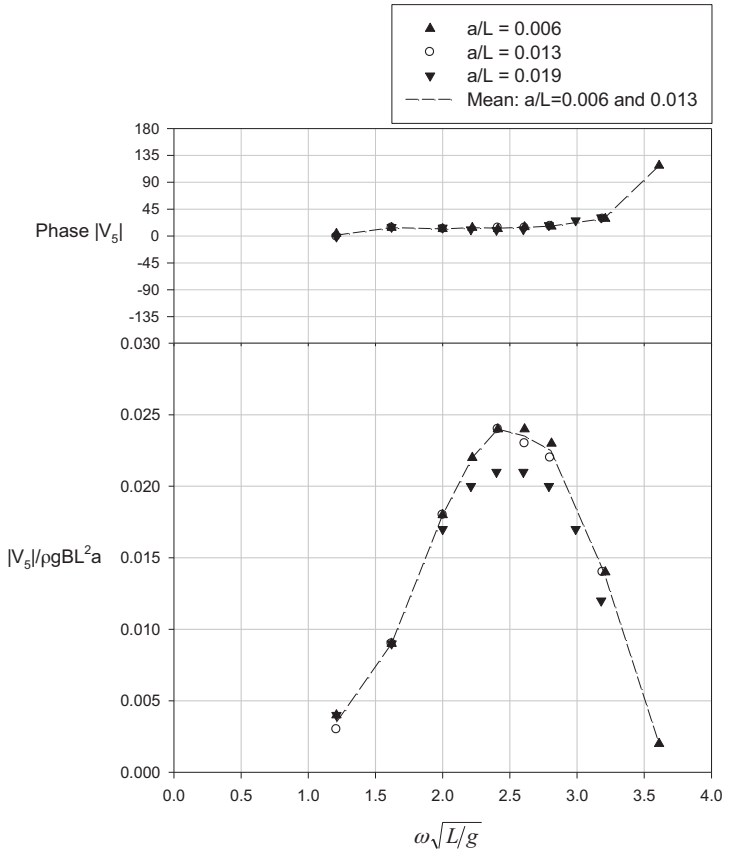

Figure 12.7. Model test results for bending moment (right-V5) at Fn = 0.25 in head seas at different wave amplitudes related to a ship's length a/L (Kukkanen 2012).

The nonlinearities are visible as differing values of RAOs for the frequencies close to resonance obtained with different wave amplitudes (denoted by small letter *a* in the Figure 12.6).

Kukkanen (2012) has investigated the effect of nonlinearities of wave induced motion and internal loads of the RoPax ship presented above. He has studied this subject with the dedicated model tests conducted in the towing tank at Aalto University and with the theoretical model. The latter is based on a Green function representation of the velocity potential of a time-domain flow with a free surface (GFM) and allows for the most important

nonlinearities of wave loads. Both, the experiments and the computations reveal un-symmetry of internal loads, resulting in different maximum values in sagging and hogging conditions. This is shown in figures 12.8, 12.9, 12.10 and 12.11 below.

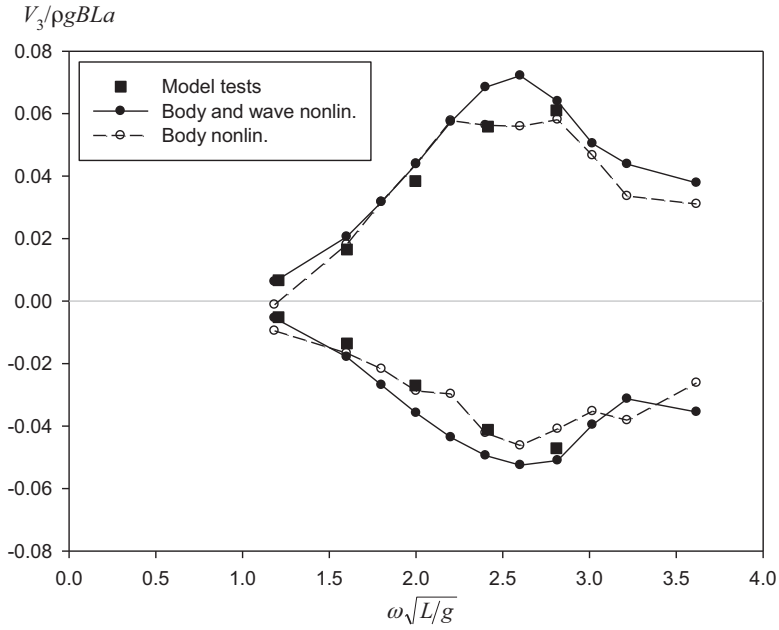

Figure 12.8 Maximum and minimum peaks of the shear force at Fn = 0.0. Calculation was carried out with the relative wave amplitude a/L = 0.013 using the body nonlinear and the body-wave nonlinear solutions.

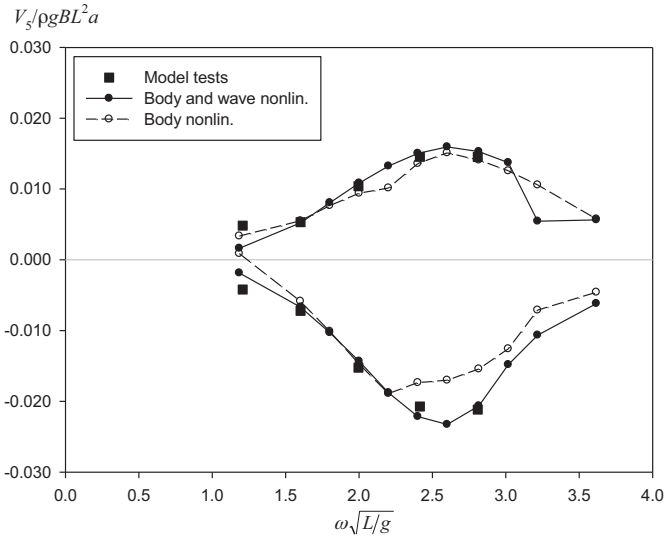

Figure 12.9 Maximum and minimum peaks of bending moment at Fn = 0.0. Calculation was carried out with the relative wave amplitude a/L = 0.013 using the body nonlinear and the body-wave nonlinear solutions.

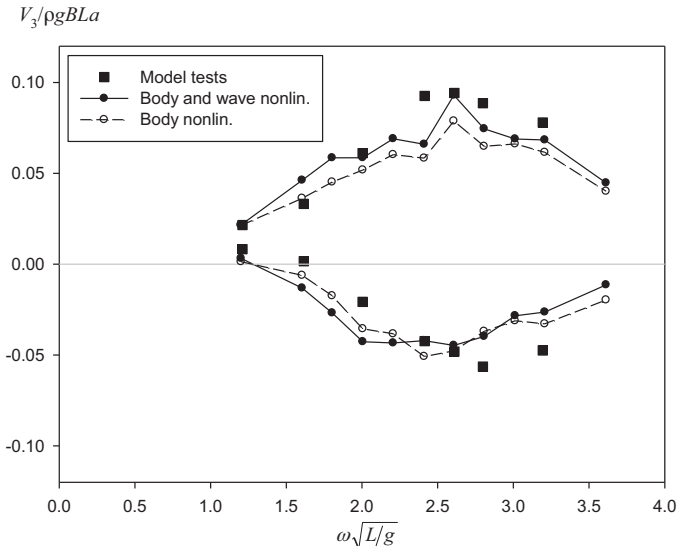

Figure 12.10 Maximum and minimum peaks of the shear at Fn = 0.25. Calculation was carried out with the relative wave amplitude a/L = 0.013 using the body nonlinear and the body-wave nonlinear solutions.

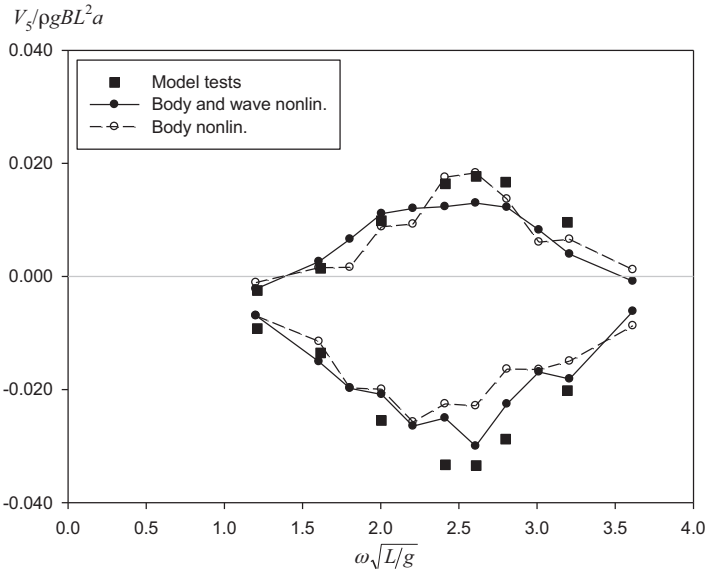

Figure 12.11 Maximum and minimum peaks of the bending at Fn = 0.25. Calculation was carried out with the relative wave amplitude a/L = 0.013 using the body nonlinear and the body-wave nonlinear solutions.

There is a clear difference in sagging and hogging maximum values of internal loads. The shear force at the ship's forepart and the bending moment at the mid-ship are significantly higher for the sagging condition. The bow flare, flat bottom at stern and load caused by the steady wave generated by hull at speed are the main contributors to this un-symmetry.

References

Bertram, V. 2000 Practical Ship Hydrodynamics, Butterworth-Heinemann, ISBN 0 7506 4851 1.

Brix, J. 1993 Manoeuvring Technical Manual, Seehafen Verlag GmbH, Hamburg

Clayton B. R. & Bishop, R.E.D. 1982 Mechanics of Marine Vehicles, London, ISBN 0 419 12110-2.

Cummins, W.E. 1962. The impulse response function and ship motions. Schiffstechnik pp. 101–109.

Faltinsen, O. M. 1990. Sea Loads on Ships and Offshore Structures, Cambridge University Press, 328 p.

Fossen, T. I. 1994. Guidance And Control Of Ocean Vehicles, J. Wiley&Sons, ISBN 0 471 94113 1.

Garrison, C. J. 1974. Dynamic response of floating bodies. Houston. Proceedings in Offshore Technology Conference, paper No. 2067, pp. 365 – 377.

Matusiak, J. 2000. Dynamics of cargo shift onboard a ship in irregular beam waves, International Shipbuilding Progress, 47, No 449 pp. 77-93

Hamamoto, M. & Kim, Y.S. 1993. A New Coordinate System and the Equations Describing Manoeuvring Motion of a Ship in Waves, J. Soc. Naval Arch., Vol 173.

IMO i.e. International Maritime Organization, SLF 49/5 Revised Intact Stability Code prepared by the Intersessional Correspondence Group.

International Maritime Organization, 2008. SLF 49/WP.2 ANNEX 2, Revised Guidance to the Master for Avoidance Dangerous Situations in Adverse Weather and Sea Conditions.

Ischida, S. et al, 2006. Evaluation of the weather criterion by experiments and its effect to the design of a RoPax ferry. In Proceedings of the 9th International Conference on Stability of Ships and Ocean Vehicles, STAB 2006, 25-29 September, 2006, Rio de Janeiro, Brazil.

Journee J. M. 1992. Strip Theory Algorithms, report MEMT 24, Delft University of Technology, Ship Hydrodynamics Laboratory.

Kreyshig, E. 1993. Advanced Engineering Mathematics. John Wiley&Sons, Inc. 7th edition.

Kukkanen, T. 2012. Numerical and experimental studies of nonlinear wave loads of ships, doctoral dissertation, VTT Science 15.

23rd International Towing Tank Conference, 2002. Report of the Specialist Committee of Extreme Ship Motions and Capsizing, Venice Italy, September 8-14, 2002, in Proceedings of the Conference, Vol. 2.

Lloyd, A.R.J.M, 1989. Seakeeping: Ship Behaviour in Rough Weather, Ellis Horwood Ltd.

Luukkainen, Niilo 2011. Modelling of Hydrodynamic Phenomena in Simulation of Ship Manoeuvring, Aalto University, School of Engineering, Department of Applied Mechanics, Master Thesis (in Finnish).

Mattila, M. 1999. An investigation of the dynamic stability of a fast RoPax vessel in waves (in Finnish), Helsinki University of Technology, Mechanical Engineering Department, Master Thesis.

Matusiak, J. 1995. Ship Buoyancy and Stability. Otatieto Oy. Helsinki 1995 (textbook in Finnish).

Matusiak, J. 2000. Dynamics of cargo shift onboard a ship in irregular beam waves, International Shipbuilding Progress, 47, No 449 pp. 77-93.

Matusiak, Jerzy 2003. On the effects of wave amplitude, damping and initial conditions on the parametric roll resonance. Proceedings of the 8th International Conference on Stability of Ships and Ocean Vehicles, Madrid, Spain, September 2003, pp. 341-348.

Matusiak, Jerzy 2003. Momentum equation applied to the problem of a propeller in oblique flow. Ship Technology Research-Schiffstechnik, Vol. 50-2003, pp. 103-105.

Matusiak, J. 2005. Ship Propulsion. Helsinki University of Technology. Ship Laboratory. Report M-176. Otaniemi 2005. Sixth edition. (in Finnish).

Matusiak, Jerzy; Hamberg, Karl, 2006. Considerations on the weather criterion applicability for the stability assessment of the large vessels. In Proceedings of the 9th International

Conference on Stability of Ships and Ocean Vehicles, Rio de Janeiro, Brasilia, 25.-29.9.2006. 447-454 (Vol 1).

Molland, A.F. &Turnock, S.R. 2007. Marine Rudders and Control Surfaces Elsevier Ltd. ISBN978-0.75-0-066944-3.

Naito, S. 1995. Generation and absorption of waves. Symposium on Wave Generation, Analysis and Related Problems in Experimental Tanks- Especially on Directional Wave. Yokohama National University, 25 September 1995. Pp. 1-27.

Newman, J.N. 1980. Marine Hydrodynamics. Cambridge, Massachusetts, The MIT Press, 402 s. Washington, D.C 1997.

Ohkusu, M. editor 1996. Advances in Marine Hydrodynamics, Computational Mechanics Publications, Southampton Boston.

Ruponen, Pekka 2004. Calculation Method for the Steering Forces of a Pod in Hybrid Propulsion. Master Thesis, Faculty of Mechanical Engineering, Helsinki University of Technology, in Finnish.

Ruponen, Pekka; Matusiak, Jerzy 2004. Calculation Method for the Steering Forces of a Pod in Hybrid Propulsion. First International Conference on Technological Advances in Podded Propulsion, Newcastle, 14.-16.4.2004. 2004, University of Newcastle, 263-275.

Salonen, E-M., 1999. Dynamiikka II. Otakustantamo 591 (in Finnish).

Söding, H. 1982. Prediction of ship steering capabilities, Schiffstechnik, Band 29, Heft 1, März 1982 pp. 3-29.

Stigler, C. 2012. Investigation of the behaviour of a RoPax vessel in stern quartering irregular long-crested waves, Student research project (Aalto University&Hamburg University of Technology.

Triantafyllou Michael S. & Hover Franz S. 2003. Manoeuvring and control of marine vehicles, Department of Ocean Engineering, Massachusetts Institute of Technology, Cambridge, Massachusetts USA.

Yoon, Hyeon Kyu et al, 2006. Application and Review on Interim Guidelines for Alternative Assessment of the Weather Criterion. In Proceedings of the 9th International Conference on Stability of Ships and Ocean Vehicles, STAB 2006, 25-29 September, 2006, Rio de Janeiro, Brazil.

Young, Ian R. 2000. Wind generated ocean waves, Amsterdam, 2000. Elsevier ocean engineering book series; 2 ISBN 0-08-043317-0.

Appendix A. Co-ordinate systems used in the context of the linear seakeeping theory

In the linear seakeeping theory and in manoeuvring normally three co-ordinate systems fixed with ship are considered. They are all right-handed systems and their origins are located at the symmetry plane of the ship. The z-axes of two of the systems are passing through the centre of gravity of ship G. In the manoeuvring the most common approach is to have motion and forces expressed in the co-ordinate system x_M,y_M,z_M, with the origin located at the vertical encompassing centre of gravity G and at the still water plane (Journee 1992). The vertically oriented z_M-axis points upwards. Another co-ordinate system used in this work, x,y,z is located at the centre of gravity of ship G and the z-axis is oriented downwards. The third co-ordinate system, the so-called Tasai's co-ordinate system, has an origin located at the water plane and at mid-ship. The co-ordinates systems are shown in Figure A.1 below.

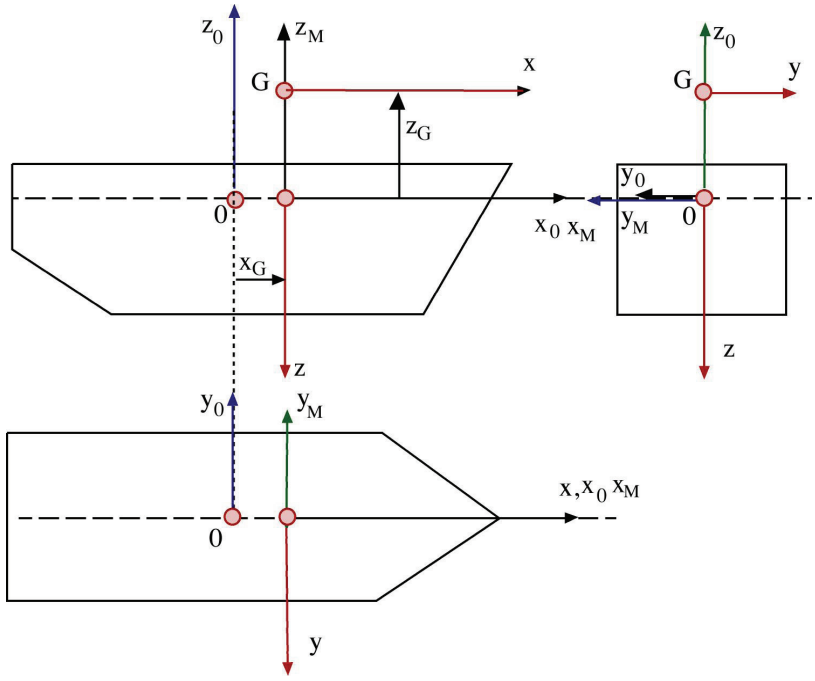

Fig. A.1 Co-ordinate systems.

The distance of the centre of gravity G from the water-plane is marked by z_G. The longitudinal (that is, the x-directional distance) of the origins is denoted by x_G.

Ship motions in terms of displacements are depicted as the co-ordinates. Angular motions are marked as ϕ_0, θ_0, ψ_0 and ϕ, θ, ψ. These are small angular motions in the co-ordinate systems x_0,y_0,z_0 and x,y,z respectively. The relation between the motion components, forces and moments in these two co-ordinate systems are as follows

$$
\begin{aligned}
&x = x_0 + z_G\theta_0,\ y = -y_0 + z_G\phi_0 - x_G\psi_0,\ z = -z_0 + x_G\theta_0 \\
&\phi = \phi_0,\ \theta = -\theta_0,\ \psi = -\psi_0 \\
&X = X_0,\ Y = -Y_0,\ Z = -Z_0 \\
&K = K_0 + z_G Y_0,\ M = -M_0 + z_G X_0 - x_G Z_0,\ N = -N_0 + x_G Y_0.
\end{aligned}
\qquad \text{(A.1)}
$$

Equations A.1 can be written in a matrix form as follows

$$\{x\} = \begin{Bmatrix} x \\ y \\ z \\ \phi \\ \theta \\ \psi \end{Bmatrix} = [T_1]\{x_0\} = \begin{bmatrix} 1 & 0 & 0 & 0 & z_G & 0 \\ 0 & -1 & 0 & z_G & 0 & -x_G \\ 0 & 0 & -1 & 0 & x_G & 0 \\ 0 & 0 & 0 & 1 & 0 & 0 \\ 0 & 0 & 0 & 0 & -1 & 0 \\ 0 & 0 & 0 & 0 & 0 & -1 \end{bmatrix} \begin{Bmatrix} x_0 \\ y_0 \\ z_0 \\ \phi_0 \\ \theta_0 \\ \psi_0 \end{Bmatrix}$$

$$\{X\} = \begin{Bmatrix} X \\ Y \\ Z \\ K \\ M \\ N \end{Bmatrix} = [T_2]\{X_0\} = \begin{bmatrix} 1 & 0 & 0 & 0 & 0 & 0 \\ 0 & -1 & 0 & 0 & 0 & 0 \\ 0 & 0 & -1 & 0 & 0 & 0 \\ 0 & z_G & 0 & 1 & 0 & 0 \\ z_G & 0 & -x_G & 0 & -1 & 0 \\ 0 & x_G & 0 & 0 & 0 & -1 \end{bmatrix} \begin{Bmatrix} X_0 \\ Y_0 \\ Z_0 \\ K_0 \\ M_0 \\ N_0 \end{Bmatrix} \quad \text{(A.2)}$$

Linear strip seakeeping theory yields the radiation forces expressed with the aid of added masses A_{ij} and damping B_{ij} coefficients in the x_0,y_0,z_0 co-ordinate system and as dependent upon the acceleration and velocities in the following form

$$\{X_0\} = \begin{Bmatrix} X_0 \\ Y_0 \\ Z_0 \\ K_0 \\ M_0 \\ N_0 \end{Bmatrix} = -[A]\{\ddot{x}_0\} - [B]\{\dot{x}_0\} = -\begin{bmatrix} A_{11} & 0 & 0 & 0 & 0 & 0 \\ 0 & A_{22} & 0 & A_{24} & 0 & A_{26} \\ 0 & 0 & A_{33} & 0 & A_{35} & 0 \\ 0 & 0 & 0 & A_{44} & 0 & A_{46} \\ 0 & 0 & A_{35} & 0 & A_{55} & 0 \\ 0 & A_{26} & 0 & A_{46} & 0 & A_{66} \end{bmatrix} \begin{Bmatrix} \ddot{x}_0 \\ \ddot{y}_0 \\ \ddot{z}_0 \\ \ddot{\phi}_0 \\ \ddot{\theta}_0 \\ \ddot{\psi}_0 \end{Bmatrix}$$

$$- \begin{bmatrix} B_{11} & 0 & 0 & 0 & 0 & 0 \\ 0 & B_{22} & 0 & B_{24} & 0 & B_{26} \\ 0 & 0 & B_{33} & 0 & A_{35} & 0 \\ 0 & 0 & 0 & B_{44} & 0 & B_{46} \\ 0 & 0 & B_{35} & 0 & B_{55} & 0 \\ 0 & B_{26} & 0 & B_{46} & 0 & B_{66} \end{bmatrix} \begin{Bmatrix} \dot{x}_0 \\ \dot{y}_0 \\ \dot{z}_0 \\ \dot{\phi}_0 \\ \dot{\theta}_0 \\ \dot{\psi}_0 \end{Bmatrix} \quad \text{(A.3)}$$

Added masses and damping coefficients in the x,y,z co-ordinate system

Added mass and damping matrices are needed in the equations of motions set with the ship's origin located in the centre of gravity and with the co-ordinates fixed with a ship (axes x,y,z). For this reason matrices $[A]$ and $[B]$ have to be transferred to the x,y,z co-ordinate system having the origin in the ship's centre of gravity. This is done as follows. Using the first of relations

(A.3) and the linearity assumptions the transformation of the motion components, velocities and accelerations can be presented as follows:

$$\begin{aligned}\{x_0\} &= [T_1]^{-1}\{x\} \\ \{\dot{x}_0\} &= [T_1]^{-1}\{\dot{x}\} \\ \{\ddot{x}_0\} &= [T_1]^{-1}\{\ddot{x}\}.\end{aligned} \tag{A.4}$$

Using expressions A.2, A.3 and A.4, the radiation forces in the body fixed co-ordinate system can be derived as follows:

$$\begin{aligned}\{X\} &= [T_2]\ \{X_0\} = [T_2]\ (-[A]\{\ddot{x}_0\} - [B]\{\dot{x}_0\}) = [T_2]\ (-[A][T_1]^{-1}\{\ddot{x}\} - [B][T_1]^{-1}\{\dot{x}\}) \\ &= -[a]\{\ddot{x}\} - [b]\{\dot{x}\},\end{aligned} \tag{A.5}$$

where added mass and damping matrices in the body-fixed co-ordinate system are given by the expressions given below:

$$[a] = [T_2]\ [A][T_1]^{-1}$$

$$= \begin{bmatrix} A_{11} & 0 & 0 & 0 & A_{11}z_G & 0 \\ 0 & A_{22} & 0 & -A_{24} - A_{22}z_G & 0 & A_{26} - A_{22}x_G \\ 0 & 0 & A_{33} & 0 & A_{35} + A_{33}x_G & 0 \\ 0 & -A_{24} - A_{22}z_G & 0 & \begin{matrix} A_{44} + 2A_{24}z_G \\ + A_{22}z_G^2 \end{matrix} & 0 & \begin{matrix} -A_{46} - A_{26}z_G \\ + x_G(A_{24} + A_{22}z_G) \end{matrix} \\ A_{11}z_G & 0 & A_{35} + A_{33}x_G & 0 & \begin{matrix} A_{55} + 2A_{35}x_G \\ + A_{33}x_G^2 + A_{11}z_G^2 \end{matrix} & 0 \\ 0 & A_{26} - A_{22}x_G & 0 & \begin{matrix} -A_{46} - A_{26}z_G \\ + x_G(A_{24} + A_{22}z_G) \end{matrix} & 0 & \begin{matrix} A_{66} - 2A_{26}x_G \\ + A_{22}x_G^2 \end{matrix} \end{bmatrix}$$

$$[b] = [T_2]\ [B][T_1]^{-1}$$

$$= \begin{bmatrix} B_{11} & 0 & 0 & 0 & B_{11}z_G & 0 \\ 0 & B_{22} & 0 & -B_{24} - B_{22}z_G & 0 & B_{26} - B_{22}x_G \\ 0 & 0 & B_{33} & 0 & B_{35} + B_{33}x_G & 0 \\ 0 & -B_{24} - B_{22}z_G & 0 & \begin{matrix} B_{44} + 2B_{24}z_G \\ + B_{22}z_G^2 \end{matrix} & 0 & \begin{matrix} -B_{46} - B_{26}z_G \\ + x_G(B_{24} + B_{22}z_G) \end{matrix} \\ B_{11}z_G & 0 & B_{35} + B_{33}x_G & 0 & \begin{matrix} B_{55} + 2B_{35}x_G \\ + B_{33}x_G^2 + B_{11}z_G^2 \end{matrix} & 0 \\ 0 & B_{26} - B_{22}x_G & 0 & \begin{matrix} -B_{46} - B_{26}z_G \\ + x_G(B_{24} + B_{22}z_G) \end{matrix} & 0 & \begin{matrix} B_{66} - 2B_{26}x_G \\ + B_{22}x_G^2 \end{matrix} \end{bmatrix}$$

Appendix B Cosine transform using FFT

Transformation of the added masses from the frequency to time domain involves an evaluation of the integral

$$K_{ij}(t) = \frac{2}{\pi}\int_0^{\omega_{\max}} B_{ij}(\omega)\cos(\omega t)\,d\omega. \tag{B.1}$$

This integral is called retardation or memory function. It can be approximated by the sum

$$K_{k,ij}(k\Delta t) = \frac{2}{\pi}\sum_{r=0}^{N-1} B_{ij}(r\Delta\omega)\cos(r\Delta\omega k\Delta t)\Delta\omega. \tag{B.2}$$

Selecting the frequency and time spacing is as follows. Time increment Δt is selected. It is the same as the time step used in the numerical integration of the equations of motion. The integer number $N=2^n$ is selected and the maximum angular frequency and frequency increament used in the Fast-Fourier-Transform (FFT) analysis are evaluated from:

$$\begin{aligned}\omega_{\max} &= 2\pi/\Delta t\\ \Delta\omega &= \omega_{\max}/N.\end{aligned} \tag{B.3}$$

yields

$$K_{k,ij}(k\Delta t) = \frac{2\Delta\omega}{\pi}\sum_{r=0}^{N-1} B_{ij}(r\Delta\omega)\cos(2\pi rk/N). \tag{B.4}$$

Expression B.4 can be evaluated using the FFT algorithm as follows

$$K_{k,ij}(k\Delta t) = \frac{N\Delta\omega}{\pi}\mathbf{FFT}(g_{ij}(x)), \tag{B.5}$$

where the original added damping discrete functions are substituted by a 'double-sided function' g(x) as follows:

$$g_{ij}(x) = B_{ij}(x) \text{ for } x = \Delta\omega, \Delta\omega N/2$$
$$g_{ij}(N\Delta\omega - x) = B_{ij}(x) \text{ for } x = 0, \Delta\omega(N/2+1) \qquad \text{(B.6)}$$

Note that as a result the retardation function B.5 is obtained at N/2 discrete time instants with a time step Δt.

The examples of the retardation functions are given in figures B.1 and B.2.

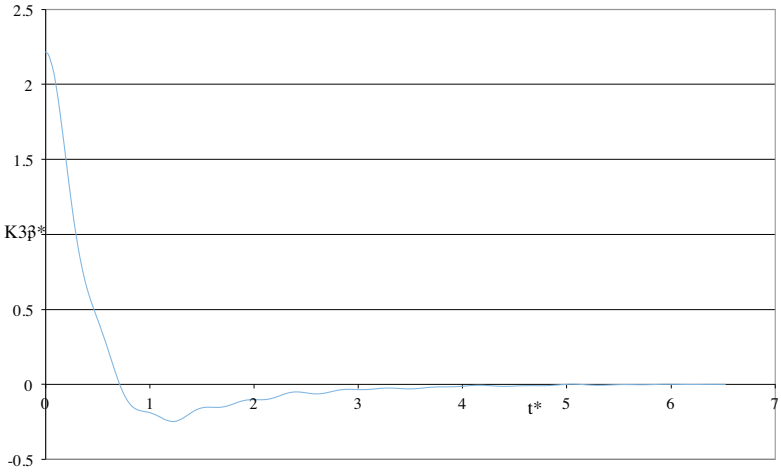

Fig. B.1 Non-dimensional heave memory (retardation) function $K_{33}^* = K_{33}/\left(M\sqrt{g/L}\right)$*. Time is made non-dimensional, too* ($t^* = t/\sqrt{g/L}$).

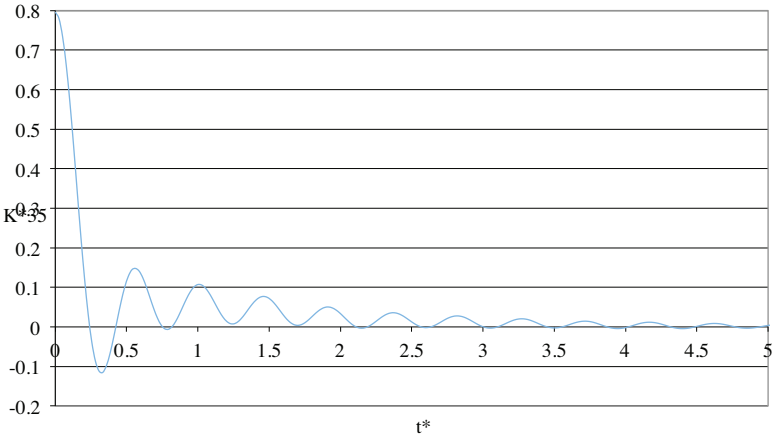

Fig. B.2 Non-dimensional heave to pitch memory (retardation) function $K_{35}^* = K_{35}/\left(ML\sqrt{g/L}\right)$*. Time is made non-dimensional, too* ($t^* = t/\sqrt{g/L}$).

Aalto-ST 11/2013

ISBN 978-952-60-5204-5
ISBN 978-952-60-5205-2 (pdf)
ISSN-L 1799-4896
ISSN 1799-4896
ISSN 1799-490X (pdf)

Aalto University
School of Engineering
Applied Mechanics
www.aalto.fi

BUSINESS +
ECONOMY

ART +
DESIGN +
ARCHITECTURE

SCIENCE +
TECHNOLOGY

CROSSOVER

DOCTORAL
DISSERTATIONS